

UC Berkeley

UC Berkeley Electronic Theses and Dissertations

Title

Enhanced Granular Media Filtration of Waterborne Pathogens: Effect of Media Amendments for Treatment of Drinking Water and Stormwater

Permalink

<https://escholarship.org/uc/item/9fz7q048>

Author

Torkelson, Andrew

Publication Date

2015

Peer reviewed|Thesis/dissertation

Enhanced Granular Media Filtration of Waterborne Pathogens: Effect of Media Amendments for
Treatment of Drinking Water and Stormwater

By

Andrew Arthur Torkelson

A dissertation submitted in partial satisfaction of the

requirements for the degree of

Doctor of Philosophy

in

Engineering – Civil and Environmental Engineering

in the

Graduate Division

of the

University of California, Berkeley

Committee in Charge:

Professor Kara L. Nelson, Chair
Professor David L. Sedlak
Professor John D. Coates

Fall 2015

Enhanced Granular Media Filtration of Waterborne Pathogens: Effect of Media Amendments for
Treatment of Drinking Water and Stormwater

Copyright 2015
By
Andrew Arthur Torkelson

Abstract

Enhanced Granular Media Filtration of Waterborne Pathogens: Effect of Media Amendments for Treatment of Drinking Water and Stormwater

By

Andrew Arthur Torkelson

Doctor of Philosophy in Engineering – Civil and Environmental Engineering

University of California, Berkeley

Professor Kara L. Nelson, Chair

Drinking water in low-income countries and stormwater in the U.S. is often contaminated with pathogens, posing health risks to local communities. In response, distributed filters are being used to provide the needed protection from exposure and infectious disease. Two examples of these distributed filters include point-of-use (POU) devices at the household scale for drinking water treatment and bioretention basins at the community scale for stormwater treatment. Sand is a common media used in distributed filters, but pathogen removal is often low due to unfavorable interactions between the sand surface and microorganisms. Removal may be increased, however, if certain amendments are added that create favorable interactions between microorganisms and the filter media, either through electrostatic attraction or hydrophobic interactions. This dissertation focused on the use of three media amendments, including a quaternary ammonium silane (QAS), zero valent iron (ZVI), and biochar, in distributed filters to improve removal of indicator bacteria and viruses from drinking water and stormwater.

In the first part of this dissertation, a QAS-coated sand was evaluated for drinking water treatment in POU filters. Varying influent water matrices were introduced to QAS-coated sand columns at representative flow rates, and the effluent was evaluated for indicator bacteria, indicator virus, and human virus removal. In basic water matrices with 1 mM NaCl and *Escherichia coli* (*E. coli*) or MS2 coliphage (MS2), removal was observed to increase with depth and decrease with increasing ionic strength, flow velocity, and experiment length. *E. coli* attached to QAS-coated sand were observed to have permeable membranes, providing evidence of inactivation. Major limitations, however, were observed when the influent contained humic acid or other viruses. Rapid fouling in the presence of humic acid was likely caused by competition for positively charged binding sites, and low PRD1 and Adenovirus 2 removal may have stemmed from steric interference between viral capsid features and the media surface.

In the second part of the dissertation, ZVI and biochar amendments were evaluated for stormwater treatment in bioretention basins in two long-term experiments. In the first experiment, stormwater columns were operated intermittently to examine *E. coli* and MS2 removal in

conventional bioretention media (CBM) and ZVI-amended media. A 1-year storm (3.2 cm) for Berkeley, CA was introduced to the columns once per week for 5.15 h. Afterwards, the columns were drained and remained in this state until the next week's storm. This pattern was repeated for 46 weeks. In CBM, *E. coli* removal increased as the columns aged and correlated with a decrease in hydraulic conductivity. Some evidence that biological activity contributed to *E. coli* removal was observed in a sodium azide experiment. In a ZVI-amended silica sand, *E. coli* and MS2 removal was above 1 log through week 11 but decreased quickly afterwards to levels observed in silica sand. The presence of other adsorbates, including natural organic matter (NOM), phosphate (PO_4^{3-}), and other organisms, likely contributed to the observed decrease in removal. In ZVI-amended CBM, *E. coli* and MS2 removal remained low throughout the experiment, likely due to the NOM, PO_4^{3-} , and organisms leached by the compost in CBM. Iron leaching was also observed in ZVI-amended CBM. In both ZVI-amended media types, large hydraulic conductivity reductions and cementation issues raised concerns over long-term permeability in the field.

In the second experiment, columns were operated as a batch system where stormwater was injected into a column and allowed to rest in the media for 24 h. After this rest period, fresh influent was injected into the column again, and the expelled effluent was evaluated for *E. coli* and MS2 removal. This pattern was repeated daily for 75 d. In biochar-amended silica sand, *E. coli* removal above 4 log was observed throughout the experiment. In iron-amended silica sand, MS2 removal above 2 log and PO_4^{3-} removal around 90% was observed after 75 d, and hydraulic conductivity did not decrease as observed in unsaturated columns.

Results from this dissertation provided insights into the limits of media amendments for pathogen removal, identified possible removal mechanisms of indicator organisms in mature bioretention basins, and demonstrated the promise of a batch configuration with increased rest periods and media amendments for long-term removal of indicator organisms.

Table of Contents

Table of Contents	i
List of Figures	iv
List of Tables	viii
Acknowledgements	ix
Chapter 1: Introduction	1
Sources of Contamination and Health Impacts	1
Removal Mechanisms and Types of Filters	2
Improved Removal Options	6
Dissertation Research Objectives	8
Dissertation Overview	10
Chapter 2: Investigation of Quaternary Ammonium Silane (QAS)-coated Sand for the Removal of Bacteria and Viruses in Point-of-Use (POU) Filters	11
Introduction	11
Materials and Methods	12
<i>Escherichia Coli</i>	13
MS2 and PRD1 Bacteriophage	13
Human Virus and Host Cells	13
Coating Procedure of QAS-Coated Sand	14
Leaching Assays (Microbial and Bromophenol Blue Methods).....	14
QAS Coverage of Silica Sand Media Measurement.....	15
QAS-coated Sand Column Experiments	15
Filtration Model Parameters	16
Bacteria Membrane Damage/Death from QAS-coated Sand Exposure	16
Fluorescence Microscopy.....	16
Results	17
QAS Coverage and Coating Stability on Silica Sand Media	17
QAS-coated Sand Column Studies	19
Loss of Culturability and Membrane Damage due to QAS-coated Sand Exposure.....	22
Discussion	23
Conclusions	26
Chapter 3: Introduction and Materials and Methods for Intermittently Fed, Unsaturated Stormwater Columns	27
Introduction	27
Materials and Methods	29
Indicator <i>Escherichia coli</i> and MS2 Coliphage.....	29
Media Preparation	29
Short-Term Column Experiment with Synthetic Stormwater	30
46-Week Column Experiment with Amended Creek Water	30
Rest Period and Sodium Azide Experiments	34

Water Chemistry	35
Clogging Model	37
Biofilm Characterization	39
Flow Cytometry and Assimilable Organic Carbon	40
Data Analysis	43
Chapter 4: Results and Discussion for Intermittently Fed, Unsaturated Stormwater Columns with Conventional Bioretention Media	44
Results.....	44
Removal of <i>E. coli</i> , MS2, Total Organic Carbon, and Phosphate	44
Hydraulic Conductivity and Clogging Model	45
Effect Biological Activity on Indicator Removal.....	47
Effect of Rest Period on Indicator Removal	48
Biofilm Characterization on Media	48
Flow Cytometry Counts of Influent and Effluent Samples.....	50
Discussion	51
<i>E. coli</i> and MS2 Removal.....	51
Effect of Biological Community on Indicator Removal	53
Biofilm Characterization and Flow Cytometry Counts	54
Conclusions	55
Chapter 5: Results and Discussion for Intermittently Fed, Unsaturated Stormwater Columns with Zero Valent Iron-Amended Media	57
Results.....	57
Short-term Column Studies.....	57
46-Week Removal of <i>E. coli</i> and MS2	57
Total Organic Carbon, Phosphate, and Flow Cytometry Counts	58
Hydraulic Conductivity and Iron Leaching.....	60
Effect of Rest Period on <i>E. coli</i> and MS2 Removal	63
Discussion	63
Short-Term <i>E. coli</i> Removal in ZVI-Amended Column	63
46-Week <i>E. coli</i> and MS2 Removal and Effect of Total Organic Carbon, Phosphate, and Background Microbial Community on Removal.....	64
Zero Valent Iron Corrosion, Hydraulic Conductivity, and Cementation.....	67
Iron in Effluent of ZVI-Amended Columns	68
Effect of Rest Period on Indicator Organism Removal.....	70
Conclusions	70
Chapter 6: A Novel Design for Stormwater Bioretention with Pulsed Feed and Saturated Bed: Evaluation of <i>E. coli</i> and MS2 Removal in Aged Columns with Different Media Amendments	71
Introduction	71
Material and Methods.....	73
Indicator <i>E. coli</i> and MS2 Coliphage	73
Media and Column Preparation	73
75-Day Column Experiment	75
Hydrophobic Interactions and Biochar.....	77
Source Water	77
Flow Cytometry and Assimilable Organic Carbon	78
Data Analysis	78
Results.....	79

<i>E. coli</i> and MS2 Removal and Hydraulic Conductivity	79
Effect of Hydrophobic Interactions on Indicator Removal in PS+BC.....	80
Total Organic Carbon and Phosphate	81
Flow Cytometry Counts of Influent and Effluent Samples.....	82
Biofilm Characterization	84
Discussion	86
<i>E. coli</i> , MS2, and Phosphate Removal.....	86
Suspended and Attached Biomass	88
Conclusions	89
Chapter 7: Conclusions	90
References	94

List of Figures

Figure 1.1 – Physico-chemical removal mechanisms of microorganisms on a single collector (Benjamin and Lawler, 2013).	3
Figure 1.2 – Sources of clogging and increased microorganism removal in aged filters.	4
Figure 1.3 – Improved microorganism removal through altered flow paths from favorable electrostatic or hydrophobic interactions (Elimelech and Song, 1992).	6
Figure 1.4 – Net positive surface charge on silica media by attaching QAS molecules.	7
Figure 2.1 – Estimated surface charge density of QAS-coated sand batches used in column experiments. Dotted lines show the charge density thresholds reported by Kügler et al. (2005). Error bars report two standard deviations, and reflect only the variability in the measurement of the coating concentration. As described in the text, it was not possible to estimate the variability of the surface area of the sand.	17
Figure 2.2 – Microbial Leach Assay Results. The columns represent the die off of <i>E. coli</i> when exposed to MilliQ water exposed to QAS-coated sand. Plain silica sand was used as the control. A decrease in <i>E. coli</i> concentration above the control was considered evidence of QAS leaching.	18
Figure 2.3 – Comparison of the predicted removal from the filtration model (Tufenkji and Elimelech, 2004) and the observed clean bed removal in QAS-coated sand columns. Columns for the <i>E. coli</i> , MS2, and PRD1 experiments were 18 cm.	20
Figure 2.4 – Removal of <i>E. coli</i> and MS2 by QAS-coated sand as a function of (A) ionic strength, (B) flow velocity, (C) presence of 20 mg/L humic acid (in 1 mM NaCl), and (D) presence of powdered activated carbon (PAC) pre-filter to remove Fluka humic acid. The flow velocity in each column test was 18 m/h unless otherwise indicated. Column lengths for each experiment are indicated on each graph. An asterisk indicates that the removal was equal to or greater than the detection limit of the assay.	21
Figure 2.5 – Fluorescence microscopy images of QAS-coated sand exposed to <i>E. coli</i> . <i>E. coli</i> were stained with SYTO-9 to image membrane-impermeable (live) cells and PI to image membrane-permeable (dead) cells.	23
Figure 3.1 – Cross-section schematic of columns for this study. (A) Upward flow orientation used during the weekly 5.15-h stormwater injections. After each 5.15-h injection, the columns were inverted to the (B) orientation to allow drainage via gravity without reversing the direction of flow. The columns stayed in the (B) orientation for the remainder of the week. Immediately prior to the next injection, the columns were inverted back to the (A) orientation to again receive stormwater.	31
Figure 3.2 – Photo of the experimental setup for the 46-week column experiment.	32
Figure 3.3 – Typical (A) <i>E. coli</i> and (B) MS2 removal changes in PS, CBM, PS+ZVI, and CBM+ZVI columns throughout a 1-year storm injection. For routine sample collection, a single sample was collected from each column after 3 pore volumes had been injected through the	

columns. Error bars represent one standard deviation.	33
Figure 3.4 – Absorption spectrum of NOM amendment created from Strawberry Creek water, wood chips, maple leaves, and American Soil and Stone compost.	36
Figure 3.5 – Sample ATP standard curves for (A) PS and (B) CBM media.	40
Figure 3.6 – Flow cytometry plots displaying the gates drawn for TCCs and HNA and LNA bacteria concentrations for effluent from (A) PS, (B) CBM, (C) PS+ZVI, and (D) CBM+ZVI columns. The forward and side scatter plots are also included.....	42
Figure 4.1 – Removal of (A) <i>E. coli</i> and (B) MS2 in PS and CBM columns during weekly stormwater injections. Stormwater was injected weekly for 5 h and samples were taken after 3 pore volumes of stormwater passed through the columns. Error bars represent one standard deviation.....	44
Figure 4.2 – Normalized effluent (A) TOC and (B) phosphate concentrations from PS and CBM columns. Samples were collected after 3 pore volumes of stormwater passed through the columns. Error bars represent one standard deviation.	45
Figure 4.3 – Hydraulic conductivity (cm/h) of PS and CBM columns during weeks 1, 8, 18, 35, and 46. Hydraulic conductivity was measured via the falling head method from duplicated columns immediately following a 5-h stormwater injection. Error bars represent one standard deviation.....	46
Figure 4.4 – Correlation between specific deposit and log removal of (A) <i>E. coli</i> and (B) MS2 for PS and CBM columns. Specific deposit was calculated using the Mays et al. clogging model (2005). The week 8 specific deposit for CBM columns could not be calculated since HC remained unchanged from the initial HC. Error bars represent one standard deviation.....	46
Figure 4.5 – (A) <i>E. coli</i> and (B) MS2 removal in PS and CBM columns fed with or without sodium azide feed. The normal feed was the same stormwater recipe used throughout the 46-week experiment. These data were collected during the week 46 regular feed. The sodium azide feed contained the stormwater recipe with 6 mM of sodium azide and was conducted on a different replicate column. The sodium azide feed was injected for 5 h on three consecutive days. Samples were analyzed for indicators on the 3 rd day. Error bars represent one standard deviation.	47
Figure 4.6 – (A) <i>E. coli</i> and (B) MS2 removal in PS and CBM columns after rest periods. Duplicate columns were first saturated with stormwater. After 24 h, stormwater was again injected, and the effluent was collected for analysis. The 0-h rest period removal data were collected from the week 46 injection in which stormwater was injected at a constant flow rate without a rest period. Error bars represent one standard deviation.....	48
Figure 4.7 – Biofilm characterization in PS and CBM columns reported as (A) ATP/cell, (B) ATP/g Media, and (C) Cells/g Media. Columns were sacrificed during weeks 8, 18, 31, and 46, and samples were taken from the top, middle, and bottom 3 cm of duplicate columns. PS data from the middle and bottom sections and CBM data from all sections were averaged due to statistical similarity ($p > 0.05$). Error bars represent one standard deviation.	49
Figure 4.8 – TCCs in the influent and effluent of (A) PS and (B) CBM columns. Samples were taken after 3 pore volumes of stormwater had been injected and measured via flow cytometry. Error bars represent one standard deviation.....	50

Figure 4.9 – Influent and PS and CBM effluent TCCs, reported as HNA and LNA bacteria concentrations, during the week 46 injection. The influent sample was taken at the beginning of the stormwater injection. Effluent samples were taken after 0.5 and 5 pore volumes of stormwater had been injected into the columns. Error bars represent one standard deviation. **51**

Figure 5.1 – *E. coli* removal through 3.2 pore volumes in PS and PS+ZVI columns. * denotes removal to the detection limit (10 CFU/mL). Error bars represent one standard deviation. **57**

Figure 5.2 – Removal of (A) *E. coli* and (B) MS2 in PS, PS+ZVI, and CBM+ZVI columns. Stormwater was injected weekly for 5 h and samples were taken after 3.2 – 3.5 pore volumes of stormwater passed through the columns. Error bars represent one standard deviation. **58**

Figure 5.3 – Normalized (A) TOC and (B) PO₄³⁻ concentrations in PS, PS + ZVI, and CBM + ZVI effluent. Error bars represent one standard deviation. **59**

Figure 5.4 – TCCs in the influent and effluent of (A) PS + ZVI and (B) CBM + ZVI columns. Samples were taken during weekly stormwater injections after 3 pore volumes and analyzed via flow cytometry. Error bars represent one standard deviation. **59**

Figure 5.5 – TCC, broken down into LNA and HNA bacteria, in the influent and effluent of PS + ZVI and CBM + ZVI during the week 46 breakthrough experiment. The influent sample was taken at the beginning of the stormwater injection. Samples from the effluent were taken after 0.5 and 5 pore volumes of stormwater had been injected. Error bars represent one standard deviation. **60**

Figure 5.6 – Hydraulic conductivity (cm/h) of PS, PS + ZVI, and CBM + ZVI columns during weeks 1, 8, 18, and 46. Hydraulic conductivity was measured in duplicate columns via the falling head method immediately following a 5-h stormwater injection. Error bars represent one standard deviation. **61**

Figure 5.7 – Fe[II], Fe[III], Tot Fe concentrations in (A) PS + ZVI and (B) CBM + ZVI effluent during weekly stormwater injections. Samples were taken after 3 pore volumes of stormwater had been injected into the columns. Error bars represent one standard deviation. **61**

Figure 5.8 – Fe[II], Fe[III], Tot Fe concentrations in PS + ZVI and CBM + ZVI effluent during the (A) week 8 and (B) week 46 injections. Samples were taken at multiple points (0.5, 2, 4, and 5 pore volumes) throughout the 5-h stormwater injection. Error bars represent one standard deviation. **62**

Figure 5.9 – (A) *E. coli* and (B) MS2 removal in PS, PS + ZVI, and CBM + ZVI columns after longer rest periods. For the 24-h rest period experiments, duplicate columns were saturated with stormwater and allowed to rest for the stated time period. Afterwards, stormwater was injected and the initial 0.5 pore volume of effluent was collected for indicator analysis. The 0-h rest period experiment is removal data from the week 46 injection in which stormwater was continually injected without a rest period. Error bars represent one standard deviation. **63**

Figure 6.1 – Experimental setup including eight columns total. **75**

Figure 6.2 – Cross-section schematic and injection/sampling regimen for columns in this study. At 9 AM on Day N, columns were injected for 0.75 h (A). After the injection, the columns rested for the next 23.25 h until 9 AM on Day N+1 (B). The columns were then injected again for 0.75 h, displacing a mixture of Day N stormwater and Day N–1 stormwater (C). This effluent was analyzed to evaluate removal performance for Day N. Afterward, the columns were allowed to

rest for 23.25 h until the next injection (D). Due to differences in porosities, PS, CBM, and PS+ZVI columns received 0.8 PVs and PS+BC columns received 0.9 PVs during injections.... 76

Figure 6.3 – Removal of (A) *E. coli* and (B) MS2 in each media type during the 75-d experiment. (C) Average *E. coli* and MS2 removal in each media type over entire 75-d experiment. Error bars represent one standard deviation. * denotes concentrations were below the detection limit (10 CFU/mL or PFU/mL). 79

Figure 6.4 – Saturated hydraulic conductivity (cm/h) of PS, CBM, PS+ZVI, and PS+BC columns on day 1 and 75 of the experiment. Error bars represent one standard deviation. 80

Figure 6.5 – Indicator *E. coli* and MS2 removal in PS+BC column with a normal and 0.1% Tween[®] 20 feed. * denotes removal to the detection limit (10 CFU/mL or PFU/mL). Error bars represent one standard deviation. 81

Figure 6.6 – Normalized (A) TOC and normalized (B) PO₄³⁻ concentrations in each media type effluent. Average effluent (C) TOC and (D) PO₄³⁻ concentration in each media type over entire 75-d experiment. Error bars represent one standard deviation. 82

Figure 6.7 – TCCs, divided into HNA and LNA bacteria counts, and the % HNA and % LNA, reported as percentage of the TCC, in the influent and effluent of (A) PS, (B) CBM, (C) PS+ZVI, and (D) PS+BC during the 75-d study. Error bars represent one standard deviation. Note the difference in scale for TCCs between media types. 83

Figure 6.8 – Average TCC, broken down into HNA and LNA bacteria concentrations, in the influent and effluent of each media type over the entire 75-d experiment. Error bars are one standard deviation. 84

Figure 6.9 – Biofilm characterization in PS, CBM, and PS+BC columns reported as (A) ATP/Cell, (B) ATP/g Media, and (C) Cells/g Media. Duplicate columns were sacrificed after the day 75 injection, and samples were taken from the top, middle, and bottom 4 cm of the media section. Error bars represent one standard deviation. 85

List of Tables

Table 1.1 – Properties of various types of filtration (Huisman and Wood, 1974; Benjamin and Lawler, 2013; Stauber et al., 2006; Davis et al., 2009; Li et al., 2012).	5
Table 2.1 – Parameters used in the filtration model to predict column removal (Tufenkji and Elimelech, 2004).	16
Table 2.2 – Bromophenol Blue (BPB) Leaching Assay. A 1:1 molar ratio of BPB:QAS in solution was observed to cause a shift in peak absorption wavelength. Standard BPB solutions without QAS had a peak wavelength around 591 nm, and standard solutions with 1:1 ratio of BPB:QAS had a peak wavelength around 604 nm.	18
Table 2.3 – Clean bed removal of <i>E. coli</i> , MS2, PRD1, Poliovirus 3, and Adenovirus 2 by QAS-coated sand columns at an ionic strength of 1 mM NaCl and filtration velocity of 18 m/h. Dashes in the standard deviation column indicate the microorganisms were removed to the detection limit in each experiment. The standard deviation was calculated based on duplicate influent and effluent samples taken from a single column experiment at 2 min. Column tests conducted with different batches of sand resulted in similar log removal levels.	19
Table 2.4 – <i>E. coli</i> in pore water and regrowth on sand grains. Sands were exposed to <i>E. coli</i> by tumbling for 24 h, followed by rinsing. Rinsed sand was re-introduced to growth media to detect <i>E. coli</i> regrowth.	22
Table 3.1 – Column and Media Characteristics.	32
Table 3.2 – Influent Characteristics. <i>E. coli</i> , MS2, and TOC added to creek water 15 minutes prior to every injection. Dissolved oxygen (DO) and alkalinity were not measured directly, but historical monitoring values of Strawberry Creek are reported here (Hans and Maranzana, 2006).	35
Table 3.3 – Specific Ultraviolet Absorbance (SUVA), Peak Wavelength, and Peak Absorbance for NOM amendment.	36
Table 3.4 – Parameters used in the clogging model to track HC changes (Mays and Hunt, 2005).	39
Table 6.1 – Biochar Source, Process Description, Feedstock, Peak Temperature (T), Surface Area (SA), and Micropore Volume ($V_{\mu\text{pore}}$) (Ulrich et al., 2015).	74
Table 6.2 – Physical and Chemical Composition of Sonoma Compost Co. Biochar (Mohanty et al., 2014).	74
Table 6.3 – Column and Media Type Characteristics.	75
Table 6.4 – Influent characteristics during 75-d study. DO was not measured directly, but historical monitoring values of Strawberry Creek indicate that levels are typically near saturation (Hans and Maranzana, 2006).	78

Acknowledgements

I want to thank Professor Kara Nelson for being such a supportive and inspiring advisor. Her constant, patient guidance gave me the chance to explore my interests and pushed me to complete experiments that were more challenging than expected. There is no doubt in my mind that I have reached this point because Kara was my advisor.

I would like to thank Professor David Sedlak and Professor John Coates for serving on my dissertation committee, and Professor Ali Boehm for her valuable advice. I also owe Sanjay Mohanty so much. During our work together, he taught me how to design filtration experiments and persevere through the inevitable difficulties.

I owe considerable thanks to all the graduate and postdoctoral students in O'Brien Hall for their help around the lab. Particular thanks are needed for Andrea Silverman, Allegra da Silva, Mi Nguyen, Jannis Wenk, and Janel Grebel. I also owe Chris Loeb considerable thanks for his help putting together 40 filters.

To Ari, you have been the best partner. Through the highs and lows, you have been my rock and inspiration. Thank you for your constant encouragement, optimism, love, and unending belief in me. I love you and cannot wait for all the adventures that lay ahead.

To Hannah, you have been my sounding board and source of sanity. During trips and weekly chats, you patiently listened to my complaints and always offered great advice and distractions. I love you and thank you for the time, laughs, and wonderful guidance.

To Mom and Dad, I owe you everything. Your unconditional love and support has enabled me to chase and reach my dreams. I love you and thank you from the bottom of my heart.

Finally, to all my family and friends, I cannot possibly express in words what your support has meant to me. Without you, I would never have reached this stage. This dissertation is for you.

*

*

*

For the drinking water research, support was provided by the Lemelson Foundation, Mulago Foundation, University of California, Berkeley Blum Center for Developing Economies, and University of California, Berkeley Sustainable Products and Solutions Program.

For the stormwater research, support was provided by Re-Inventing the Nation's Urban Water Infrastructure (ReNUWIIt), an Engineering Research Center (ERC) funded by the U.S. National Science Foundation (NSF) (Grant # EEC-1028968).

Chapter 1: Introduction

Waterborne pathogens, including viruses, bacteria, protozoa, and helminths, pose health risks with exposure leading to gastrointestinal disease. Water treatment processes are therefore necessary to prevent this exposure by removing or inactivating several types of pathogens. One such treatment process for removing pathogens is granular media filtration. Filtration passes water through porous media by gravity or pressure and can remove pathogens under specific conditions (Huisman and Wood, 1974). This dissertation focused on filtration applications for drinking water treatment in low-income countries and stormwater treatment in the U.S. and investigated the use of media amendments for enhanced removal of bacteria and viruses.

Sources of Contamination and Health Impacts

Pathogen contamination of water sources remains a frequent problem for both drinking water sources in low-income countries (WHO, 2007) and stormwater in the U.S. (CDC, 2011). In low-income countries, this contamination stems from unsafe drinking water, sanitation, and hygiene (WASH) practices and is often transmitted through fecal-oral routes (UNICEF/WHO, 2009). Human fecal markers have been frequently found in the household environment in soil (Pickering et al., 2012) and on hands (Mattioli et al., 2014), and animal fecal markers have been found in both household and community environments (ponds and groundwater sources) (Schriewer et al., 2015). Thus, surface water collected as the drinking water source (Hunter et al., 2010) and water stored in the house (Jensen et al., 2002) is often contaminated with pathogens and their indicator organisms. Without adequate drinking water treatment, consuming this water can lead to infectious diseases, accounting for 1.5% of the total global disease burden and 58% of diarrheal disease (Prüss-Ustün et al., 2014). Highly endemic diarrhea is the greatest concern (Clasen et al., 2007), accounting for nearly 5.5% of overall deaths in children under five (Prüss-Ustün et al., 2014). Although the United Nations met the Millennium Development Goal (MDG) for drinking water access in 2010 (50% reduction in people without access to improved water sources from a 1990 baseline), the problem still impacts low-income communities, particularly in rural areas. In 2015, 663 million people still lack access to improved drinking water sources, and 80% of these people live in rural areas (WHO, 2015).

In the U.S., the Environmental Protection Agency (EPA) has estimated that nonpoint pollution from stormwater runoff has impaired 13% of river segments, 18% of lakes, and 32% of estuaries surveyed (U.S. EPA, 2009). Stormwater can contain a highly variable mixture of contaminants, including suspended solids, nutrients, heavy metals, trace organic contaminants, and pathogens (Grebel et al., 2013) and has been linked to water quality and health impacts in urban environments. Stormwater and precipitation events have been blamed for beach closures in Southern California (Marsalek and Rochfort, 2004; Schiff et al., 2003) and linked to recreational waterborne illness in swimmers (Colford et al., 2012), waterborne disease outbreaks (Curriero et al., 2001), and pediatric emergency room visits for acute gastrointestinal illness (Drayna et al., 2010). Several types of human pathogens and indicator organisms have been detected in stormwater, including pathogenic bacteria (*Salmonella* spp. and *Staphylococcus aureus*) (Walters et al., 2011), human viruses (Adenovirus, Rotavirus, and Enterovirus) (Sidhu et al., 2013), fecal

indicator bacteria (FIB) (total and fecal coliforms, *Escherichia coli*, and *Enterococcus faecalis*) (Staley et al., 2012), and bacteriophage (F+ coliphage) (Cizek et al., 2008). Contamination has been traced to several sources and can depend on surrounding land use. Human sewage pollution in urban environments is a common reservoir of bacteria and viruses. Researchers have detected pathogenic bacteria, human viruses, and indicator organisms in urban runoff during storms and dry weather using microbial source tracking techniques (Sidhu et al., 2012; Sidhu et al., 2013), attributing their presence to widespread sewage pollution from sanitary sewer leaks/exfiltration to the stormwater sewers (Sauer et al., 2011; Sercu et al., 2011). Stormwater runoff from high-density residential land with sewer systems, in fact, had higher indicator bacteria concentrations compared to low-density residential land with septic tanks or commercial land (Selvakumar and Borst, 2006; Young and Thackston, 1999). Viruses, highly specific to their hosts (Gerba and Rose, 1990), are typically limited to human sewage sources, but bacteria contamination has also been traced to feces from pets, raccoons, and birds (Ram et al., 2007) and non-fecal, environmental reservoirs, including temperate or subtropical soils (Byappanahalli et al., 2012) and grasses (Ott et al., 2001).

While numerous strains of pathogens and indicator organisms have been detected in stormwater, the concentrations can be highly variable. Due to the difficulty of measuring low, variable concentrations, human pathogens are seldom monitored in stormwater. Instead, indicator organisms are the focus of most monitoring studies and regulations (Olivieri et al., 2007). Recreational water quality criteria and total maximum daily loads (TMDL) are based on FIB concentrations (Boehm et al., 2009), and stormwater flows have been frequently observed to exceed these standards (Parker et al., 2010). It should be noted that correlations have yet to be established in stormwater between indicator organisms and pathogen concentrations (Brownell et al., 2007; Selvakumar and Borst, 2006). Furthermore, the relationship between indicator organisms, pathogens, and recreational water illness is unknown (Boehm et al., 2009). However, under current TMDL and recreational water standards, FIB contamination in stormwater presents a barrier to nonpotable use of stormwater (Pitt and Clark, 2012). In addition, indicator viruses are viewed as a particular concern when considering stormwater for groundwater replenishment (Pitt et al., 1999).

Removal Mechanisms and Types of Filters

In granular media filters, microorganisms are removed by a two-step process. First, the microorganism must be transported to a filter media collector. The transport step, shown in Figure 1.1, occurs through fluid motion, gravity settling, and Brownian diffusion. Viruses, with diameters less than one μm , are typically transported via Brownian diffusion. Protozoan cysts and helminth eggs, with diameters larger than 10 μm , are transported by interception, sedimentation, and straining. Bacteria, with diameters around one μm , are usually transported via a combination of the previously mentioned transport processes. Second, the microorganism must attach to the filter media collector. The attachment step is largely governed by short-range forces, including van der Waals interactions, electrical double layer interactions, steric interactions, and hydrophobic interactions (Benjamin and Lawler, 2013). The effect of these interactions is captured in an empirical attachment coefficient α , defined as the fraction of predicted microorganism/collector collisions leading to attachment. Depending on the microorganism and collector's surface characteristics, α is often much lower than one (Tufenkji

and Elimelech, 2004).

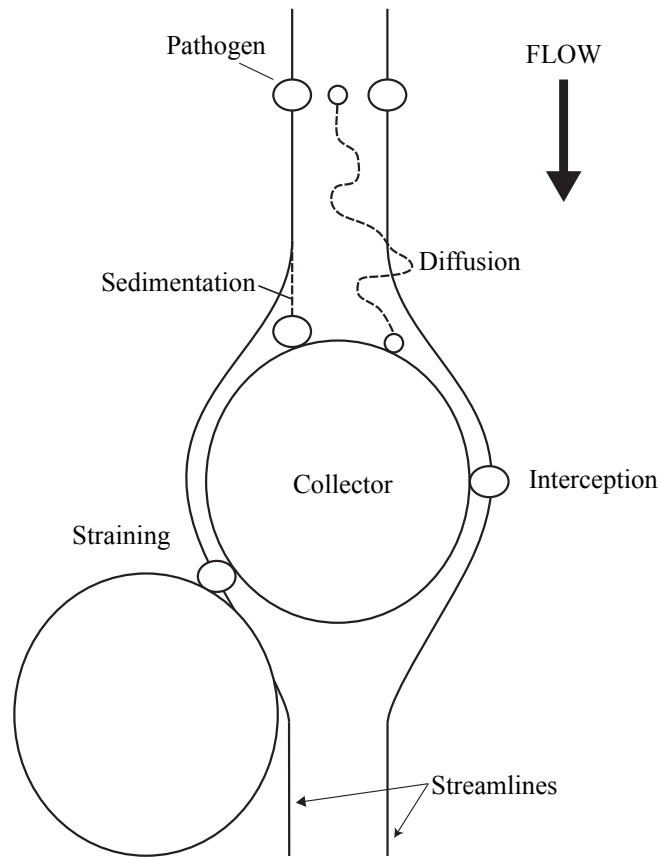


Figure 1.1 – Physico-chemical removal mechanisms of microorganisms on a single collector (Benjamin and Lawler, 2013).

As a filter ages, the flow velocity eventually decreases due to the restriction of pore spaces and an increase in head loss. This process, referred to as clogging, can occur via abiotic and biotic processes, as shown in Figure 1.2. The abiotic process involves the accumulation of suspended solids in the pore space between collectors (Mays and Hunt, 2005). The biotic process can occur in two ways. First, attached biomass can form extracellular polymeric substances (EPS) to provide structural and functional integrity to the biofilm (Wingender et al., 1999) or protection from desiccation (Roberson and Firestone, 1992). Second, microorganisms can produce gas bubbles as a product of respiration (Ronen et al., 1989). In either process, the reduction in flow velocities generally leads to an increase in microorganism removal through increased contact times with filter media, reduced distances between microorganism and filter collectors (Yates and Yates, 1987), increased exposure to a biofilm (Bellamy et al., 1985), and increased exposure to air-water interfaces from gas production (Wan et al., 1994). In addition to clogging, aging of the filter also exposes microorganisms to decay stresses via predation or enzyme production from the larger microbial community (Elliott et al., 2011; Weber-Shirk and Dick, 1997).

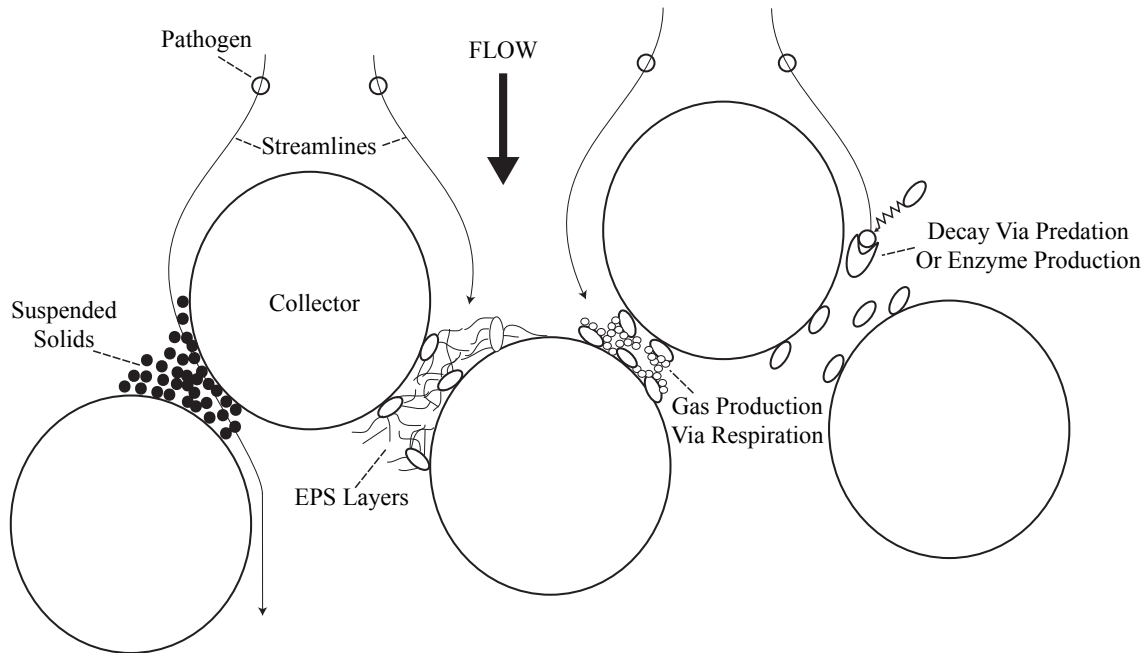


Figure 1.2 – Sources of clogging and increased microorganism removal in aged filters.

Historically, gravity filtration has been conducted in two types of filters: (1) slow sand filters and (2) rapid sand filters. Slow sand filters, operated in the U.S. since the late 19th century, typically contain finer sand and lower elevation heads than rapid sand filters (Fox et al., 1984; Huisman and Wood, 1974). The aging, biological activity, and clogging process shown in Figure 1.2 occurs in both filter types but is more prominent in slow sand filters. Slow sand filters are operated with 1 – 1.5 m of constant elevation head and slow flow velocities between 0.08 – 0.4 m/h. Due to this slow flow velocity, large particles in the influent typically settle onto the top of the media, forming a biologically active cake layer called the *Schmutzdeke*. This layer is usually a few centimeters thick and contains a biological community that includes numerous types of algae, bacteria, protozoa, and plankton. The *Schmutzdeke* thickens over time as more particles settle, and a biofilm can also form in the underlying media. Larger pathogens, such as protozoan cysts and helminth eggs, are removed in the *Schmutzdeke* via size exclusion or straining mechanisms (Huisman and Wood, 1974). Smaller pathogens, including bacteria and viruses, are removed more efficiently in aged media due to biofilm and microbial activity (Wheeler et al., 1988). Regeneration is possible by scraping off the *Schmutzdeke* or harrowing (raking the *Schmutzdeke* into the sand so all biological activity is not lost) if flow velocities have decreased too much (Huisman and Wood, 1974). In rapid sand filters, higher elevation head (1.5 – 3 m) and larger diameter media permit flow velocities between 5 – 24 m/h (Huisman and Wood, 1974). The residence time, therefore, is shorter than slow sand filters, and pathogen removal relies more heavily on depth filtration and physico-chemical mechanisms than biological aging. Microorganism removal is typically low, and rapid sand filters are mainly used for suspended solids removal and polishing before further disinfection (Logsdon and Lippy, 1982). Clogging in rapid sand filters is limited by frequent cleaning at specific head losses by backwashing with high flow rates and air scouring (Benjamin and Lawler, 2013).

Additional categories of filtration include biosand filters and bioretention basins. These filters share some characteristics with slow sand filters (development of *Schmutzdecke*) but are operated in different configurations. Both biosand filters and bioretention basins are operated intermittently without a constant elevation head above the top filter surface. Instead, the elevation head decreases as influent drains through the media. Biosand filters, intended for household-scale drinking water treatment in low-income countries, include shallower bed depths, broader media size distribution, lower elevation heads, and higher flow velocities than slow sand filters (Elliott et al., 2008). These filters are typically operated once per day wherein a single charge is added to the filter (typically near the pore volume of the filter) and allowed to rest in the media for 24 h. Due to this retention time, the average flow velocity over 24 h is similar to flow velocities for slow sand filters. Higher bacteria and virus removal have been reported with this long retention time (Elliott et al., 2011; Jenkins et al., 2011). Media aging and microbial activity have also been shown to be important factors in bacteria and virus removal (Elliott et al., 2011; Wang et al., 2014). Similar to slow sand filters, aging can also lead to a reduction in flow velocities and *Schmutzdecke* scraping is recommended for regeneration.

Bioretention basins are used in many distributed stormwater catchments in the U.S. and collect influent only during storms. Flow velocities, typically around 0.5 m/h, are limited by the low permeability of conventional bioretention media and native soils (He and Davis, 2011). Current designs do not allow for extended retention times in the filter media. FIB removal has been observed throughout the basin depth and can depend on media aging and infiltration rate (Li and Davis, 2009; Zhang et al., 2011). Virus removal has also been observed in one long-term study of columns in the laboratory (Li et al., 2012). No known research has been conducted on the influence of microbial activity on microorganism removal or media regeneration as flow velocities decrease with aging. A summary of the features of each filter type is included in Table 1.1.

Table 1.1 – Properties of various types of filtration (Huisman and Wood, 1974; Benjamin and Lawler, 2013; Stauber et al., 2006; Davis et al., 2009; Li et al., 2012).

Filtration Type	Flow Velocity (m/h)	Depth (m)	Pathogen Removal	Removal Mechanism	Regeneration
Bioretention Basin	0.05	0.7 – 1	B, some V	<i>Schmutzdecke</i> , Media Aging, Depth Filtration	?
Slow Sand Filtration	0.08 - 0.4	0.6 – 1.2	B, V	<i>Schmutzdecke</i> , Straining	Remove Cake
Biosand Filtration	1.1	0.4	B, some V	<i>Schmutzdecke</i> , Media Aging, Depth Filtration	Remove Cake
Rapid Sand Filtration	5-24	0.6 – 1.2	Low	Depth Filtration	Backwash

Improved Removal Options

To enhance microorganism removal in granular filters, both the transport rate and attachment efficiency to collectors must be increased. This two-step process can be improved by producing favorable interactions between the collector and microorganism, which can change a microorganism's trajectory toward the collector for attachment (Figure 1.3) or improve attachment efficiency.

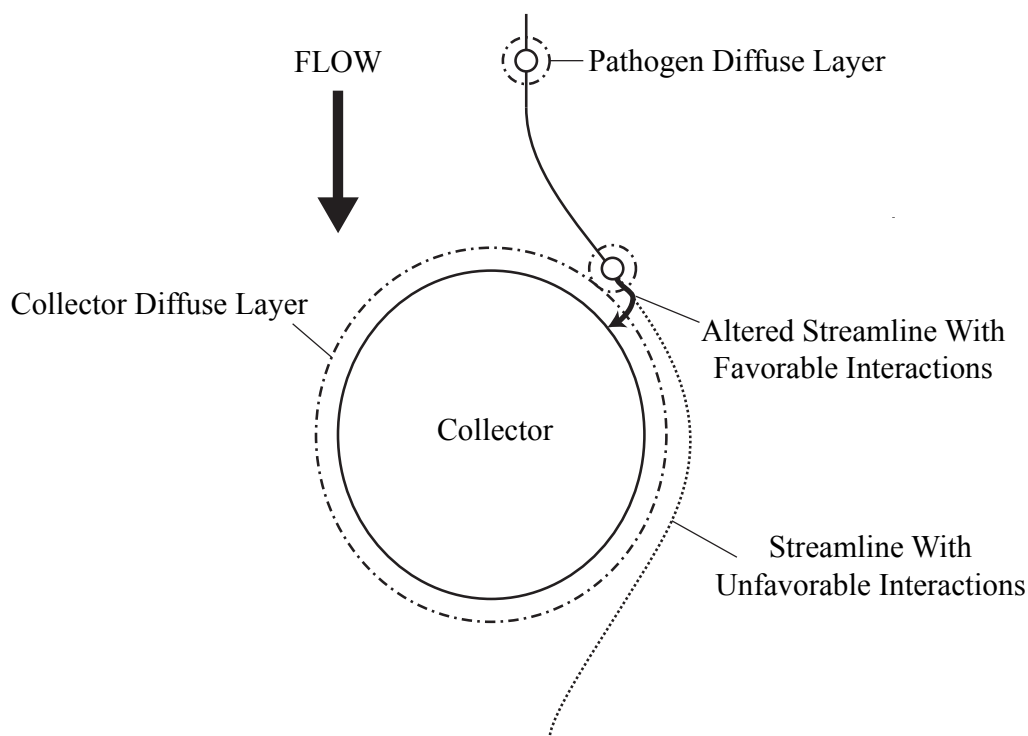


Figure 1.3 – Improved microorganism removal through altered flow paths from favorable electrostatic or hydrophobic interactions (Elimelech and Song, 1992).

These favorable interactions can be created either by manipulating a collector's surface charge or hydrophobicity. Surface characteristics and the surrounding solution chemistry are the main influences on a collector's surface charge (Benjamin, 2002). At pH 7, typical filter media and the majority of microorganisms exhibit a net negative charge (Kosmulski, 2011; Michen and Graule, 2010). The similar surface charges, therefore, inhibit microorganism attachment to filter media by electrostatic repulsion. In the case of opposite surface charges, in which the filter media is net positive and the microorganism is net negative, microorganism transport and attachment would increase due to electrostatic attraction. As show in Figure 1.3, the net positive charge layer from filter media can extend further into the surrounding bulk solution at low ionic strengths and

change the trajectory of a net negatively charged microorganism toward the collector for attachment (Elimelech and Song, 1992). Large increases in deposition rates under these electrostatically attractive conditions have been observed for particles with similar diameters as bacteria and protozoan cysts (Elimelech, 1994). Although smaller particles with diameters similar to viruses did not have higher deposition rates, increased virus removal has been observed from electrostatic attraction (Foppen et al., 2006; Ryan et al., 2002). Thus, filter media with a net positive surface charge may enhance the removal of bacteria and viruses. A collector's hydrophobicity is also influenced by the collector's surface characteristics. Silica sand, typically containing low organic carbon content, has low surface hydrophobicity (Abit et al., 2012). Microorganism surfaces also have low hydrophobicity, but specific surface proteins on virus capsids (Gerba, 1984) and outer proteins and surface fibrils on bacteria membranes (Rosenberg and Kjelleberg, 1986) may have hydrophobic regions exposed to the surrounding solution. Thus, if the filtration media's hydrophobicity were to increase, the attachment efficiency of a microorganism could potentially increase by interaction between these surface proteins and the hydrophobic collector.

Two methods for producing a net positive surface charge on filter media are: (1) covalently binding a positively charged functional group, such as a quaternary nitrogen group; or, (2) adding minerals with positive surface charge, such as iron oxides. The first method can be achieved by binding quaternary ammonium silanes (QAS) to silica sand media as shown in Figure 1.4. The condensation reaction produces covalent bonds between the silica surface and QAS molecules and creates links between adjacent QAS molecules. If the QAS density on the silica sand surface is high enough, the N^+ atoms can alter the silica sand surface to exhibit a net positive charge.

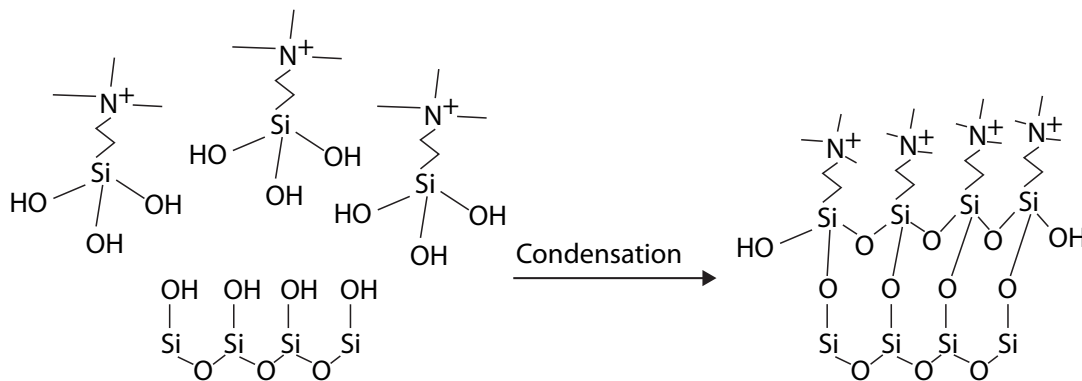
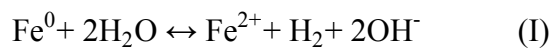
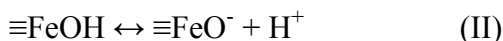
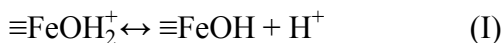


Figure 1.4 – Net positive surface charge on silica media by attaching QAS molecules.

The second method involves the addition of iron oxides by mixing zero valent iron (ZVI) with silica media. In the presence of water, ZVI corrodes due to the following reactions in (I) anoxic and (II) oxic environments:



After ZVI oxidation, ferrous iron (Fe^{2+}) further oxidizes to form amorphous ferric iron (Fe^{3+}) hydroxides, which may then change into other stable iron oxides and/or iron oxyhydroxides (Furukawa et al., 2002; Noubactep, 2010). The positive surface charge arises from the presence of these iron hydroxides, iron oxides, and iron oxyhydroxides from the following acid/base chemistry:



While typical filter media, like sand and soil, has a point of zero charge (PZC) between 2 – 5, iron oxides have PZCs ranging between 5 – 9 (Kosmulski, 2011). Hence, at pH 7, any iron hydroxide, iron oxide, or iron oxyhydroxide with a PZC above 7 will have a positive charge while sand will have a negative charge (Harvey and Ryan, 2004). At high enough concentrations, these iron oxides can thus change the surface charge from net negative to net positive.

Hydrophobicity in silica sand media can be increased by adding hydrophobic amendments such as biochar. Biochar is a stable organic carbon material created when biomass, typically wood chips, manure, or municipal solid waste, is heated at high temperatures (300 – 1000°C) in the absence of oxygen (Xie et al., 2015). This process produces a material with high surface areas, microporosity, and hydrophobic surfaces. When added to silica sand at a 5% by weight ratio, biochar can increase the organic carbon content by 4% and subsequently increase the filter media's hydrophobicity (Mohanty et al., 2014).

Dissertation Research Objectives

Enhanced filtration with media amendments can best be applied in distributed systems where filters are the only treatment barrier and require high pathogen removal. Two opportunities fulfilling these requirements have been identified. The first opportunity concerns drinking water treatment in low-income communities at the household scale. In response to endemic diarrhea from unsafe WASH practices, household water treatment and safe storage (HWTS) has been introduced to reduce exposure to pathogenic organisms in drinking water. The WHO has recommended removal targets between 2 – 3 log of bacteria, viruses, and protozoa for a HWTS option to be considered protective (WHO, 2011). Current HWTS options, however, are not effective against all types of pathogens, may conflict with local consumer preferences, require long ripening times, and entail high user input. For example, biosand filters have been observed to remove both bacteria and viruses, but long ripening times are required to acquire the necessary microbial activity for removal (Wang et al., 2014). Other options, such as chlorination, leave an undesired aftertaste and can require long contact times for protozoan cyst removal (Sobsey et al., 2008). Point-of-use (POU) filters, however, can address these issues with enhanced filtration media. These filters are designed as a dual-chamber device that can hold up to 20 liters. Untreated water is poured into the top chamber, and water drains via gravity through a replaceable treatment cartridge into the bottom chamber for consumption (Kols, 2010). With enhanced filtration media, the treatment cartridge can operate like a rapid sand filter in that larger diameter media can maintain higher flow rates and microorganism removal can occur by adsorption along the cartridge's depth.

The goal of the first part of this dissertation (Chapter 2) was to investigate whether a QAS-coated silica media could improve bacteria and virus removal in a POU filter. An 18-carbon QAS molecule was selected for this coating for both its positively charged ammonium group and hydrophobic alkyl carbon chain. Furthermore, QAS compounds have been used extensively as disinfectants and antiseptics due to their antimicrobial properties (Fraise et al., 2008). QAS-coated sand was packed into columns and exposed to a wide range of influent water chemistries and microorganisms. Specific objectives included:

- Quantify the quaternary ammonium coverage of silica media and determine whether QAS-coated media exhibited antibacterial properties.
- Evaluate QAS-coated sand removal of indicator bacteria, indicator viruses, and human viruses in short-term column experiments.
- Compare observed removal in QAS-coated sand to predicted removal from a filtration model.
- Determine the impact of influent water quality, including ionic strength and natural organic matter (NOM), on QAS-coated media performance.
- Evaluate the effectiveness of a prefilter with powdered activated carbon (PAC) in source water with NOM to determine if a multistage filter improves performance.

The second opportunity concerns stormwater treatment in bioretention basins in the U.S. Bioretention basins contain a top layer with plants and mulch, an underlying layer filled with a mixture of sand and compost (conventional bioretention media; CBM), and a bottom storage layer containing gravel. Stormwater is pooled above the top layer and then slowly filters through the CBM to either infiltrate the groundwater or discharge to a storm sewer via an underdrain. Bioretention basins were originally intended to reduce the frequency of combined sewer overflows by reducing peak storm flow rates, but subsequent studies have also observed water quality improvements after infiltration through the CBM (Davis et al., 2009). Laboratory CBM column studies with synthetic stormwater have demonstrated their potential for pathogen removal, reporting increased *E. coli* removal with time up to 3-log (Zhang et al., 2011). Little work, however, has been conducted on removal mechanisms to explain why removal increases with time or what impact the microbial community has on removal. Furthermore, enhanced filtration media, in the form of ZVI or biochar amendments, may be able to increase indicator bacteria and virus removal in these basins in short-term experiments and over numerous storm seasons. ZVI amendments have been shown to improve heavy metal (Rangsivek and Jekel, 2005) and phosphate (Erickson et al., 2012) removal from stormwater, but no study to our knowledge has been conducted on indicator organisms. Biochar has been observed to increase FIB removal in short-term studies (Abit et al., 2012; Mohanty et al., 2014; Mohanty and Boehm, 2014), but no work has been published on longer-term experiments or indicator viruses.

The goal of the second part of the dissertation (Chapters 3 – 6) was to investigate removal mechanisms in CBM media and evaluate the performance of ZVI and biochar amendments during longer-term experiments. A 46-week experiment, in which 40 columns with different media were injected with stormwater once per week, was conducted to determine the effectiveness of ZVI amendments. A 75-day experiment in which columns were operated like biosand filters (injected with stormwater that was allowed to rest in the filter media for 24 h) was conducted to determine whether rest periods and ZVI or biochar amendments could improve

indicator organism removal. Specific objectives included:

- Track indicator organism removal in CBM media with age and investigate whether microbial activity contributes to removal in CBM media.
- Evaluate the effectiveness of ZVI amendments in removing indicator bacteria and viruses in short-term (1 storm over 1 week) and long-term (46 storms over 46 weeks) experiments.
- Determine whether rest periods can improve indicator bacteria and virus removal in CBM media and media with ZVI and biochar amendments.

Dissertation Overview

This dissertation is divided into two parts. The first part focuses on drinking water treatment at the household scale, and the second part examines stormwater treatment in bioretention basins. The second part on stormwater is further divided into two parts to describe separate long-term column experiments.

Part 1 of this dissertation (Chapter 2) includes a detailed investigation into the use of a quaternary ammonium compound (QAC) to create an anti-microbial filter media for use in a POU-filter in low-income countries. A quaternary ammonium silane (QAS) was covalently bonded to silica media and evaluated for indicator bacteria, indicator virus, and human virus removal in short-term column experiments. Anti-bacterial properties were also investigated using live/dead stains. The findings demonstrated higher removal of both bacteria and viruses than plain sand, but fouling occurred quickly in the presence of humic acid and low removal was observed of specific viruses (PRD1 and Adenovirus 2).

Part 2 of this dissertation includes a description of two stormwater experiments. Part 2A (Chapters 3, 4, and 5) describes a 46-week experiment designed to investigate indicator bacteria, virus, and phosphate removal from stormwater in unsaturated columns packed with CBM and media with ZVI amendments. Chapter 3 introduces the experiment and explains the materials and methods developed for the experiment. Chapter 4 reports results from columns packed with CBM. Chapter 5 reports results from the columns packed with ZVI-amended media. The findings demonstrated the importance of aging, clogging, and biofilm activity for *E. coli* removal in CBM. The ZVI-amended media increased *E. coli* and MS2 removal as compared to silica sand for 11 weeks. *E. coli* and MS2 removal reduced afterwards due to interference from organic matter, phosphate, and other microorganisms.

Part 2B (Chapter 6) includes a final experiment investigating a pulsed, effluent controlled bioretention basin design with ZVI and biochar amendments. Columns were injected daily for 75 days, and the biochar-amended media performed the best of all media types.

The implications of this research and future work are discussed in the Conclusion section (Chapter 7).

Part 1 – Drinking Water Treatment

Chapter 2: Investigation of Quaternary Ammonium Silane (QAS)-coated Sand for the Removal of Bacteria and Viruses in Point-of-Use (POU) Filters

The following chapter is adapted from Torkelson et al. (2012) Investigation of quaternary ammonium silane (QAS)-coated sand filter for the removal of bacteria and viruses from drinking water. *Journal of Applied Microbiology*. 113(5), 1196-1207, with permission from Allegra K. da Silva, David C. Love, Jee Yeon Kim, John P. Alper, Brian Coox, Jeff Dahm, Peter Kozodoy, Roya Maboudian, & Kara L. Nelson. Copyright 2012, The Society for Applied Microbiology

Introduction

Unsafe drinking water, sanitation, and hygiene (WASH) practices contribute to the global disease burden, increasing the number and severity of infectious diseases. Low-income countries bear the largest disease burden from unsafe WASH, which is the 2nd leading risk factor for disability-adjusted life years (DALYs) and 4th leading risk factor for mortality (WHO, 2009). The greatest concern with unsafe water and sanitation practices is highly endemic diarrhea (Clasen et al., 2007). Diarrhea is particularly dangerous for children under five, accounting for nearly 5.5% of overall deaths (Prüss-Ustün et al., 2014). The United Nations is addressing unsafe WASH related DALYs through the Millennium Development Goals (MDGs), targeting a 50% reduction in people without access to improved water sources and sanitation by 2015 (1990 baseline). In 2015, however, 663 million people still lacked access to improved water sources, a figure that does not account for the water quality of the supply. 80% of this population currently resides in rural settings beyond the reach of urban centralized water treatment (WHO, 2015).

Household water treatment and safe storage (HWTS) has been introduced as part of the solution to provide safe drinking water around the globe. HWTS seeks to provide users with the means to treat unsafe water at the point of use (POU), and prevent recontamination during storage. In 2007, HWTS was estimated to reach 18.8 million users, employing boiling, chlorination, ceramic filtration, solar disinfection (SODIS), and biosand filtration (Clasen, 2009). Several meta-analyses evaluating the effectiveness of water quality interventions have reported HWTS to be effective in reducing the overall incidence of diarrhea by about 30% (Fewtrell et al., 2005; Arnold and Colford, 2007; Clasen et al., 2007; Waddington et al., 2009), and 42% in children under five (Waddington et al., 2009). Due to the effectiveness of water quality interventions, the World Health Organization (WHO) has called for a scale-up of HWTS (Clasen, 2009). While current HWTS technology has proven effective at reducing diarrheal disease incidence, further technology development and consumer preference research is still necessary to improve pathogen removal and increase adoption. The current HWTS options are not effective against all types of pathogens (e.g. chlorination against protozoan cysts, ceramic and biosand filters against viruses), may leave undesirable aftertastes (chlorination), or require extensive time (SODIS)

(Sobsey et al., 2008). An ideal HWTS would provide high levels of removal or inactivation of waterborne viruses, bacteria, and protozoan cysts (WHO, 2011), be affordable and readily available, reflect user preferences, and require little user input and training.

The purpose of this research was to investigate the ability of quaternary ammonium compounds (QACs) immobilized on granular media to remove bacteria and viruses. QACs are a group of chemicals known for their antimicrobial properties. These compounds have been studied and used as disinfectants and antiseptics in hospitals for nearly a century, are available off patent, and cost very little (Fraise et al., 2008). QACs are surfactants consisting of a positively charged nitrogen atom with four alkyl chain substituents, providing both hydrophilic and hydrophobic regions. In solution, QACs' antimicrobial activity is attributed to membrane/envelope disruption by the charged nitrogen atom and hydrophobic alkyl chain (Gilbert and Moore, 2005). The efficiency is dependent upon the alkyl chain length (Gilbert and Al-taa, 1985; Daoud et al., 1983), microorganism (Maillard, 2002), and contact time (Nakagawa et al., 1984).

Quaternary ammonium silanes (QAS) are a silanized version of QAC that can covalently bond to hydroxylated surfaces such as silica sand; the coatings are reported to be further stabilized by cross-links between QAS molecules (Witucki, 1993). Prior research reports that while tethered QAS molecules have limited movement, antimicrobial activity still occurred without entrance into the cell (Isquith et al., 1972), and surface immobilization did not impede the ability of QAS molecules to disrupt cell walls (Brizzolara and Stamper, 2007). High concentrations of surface bound QAS molecules were capable of causing cell membrane disruption by inducing cation exchange with calcium ions (Kügler et al., 2005; Murata et al., 2007). In addition, the positively charged nitrogen atom and hydrophobic chains facilitate removal of microorganisms by attachment to the coated surfaces through hydrophobic and electrostatic interactions. It is expected that these enhanced interactions, however, may be compromised under the water quality conditions in typical water supplies. Prior studies have shown promising results for the removal of *Escherichia coli* (*E. coli*), MS2 coliphage, and *Cryptosporidium parvum* oocysts with QAS-coated zeolite filters (Abbaszadegan et al., 2006).

In Part 1, we evaluated the ability of QAS-coated sand media to remove bacteria and viruses under conditions relevant to point-of-use (POU) water treatment. We report on experiments demonstrating the microorganism removal performance under different solution chemistries, flow rates, and the antibacterial activity of QAS-coated sand.

Materials and Methods

A quaternary ammonium silane (QAS) was coated onto silica sand and evaluated as a filtration media in column experiments. Columns were packed with the QAS-coated media and challenged to evaluate the removal of bacteria (*E. coli*), bacteriophage (MS2 and PRD1), and human viruses (poliovirus and adenovirus). In addition, the columns were challenged to remove *E. coli* or MS2 under different ionic strengths and in the presence of natural organic matter (NOM). Pre-filters of powdered activated carbon (PAC) were tested with source water containing NOM to determine the effectiveness of a multistage filter.

Escherichia Coli

Escherichia coli F_{amp} (ATCC #700891) were grown the night before each experiment in tryptic soy broth containing 0.015 g/L of ampicillin and streptomycin. A frozen *E. coli* F_{amp} culture was grown in a 37 °C incubator overnight. This overnight culture was then re-propagated the morning of an experiment to an optical density of 1.0 at a wavelength of 600 nm. *E. coli* were concentrated by centrifugation at 8000 × g for 5 min, the supernatant was discarded, and the pellet was rinsed three times in a 1 × phosphate buffer solution (PBS) solution. The spread plate technique on selective agar containing 0.015 g/L of ampicillin and streptomycin was used to enumerate *E. coli* concentrations in duplicate as colony forming units (CFU) in 100 µL inocula from each sample during column experiments.

MS2 and PRD1 Bacteriophage

MS2 and PRD1 were propagated using broth enrichment (EPA Standard Method 1601) in *E. coli* F_{amp} and *Salmonella typhimurium* LT2, respectively. The bacteriophage plaque assay was conducted using the double agar layer (DAL) method with 100 µL inocula to determine plaque forming unit (PFU) concentrations in duplicate from influent and effluent samples during column studies.

Human Virus and Host Cells

Adenovirus type 2 was obtained from Mark Sobsey (University of North Carolina, Chapel Hill) and Poliovirus type 3 was provided by Alexandria Boehm (Stanford University). Adenovirus type 2 and Poliovirus type 3 were cultured in A549 cells (ATCC CCL-185) and HeLa cells (ATCC CCL-2), respectively. PFU concentrations from column studies were enumerated in duplicate after 6 d of incubation for adenovirus and 3 d of incubation for poliovirus.

Adenovirus type 2 and Poliovirus type 3 were propagated in Corning T-150 flasks. Virus propagation was performed by suctioning off maintenance media (30 mL Dulbecco's modified eagles medium (D-MEM), Invitrogen) followed by inoculating the cell culture monolayer with 2 mL of virus inocula for a multiplicity of infection between 0.01 – 0.1. Flasks were incubated at 37 °C and 5% CO₂ with gentle agitation every 15 min for 60 min to enhance virus attachment and prevent monolayers from drying. Following viral attachment, maintenance media, 10% fetal bovine serum (FBS, Invitrogen) for adenovirus or 2% FBS for poliovirus, and penicillin/streptomycin (100 U/mL final concentration each, Invitrogen) were added to the flasks and incubated until a cytopathic effect was observed. Virus stocks were prepared by freezing and thawing the flasks three times to release intracellular viruses. Cell debris was removed via chloroform extraction (1:3 v:v), centrifugation (4000 × g for 10 min) in 50-mL conical bottom centrifuge tubes (Fisher Scientific), and filtration through a 0.22-µm filter. The virus stocks were stored at -80 °C.

Virus plaque assays were performed in 6-well plates with 100-µL viral inocula in duplicate. D-MEM was used as the diluent followed by the 60-min virus attachment step as above. Following viral attachment, the wells received a 3-mL 0.075% agarose overlay [(low melting agarose,

Fisher Scientific), 2 × MEM diluted to 1 × (Invitrogen), 10% FBS for adenovirus or 2% FBS for poliovirus, and 100 U/mL final concentration of penicillin and streptomycin].

Coating Procedure of QAS-Coated Sand

Silica sand (50-70 mesh, Sigma-Aldrich) was coated with the QAS compound dimethyloctadecyl [3-(trimethoxysilyl) propyl] ammonium chloride (42% w/w methanol solution, Sigma-Aldrich). To remove metal impurities, the sand was soaked in 12 N HCl overnight, and rinsed in MilliQ water until the pH returned to 5.5. Next, the sand was soaked for 8 h in a 1 M NaOH to hydroxylize the SiO₂ surface, and rinsed with MilliQ water until the pH returned to 5.5. The sand was then mixed for 24 h in the coating solution at a 2:3 volume ratio of sand: coating solution. The coating solution was a 1.2% v/v QAS solution in ethanol at pH 3 (pH adjusted with 1 N HCl). After 24 h, the coating solution was drained and the sand was placed in a 100° C oven overnight, rinsed in ethanol for 5 min, and then rinsed three times in DI water for 5 min each. Following the last rinse, the sand was placed in the 100° C oven overnight.

Leaching Assays (Microbial and Bromophenol Blue Methods)

Two approaches, one microbiological and one chemical, were employed to quantify QAS leaching from each batch of coated sand. The leachate solution used in leaching experiments was created by mixing 1 g of QAS-coated sand with 10 mL of MilliQ water in a 15-mL centrifuge vial for 48 h, then recovering the liquid supernatant after centrifugation at 5000 × g for 15 min. In the microbiological approach, equal volumes of *E. coli* (at 10⁵ CFU/mL) and leachate solution were mixed by vortexing five times and allowed to rest for 10 min. A mixture of uncoated sand with the *E. coli* solution was used as a control. The mixture was then diluted and plated for counting. A decrease in the culturable concentration of *E. coli* in the QAS-coated sand mixture greater than the decrease observed in the control was interpreted as evidence of QAS leaching.

The chemical approach involved mixing dilutions of bromophenol blue (BPB) with the leachate solution since an electrostatic complex occurs between QAS and BPB molecules. 2.5 mL of the supernatant was mixed with 2.5 mL of diluted BPB solutions (BPB concentrations of 6×10⁻⁵, 6×10⁻⁶, and 6×10⁻⁷ M). A mixture of uncoated sand with each BPB dilution was used as a control. The mixture was vortexed, the absorbance measured on a UV-VIS spectrometer at 600 nm, and the peak absorbance wavelength recorded. A 1:1 ratio of BPB:QAS was observed to cause a shift in the peak absorption wavelength, such that a BPB solution without QAS had a peak absorption wavelength around 592 nm while a BPB solution with QAS had a peak absorption wavelength near 605 nm. Thus, a shift in the peak absorption wavelength from 592 nm to 605 nm was interpreted as evidence of QAS leaching from the sand batch, and the QAS concentration was estimated to be similar to the minimum BPB concentration necessary to cause a shift in the peak absorption wavelength. QAS-coated sand batches were used in experiments if they: 1) did not cause inactivation of *E. coli* greater than the plain sand control and 2) did not cause a shift in the peak absorption wavelength in the BPB solution containing 6×10⁻⁶ M or higher. It should be noted that there was evidence of leaching in some sand batches that were

not used for further experiments. We were not able to determine what step(s) in the coating process were responsible for producing leaching vs. non-leaching coatings. The QAS compound we used has been tested extensively and found to exhibit low toxicity. Mutagenicity and teratogenicity tests in albino rats were negative and the LD50 was found to be 12.3 g/kg body weight (Du Pont de Nemours and Co, 1992). Assuming this LD50 applies to humans, if the compound was present in water at the detection limit of our BPB leaching assay, a user would need to drink > 200,000 liters in one sitting to reach the reported LD50. Future research should examine whether long-term use of the QAS-coated sand will cause leaching at higher levels.

QAS Coverage of Silica Sand Media Measurement

1 g of coated silica sand was placed in a 15-mL centrifuge tube with 10 mL of bromophenol blue (BPB) dye. The sand/BPB mixture was vortexed five times and rotated overnight to fully coat the sand. The next day, the BPB liquid was discarded and 10 mL of DI water was added, vortexed 6 – 10 times, and discarded. The DI water rinse was repeated five times to remove any excess dye. 10 mL of a soap buffer solution (1.8 L DI water, 0.2 L 1×phosphate buffer solution (PBS), and 40 g dissolved Fischer Sparkleen soap #1) was then mixed with the dyed sand. The soap buffer solution weakened the BPB:QAS complex on the sand surface, releasing BPB back into solution. The sample was centrifuged for 15 min at 8000 × g to remove colloids, and the solution absorbance measured using a UV-VIS spectrometer. The measured absorbance was related to BPB molarity through a standard curve. Each mole of BPB was assumed to correspond to one mole of N^+ . We attempted to measure the silica sand's surface area by obtaining nitrogen adsorption isotherms on an Autosorb 1 (Quantachrome) and then analyzing the data using the Brunauer-Emmet-Teller (BET) method. The coverage data were then converted to surface charge density (N^+/cm^2).

QAS-coated Sand Column Experiments

Filtration columns packed with QAS-coated sand were challenged with various microorganisms and water qualities. The columns were created from 25-mL pipette tubes (1.2 cm diameter) that were cut to the desired length (4.5 – 30 cm depending on the experiment). The column diameter (1.2 cm) to average sand grain diameter (0.25 mm) ratio was 48, a value above a threshold of 30 found to minimize wall effects (Cohen and Metzner, 1981). The columns were packed by wetting the QAS-coated sand with ethanol and then gradually pouring the sand into the column. A hand-held massager was used to enable tight packing. A Masterflex peristaltic pump delivered influent at the desired flow rate (15 and 36 mL/min). Once packed, the column and pump tubing were rinsed with a 70% ethanol solution for 10 min to remove any pre-challenge contamination, followed by 30 min rinse with MilliQ water and 30 min rinse with 1 mM NaCl. The challenge water was spiked with microorganisms ($\sim 10^5$ CFU or PFU/mL) and then introduced for 60 – 120 min with samples taken every 20 – 30 min. Various influent conditions, such as ionic strength (1 mM, 10 mM, and 100 mM NaCl), flow velocity (3.6 m/h, 7.2 m/h, and 18 m/h), and natural organic matter (20 mg/L Fluka humic acid), were then altered to evaluate the effectiveness of the QAS-coated sand media. An equivalent sized column of powdered activated carbon (PAC) was placed before the QAS-coated sand column to evaluate the effectiveness of a dual media filter when NOM was present in the source water (20 mg/L of Fluka humic acid).

Filtration Model Parameters

The parameters used in the filtration model to determine the predicted column removal are included in Table 2.1 (Tufenkji and Elimelech, 2004).

Table 2.1 – Parameters used in the filtration model to predict column removal (Tufenkji and Elimelech, 2004).

Description	Symbol	Units	Value
Diameter of Collector	d_c	mm	0.25
Fluid Approach Velocity	U	m/h	18
Particle Density	p_p	kg/m ³	1050
Fluid Temperature	T	k	298
Porosity	f	-	0.36
Fluid Density	p_w	kg/m ³	997
Boltzmann Constant	K	J/k	1.38×10^{-23}
Dynamic Viscosity	u	Ns/m ²	0.001002
Hamaker's Constant	A	J	1×10^{-20}

Bacteria Membrane Damage/Death from QAS-coated Sand Exposure

Loss of culturability from exposure to QAS-coated sand was assessed with the following assay. 2 g of QAS-coated sand was exposed to 5 mL of a stationary phase *E. coli* suspension. The mixture was vortexed five times and then placed in a 37° C incubator for 24 h. After 24 h, the supernatant was plated to determine whether *E. coli* in the solution had adhered to the sand. The remaining sand was then rinsed with 50 mL of a 170 mM NaCl and 0.5 mM NaHCO₃ salt solution at pH 7. The rinse step with the salt solution was repeated two times. In the final rinse step, a small sample of rinse solution was plated to determine whether the final rinsate contained unbound *E. coli*. Finally, the 2 g of QAS-coated sand was placed in growth media and incubated to observe whether adhered bacteria were culturable. A sample of uncoated sand was used as an experimental control.

Fluorescence Microscopy

Fluorescence microscopy was used to observe bacterial membrane damage from QAS-coated sand exposure. An *E. coli* suspension was exposed to QAS-coated sand for 24 h and then stained with the BacLight Live/Dead kit (Invitrogen) to image cell membrane permeability. Sand grains were placed on a microscope slide for viewing. Cells stained with SYTO-9 were interpreted as membrane-impermeable (potentially viable) and cells stained with propidium iodide (PI) were interpreted as membrane-permeable (dead or damaged) cells.

Results

QAS Coverage and Coating Stability on Silica Sand Media

The QAS coverage of the silica sand media, represented as the surface charge density (N^+/cm^2), is shown in Figure 2.1. The charge density was calculated by dividing the total moles of N^+ by the surface area of the sand. However, the measured surface area was below the detection limit for the BET analyzer; thus, the approximate detection limit of $0.1 \text{ m}^2/\text{g}$ was used for the calculations. The different sands labeled in Figure 1 (Q206, Q208, Q213, Q215, and Q216) refer to the batches of QAS-coated sand used in the experiments reported here. The surface charge density in the batches ranged from 6×10^{13} – $1 \times 10^{14} \text{ N}^+/\text{cm}^2$. A surface charge density threshold for bactericidal activity has been suggested at $10^{12} \text{ N}^+/\text{cm}^2$ for *E. coli* in a dividing state and $10^{14} \text{ N}^+/\text{cm}^2$ for *E. coli* in a stationary state (Kügler et al., 2005). $10^{15} \text{ N}^+/\text{cm}^2$ has also been reported as a surface charge density threshold for antibacterial surfaces (Murata et al., 2007). Thus, we estimate that the QAS-coated sands exhibited charge densities at or just below threshold values determined by Kügler et al. (2005), and below the value determined by Murata et al. (2007). However, the actual charge density is likely underestimated because the surface area of the sand may be lower than what was assumed for the calculation.

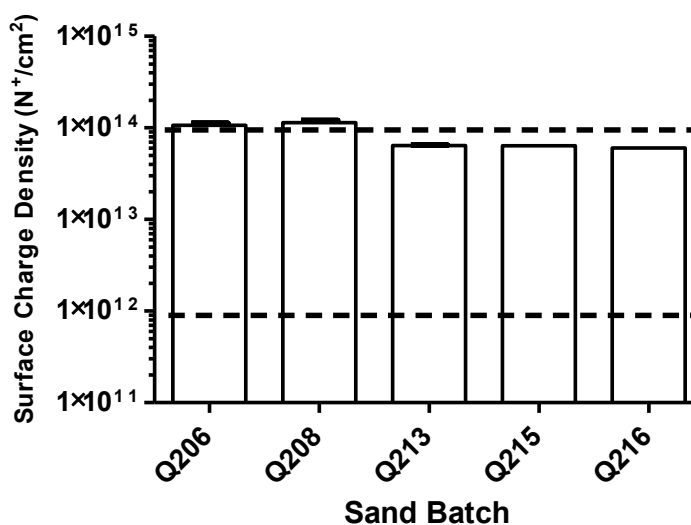


Figure 2.1 – Estimated surface charge density of QAS-coated sand batches used in column experiments. Dotted lines show the charge density thresholds reported by Kügler et al. (2005). Error bars report two standard deviations, and reflect only the variability in the measurement of the coating concentration. As described in the text, it was not possible to estimate the variability of the surface area of the sand.

In addition to verifying the coating density of each batch of sand used for experiments (Figure 1), each batch was tested for leaching using an *E. coli* bioassay and a bromophenol blue assay, and only sand batches that did not leach were used for experiments. These results are included in Figure 2.2 and Table 2.2.

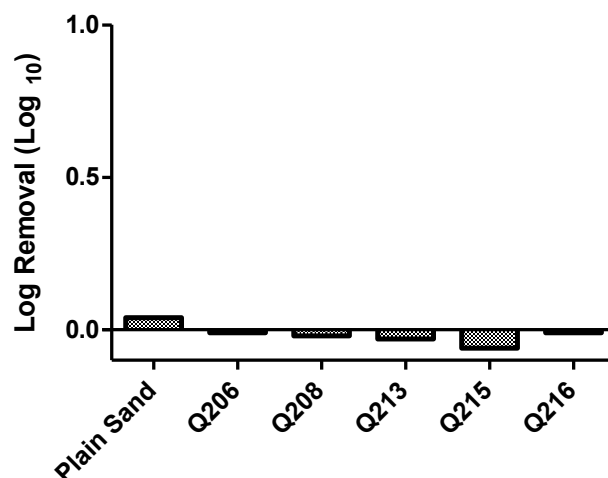


Figure 2.2 – Microbial Leach Assay Results. The columns represent the die off of *E. coli* when exposed to MilliQ water exposed to QAS-coated sand. Plain silica sand was used as the control. A decrease in *E. coli* concentration above the control was considered evidence of QAS leaching.

Table 2.2 – Bromophenol Blue (BPB) Leaching Assay. A 1:1 molar ratio of BPB:QAS in solution was observed to cause a shift in peak absorption wavelength. Standard BPB solutions without QAS had a peak wavelength around 591 nm, and standard solutions with 1:1 ratio of BPB:QAS had a peak wavelength around 604 nm.

Sample	BPB Dilution	BPB Concentration (M)	Peak Wavelength (nm)
Plain Sand	0.1	6.E-05	591
	0.01	6.E-06	591
	0.001	6.E-07	591
Q206	0.1	6.E-05	591
	0.01	6.E-06	591
	0.001	6.E-07	592
Q208	0.1	6.E-05	591
	0.01	6.E-06	593
	0.001	6.E-07	604
Q213	0.1	6.E-05	591
	0.01	6.E-06	591
	0.001	6.E-07	591
Q215	0.1	6.E-05	591
	0.01	6.E-06	591
	0.001	6.E-07	592
Q216	0.1	6.E-05	591
	0.01	6.E-06	591
	0.001	6.E-07	593

QAS-coated Sand Column Studies

The results from clean bed filtration experiments using QAS-coated sand challenged with *E. coli* and several viruses are summarized in Table 2.3. Clean bed filtration refers to the initial microorganism removal of a packed column before the surface was altered by significant accumulation of particles. Samples for quantifying clean bed removal were collected within four pore volumes of starting a challenge. The log removal of *E. coli* and MS2 was similar, and increased approximately linearly as the height of the coated sand columns increased, consistent with filtration theory. For example, a 9-cm column achieved 1.7-log removal of *E. coli* while the 18-cm column achieved roughly double this log removal value, or 4.1-log removal. No difference in log removal of *E. coli* was observed between the 18-cm and 30-cm columns because *E. coli* were removed to the detection limit in both experiments. The clean bed removals of PRD1, Poliovirus 3, and Adenovirus 2 were investigated with a single column length. Poliovirus 3 removal in a 9-cm column was similar to the removal of MS2. In contrast, clean bed removals of bacteriophage PRD1 and Adenovirus 2 were much lower, with observed removals of 1.2-log in an 18-cm column and 0.36-log in a 9-cm column, respectively.

Table 2.3 – Clean bed removal of *E. coli*, MS2, PRD1, Poliovirus 3, and Adenovirus 2 by QAS-coated sand columns at an ionic strength of 1 mM NaCl and filtration velocity of 18 m/h. Dashes in the standard deviation column indicate the microorganisms were removed to the detection limit in each experiment. The standard deviation was calculated based on duplicate influent and effluent samples taken from a single column experiment at 2 min. Column tests conducted with different batches of sand resulted in similar log removal levels.

	Column height (cm)	Challenge concentration (CFU/mL or PFU/mL)	Effluent concentration (CFU/mL or PFU/mL)	Log removal (CFU/mL or PFU/mL)	Standard Deviation of Log removal
<i>E. coli</i>	4.5	5.2×10^4	2.2×10^3	1.4	0.045
	9	6.9×10^4	1.5×10^3	1.7	0.087
	18	1.1×10^5	< 9.0	> 4.1	-
	30	1.1×10^5	< 9.0	> 4.1	-
MS2	9	3.8×10^7	5.9×10^5	1.8	0.058
	18	2.4×10^5	< 9.0	> 4.4	-
PRD1	18	3.0×10^5	2.0×10^4	1.2	0.011
Poliovirus 3	9	1.3×10^5	1.5×10^3	1.9	0.10
Adenovirus 2	9	1.8×10^6	7.8×10^5	0.36	0.092

In Figure 2.3, the observed clean bed removal from column experiments was compared to the predicted clean bed removal using the filtration model presented by Tufenkji and Elimelech (2004). In the model, the attachment coefficient (α) was assumed to be one. The comparison was conducted with observed clean bed removal data from 18-cm columns for *E. coli*, MS2, and PRD1. For *E. coli* and MS2, the predicted clean bed removals were significantly lower than the observed removals (0.37 log versus 4.1 log for *E. coli*, and 1.5 log versus 4.4 log for MS2). The predicted and observed removals of PRD1, however, were much closer to the observed removal (0.92 log versus 1.2 log).

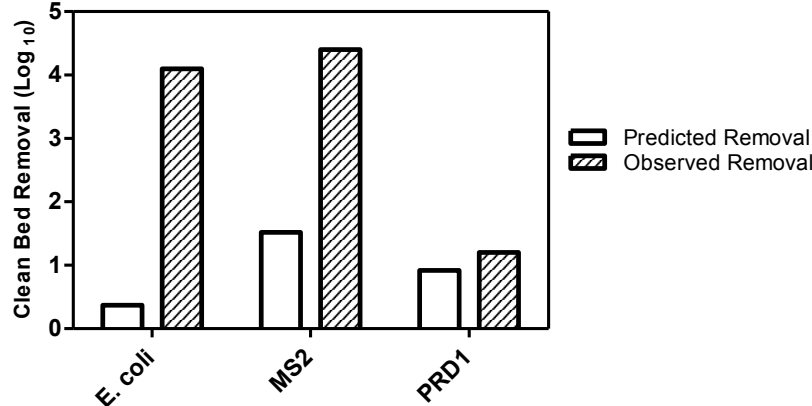


Figure 2.3 – Comparison of the predicted removal from the filtration model (Tufenkji and Elimelech, 2004) and the observed clean bed removal in QAS-coated sand columns. Columns for the *E. coli*, MS2, and PRD1 experiments were 18 cm.

The removal of *E. coli* and MS2 by QAS-coated sand as a function of ionic strength (IS), flow rate (*E. coli* only), and in the presence of NOM (Fluka humic acid) is shown in Figure 2.4. The removal of both *E. coli* and MS2 was higher in 1 and 10 mM NaCl solutions compared to 100 mM NaCl (Figure 2.4A). A decrease in removal over time was observed for both *E. coli* and MS2, likely because the positively charged sites on the QAS-coated media became covered by microorganisms. The removal of *E. coli* increased as the filtration velocity decreased from 18 m/h to 3.6 m/h (Figure 2.4B). This trend follows expected behavior from filtration theory. Slower flow velocity is expected to increase removal due to longer transport times and lower hydrodynamic forces. In addition, *E. coli* removal decreased over time more quickly at 18 m/h than at 7.2 m/h (it is not possible to compare to 3.6 m/h because three of the data points were at the detection limit). The removals of *E. coli* and MS2 in the presence of 20 mg/L of humic acid dropped dramatically by 20 min in the QAS-coated columns, to levels comparable to uncoated silica sand columns challenged without humic acid (Figure 2.4C). The humic acid likely competes with *E. coli* and MS2 for positively charged attachment sites on the media's surface. In addition, the humic acid may coat the microorganisms, altering their surface characteristics and further decreasing attachment (Yuan *et al.*, 2008; Pham *et al.*, 2009). By preceding the QAS-coated sand column with a PAC pre-filter, the dual media column was capable of removing *E. coli* in 20 mg/L of humic acid to the detection limit for 120 min (Figure 2.4D). For MS2, the PAC pre-filter and QAS-coated sand column fouled completely by 120 min when challenged with 20 mg/L of humic acid. However, this performance was greatly improved over a single QAS-coated sand column challenged with humic acid, which failed within 30 min.

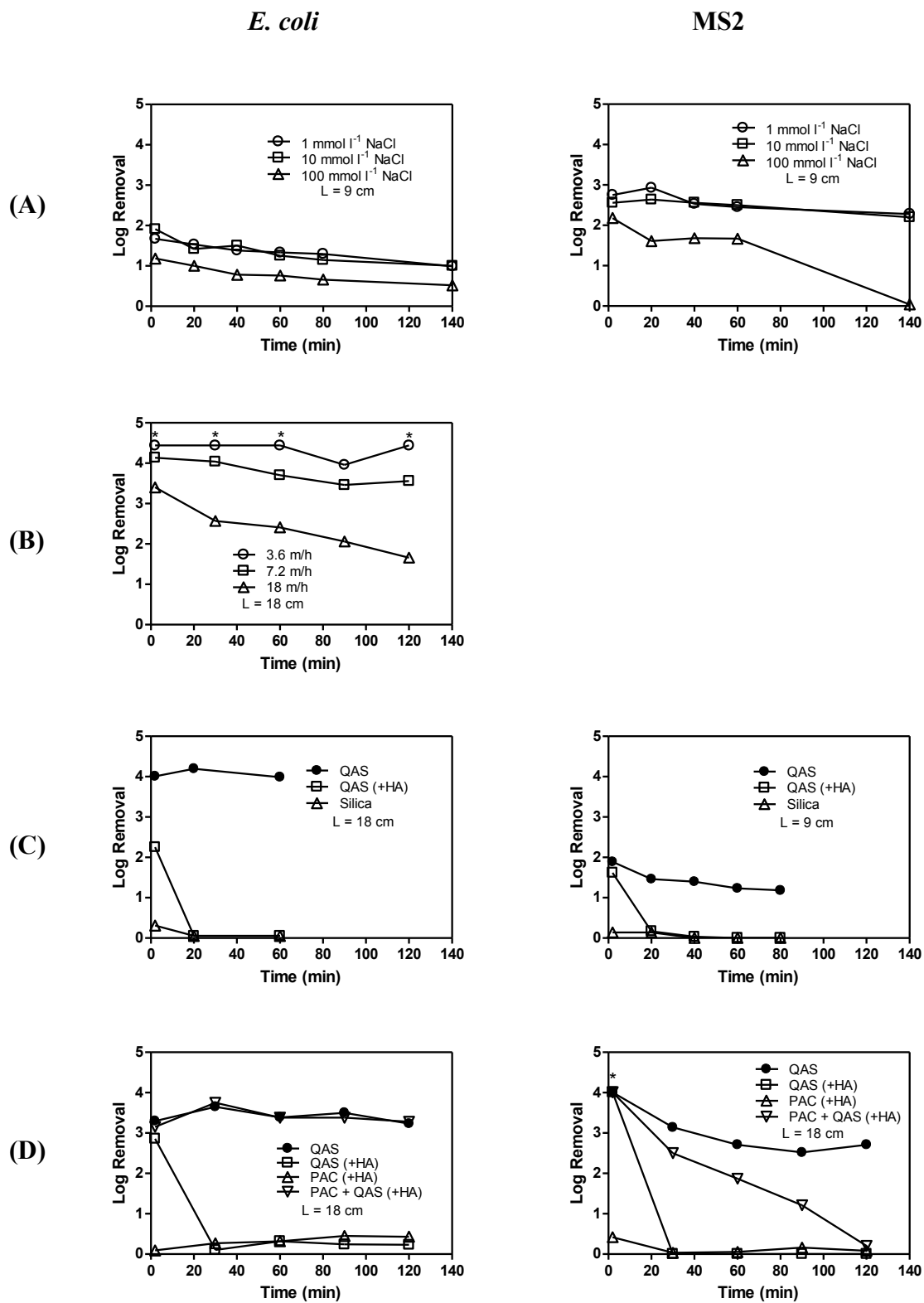


Figure 2.4 – Removal of *E. coli* and MS2 by QAS-coated sand as a function of (A) ionic strength, (B) flow velocity, (C) presence of 20 mg/L humic acid (in 1 mM NaCl), and (D)

presence of powdered activated carbon (PAC) pre-filter to remove Fluka humic acid. The flow velocity in each column test was 18 m/h unless otherwise indicated. Column lengths for each experiment are indicated on each graph. An asterisk indicates that the removal was equal to or greater than the detection limit of the assay.

Loss of Culturability and Membrane Damage due to QAS-coated Sand Exposure

The qualitative results from the *E. coli* antibacterial assay are reported in Table 2.4. Following exposure to 10^4 CFU/mL of *E. coli* for 24 h and rinsing with a salt buffer, uncoated sand that was placed in a growth media showed growth of *E. coli*, whereas no growth was observed for the coated sand. The observed growth after exposure to the uncoated sand may be attributed to residual *E. coli* in the pore water, since *E. coli* were present in the supernatant after the final rinsing step. Conversely, no active *E. coli* were present in the pore water or rinsate after exposure to QAS-coated sand. These results suggest the *E. coli* adhered to the QAS-coated sand media were inactivated.

Table 2.4 – *E. coli* in pore water and regrowth on sand grains. Sands were exposed to *E. coli* by tumbling for 24 h, followed by rinsing. Rinsed sand was re-introduced to growth media to detect *E. coli* regrowth.

Media	<i>E. coli</i> in Exposed PBS (CFU/mL)	<i>E. coli</i> in Supernatant After Rinsing (CFU/mL)	<i>E. coli</i> Regrowth in Media with Rinsed, Pre-exposed Sand		
			A	B	C
Uncoated sand (control)	590	120	+	+	+
QAS-coated sand	0	0	-	-	-

Further qualitative evidence of bacterial membrane damage is presented in Figure 2.5. A representative field of view is shown in which the sand grains are visible under bright field microscopy and stained bacteria are visible using fluorescence microscopy. No bacteria were visible on the uncoated sand, suggesting that minimal adherence of *E. coli* occurred, consistent with the column studies. On the coated sand, however, bacteria stained with both PI and SYTO-9 were visible, indicating that adhesion occurred, and that some *E. coli* became membrane permeable. The presence of these dead or damaged *E. coli* cells on the QAS-sand surface provide evidence that the QAS coated surface has antimicrobial properties. We confirmed that the vast majority of bacteria in the *E. coli* stock solution before exposure to QAS-coated and uncoated sands were intact and not permeable to PI.

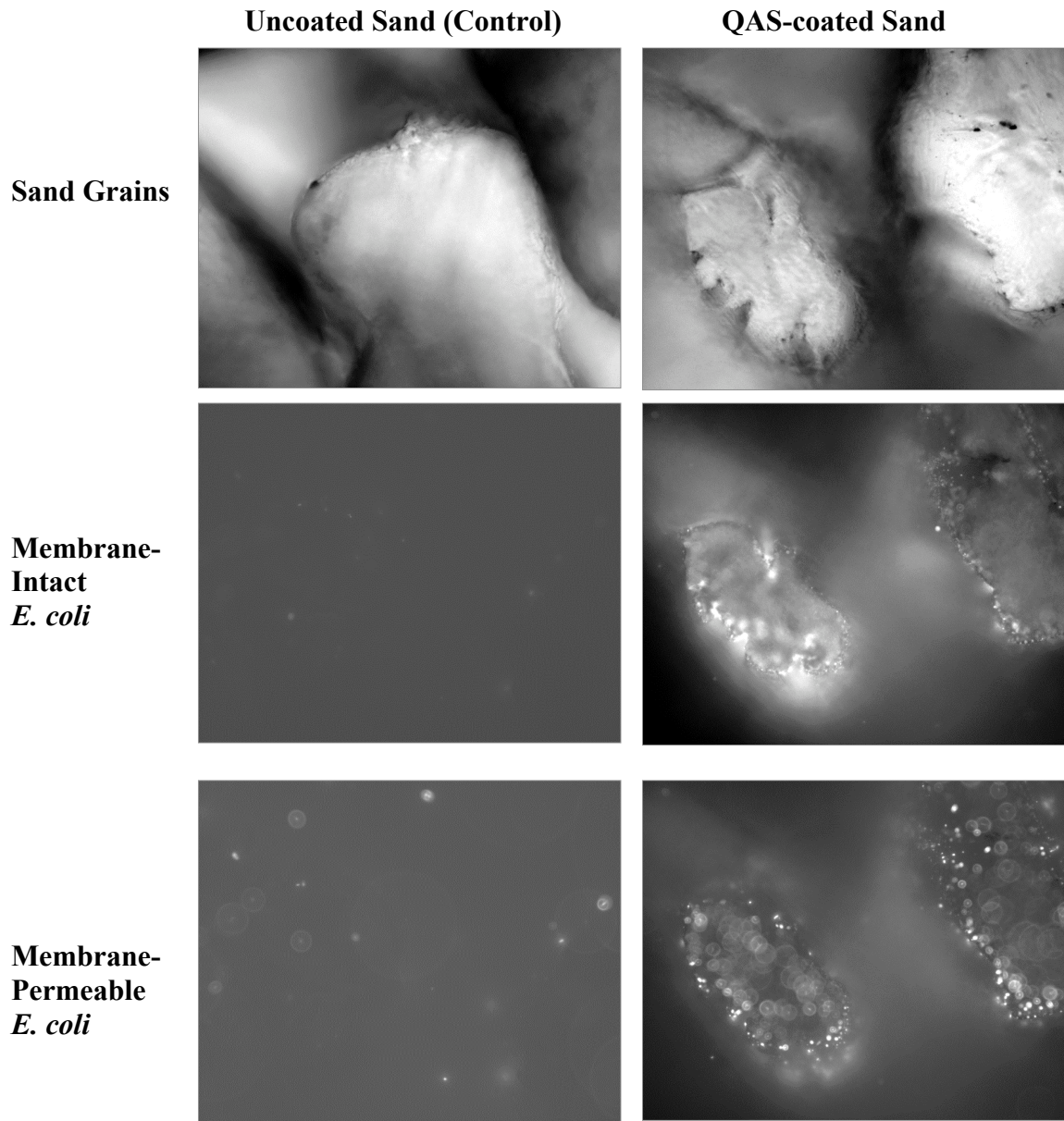


Figure 2.5 – Fluorescence microscopy images of QAS-coated sand exposed to *E. coli*. *E. coli* were stained with SYTO-9 to image membrane-impermeable (live) cells and PI to image membrane-permeable (dead) cells.

Discussion

The results from this study demonstrate the effectiveness of fresh QAS-coated silica sand as a filtration medium for treating pure water solutions containing viruses and bacteria. However, the results also highlight major shortcomings of the media that need to be addressed before it can be recommended for use in a HWTS device.

The surface charge density measurements seem to return reasonable values ($6 \times 10^{13} - 1 \times 10^{14} \text{ N}^+/\text{cm}^2$; Figure 1). Assuming the Si-O-Si bond is about 0.161 nm (Baur, 1977) each QAS molecule would occupy approximately 0.026 nm^2 if cross-linking was complete, and the theoretical charge density limit for a homogeneous monolayer would be around $4 \times 10^{15} \text{ N}^+/\text{cm}^2$. This calculation assumes the quaternary ammonium groups do not limit the coating density due to steric hindrance or electrostatic repulsion. The experimentally determined coating density of γ -aminopropyltrimethoxysilane, a primary amine QAS with a one-carbon alkyl chain, was found to be on the order of about $10^{14} \text{ N}^+/\text{cm}^2$ when deposited in the vapor phase (Ek et al., 2003). Vapor phase deposition is known to yield well-formed, dense monolayers of methoxy silanes. Thus, our estimate of the coating density on sand suggests that it is at the upper limit for a monolayer. However, the coating on sand may not exist as a monolayer. We attempted to characterize QAS coatings using the same coating chemistry on planar surfaces using AFM, contact angle measurements, and ellipsometry. These measurements suggested that the coatings were very heterogeneous and included clumps (Alper, 2010). Thus, it is possible that the surface coatings on sand were characterized by areas of high charge density where the QAS existed in clumps with cross-linking chains extending from the surface, and other areas with low or no coverage.

We also used a conservative measurement of the sand's surface area. The BET analysis conducted to determine the silica sand's surface area returned the result that the surface area was less than $0.1 \text{ m}^2/\text{g}$. A surface area of $0.1 \text{ m}^2/\text{g}$ was used in the estimate, but the sand's actual surface area may be lower. A perfect sphere of sand with diameter 0.25 mm has a theoretical surface area of $0.014 \text{ m}^2/\text{g}$ (Blott et al., 2004). Therefore, the average surface charge density of the QAS-coated sand may actually be higher than our estimate of about $10^{14} \text{ N}^+/\text{cm}^2$. A higher coating density, or patches with higher density, would contribute to greater bactericidal activity according to reports in the literature on threshold charge densities, which range from $10^{12} - 10^{15} \text{ N}^+/\text{cm}^2$ (Kügler et al., 2005; Murata et al., 2007). It should be noted that these threshold values were determined for quaternary ammonium architectures employing polymer brushes, which may have other characteristics that contribute to their bactericidal properties as well.

The results from the *E. coli* regrowth test in Table 3 demonstrate that the coated sand has at least some bactericidal activity. The pre-exposed QAS-coated sand did not allow bacteria regrowth in a growth media, implying the bacteria adhered to the surface were inactivated. More qualitative evidence of antibacterial activity was observed with the PI stain. Some bacteria adhered to the QAS-coated sand particle were shown to be permeable to PI, suggesting the cells were dead and/or damaged. A similar experiment could not be conducted, however, on viruses. Not much is known about the effectiveness of QAS compounds on non-enveloped viruses, although some efficacy was observed against MS2 in solution. While a QAS concentration as low as 10^{-5} M was observed to cause a 0.91-log reduction of MS2, it remains unclear whether these results were from inactivation or aggregation (data not shown). Natural iron oxide surfaces on sand (which are also positively charged) have been reported to cause inactivation of MS2 and PRD1, but the time scale (~ 30 days) was much longer than that used in our experiments (Ryan et al., 2002).

The QAS-coated sand media demonstrated high removal of *E. coli*, MS2, and Poliovirus 3.

Importantly, the removal was much higher than the predicted values from the filtration model for *E. coli* and MS2 (Tufenkji and Elimelech, 2004). This increased removal was likely due to attractive double layer interactions between the sand media and microbe. At low ionic strength, the attractive double layer extends over larger distances and is responsible for the increased transport of colloids onto the collector surface. In fact, small particles are capable of changing their trajectory in a filter toward collectors when encountering attractive electrostatic forces (Elimelech and Song, 1992). At higher ionic strengths, removal was lower due to the effect of charge shielding at the highest IS. Based on the results of a theoretical modeling, Elimelech and Song (1992) reported that deposition rates of particles onto an oppositely charged collector exhibit a strong dependence on IS and suggested a critical IS value of 1 mM. Below this critical value, the electric double layer's range expands with decreasing IS. Thus, attractive electrostatic interactions would be expected to enhance transport of the net negatively charged microorganisms to the net positively charged coating. Above this critical IS value, however, the electric double layer is compressed considerably and electrostatic attraction is not expected to enhance transport (Elimelech and Song, 1992). In experimental studies with ionic strengths ranging from 20 – 200 mM, Yuan et al. (2008) found no change in the deposition rate of MS2 onto a positively charged poly-L-lysine (PLL) layer. In addition, Pham et al. (2009) observed no increase in the deposition rate of MS2 onto a PLL layer in solutions with IS between 0.3 – 3 mM. Together, these studies suggest removal should be similar throughout an IS from 0.3 – 200 mM. In contrast, we observed lower removal of *E. coli* and MS2 at 100 mM than at 1 and 10 mM. One important difference is that our experiments were conducted with a monovalent cation (Na^+), whereas the Yuan et al. (2008) and Pham et al. (2009) studies were conducted with divalent cations (Ca^{2+} and Mg^{2+}). Pham et al. (2009) suggest that divalent cations may undergo specific interactions with carboxylate groups on virus surfaces, so that the effect of the cations cannot be explained simply by electrostatic interactions. The Yuan et al. (2008) and Pham et al. (2009) studies were also conducted with single layer, planar, positively charged surfaces, whereas our experiments used columns packed with net positively charged sand. In the coated porous media the microorganisms experience a complex and heterogeneous environment, in which ions may alter many types of surface interactions.

In this study, removals of PRD1 and Adenovirus 2 were much lower than removals of MS2 and Poliovirus 3. The relative removals of these viruses are roughly consistent with that reported for their removal by coagulation and filtration (simulating conventional drinking water treatment), but the reported removals also varied considerably for different conditions (Abbaszadegan et al., 2007; Mayer et al., 2008; Abbaszadegan et al., 2008). The differences in removal are likely due to differences in the capsid properties of the viruses. A comparison of isoelectric points (IEP) does not provide much insight, as MS2, PRD1, and Adenovirus 2 all have IEPs significantly below the pH used in our experiments (reported values are 3.9, 4, and 2.6, respectively), (Dowd et al., 1998; Michen and Graule, 2010), whereas poliovirus strains can exist in two interconvertible states with IEPs around 4.5 and 7.1 (Michen and Graule, 2010). However, IEP does not provide information about net surface charge. Based on electrophoretic mobility measurements, the net surface charge of MS2 is less negative at neutral pH than PRD1, and thus cannot explain the four-fold greater removal of MS2 than PRD1 observed in our setup (Abudalo et al., 2005; Redman et al., 1997). Information on the electrophoretic mobility of adenovirus has not been published. Other capsid features are likely to contribute, for example the Adenovirus 2 capsid has been shown to include a receptor-binding site formed by five copies of a penton base.

Lower than expected removal of viruses (PhiX174) in ceramic depth filters has been attributed to steric interactions between similar viral capsid features (knobs) and media surface (Michen et al., 2011). The PRD1 capsid does not have a similar penton base structure, which could account for different interactions at the coated sand surface (Rydman et al., 1999).

The major limitation to the effectiveness of QAS-coated media is the fouling of columns. As seen in the results in Figure 3, *E. coli* and MS2 removal decreased throughout each experiment. In the experiments using MilliQ water, the reduction in removal was presumably due to biofouling from cells or virus themselves, or their debris as they disintegrated. The reduction in removal was much more pronounced when the challenge water included NOM. If the laboratory columns are scaled up to a size typical for a media cartridge in a POU filter (~9.5 cm diameter), our results suggest that the cartridge would foul after treating less than 68 liters, which is clearly unacceptable performance. When a PAC pre-filter was used, the fouling due to NOM was eliminated in the *E. coli* experiment, illustrating that the main role that NOM played was competing for attachment sites on the coated media. The PAC pre-filter did not completely prevent fouling when the column was challenged with MS2; one possible explanation is that NOM coated the surface of the MS2 particles, reducing their attachment efficiency (Pham *et al.*, 2009). Since NOM is present in significant concentrations in most surface waters, it is clear that more research is needed to develop approaches for increasing the lifetime of the QAS-coated media, and/or regenerating it, if QAS coated sand is to be a feasible option for HWTS.

Conclusions

Overall, the findings from this study demonstrate the ability of filtration using QAS-coated media to remove bacteria and viruses from water. However, this study also identified major limitations and barriers to use of the coated media in a POU filter. These major limitations include: (1) rapid fouling due to the microorganisms or NOM, which contributed to an unacceptable filter lifetime, and (2) low removal of bacteriophage PRD1 (a model virus) and Adenovirus 2. A two-stage device with a PAC column followed by QAS-coated sand had improved removal of bacteria and viruses from water containing NOM. This idea could be extended to other multi-stage designs that included other media, such as metal oxide surfaces, which may further improve removal of NOM as well as viruses. QAS-coated media may also be a useful polishing step to remove viruses from other HWTS filters that target bacterial removal. However, more research is needed on the long-term performance and possible leaching of QAS-coated media, additional options to reduce fouling and regenerate the media, and the inactivation mechanisms of bacteria and viruses by QAS-coatings.

Part 2A – Stormwater Treatment

Unsaturated Column Experiment

Chapter 3: Introduction and Materials and Methods for Intermittently Fed, Unsaturated Stormwater Columns

Introduction

Stormwater, increasing in volume with urbanization (NRC, 2008), has traditionally been managed in municipalities by building storm sewers to collect flows and discharge them to surface waters (Pitt and Clark, 2008). However, water quality concerns have arisen as urban stormwater has been identified as a major nonpoint source of pathogens in surface waters (Brownell et al., 2007; Marsalek and Rochfort, 2004). Due to the difficulty of measuring human pathogens, researchers typically monitor stormwater for indicator organisms (Olivieri et al., 2007), and recreational water standards and total maximum daily loads (TMDLs) are based on fecal indicator bacteria (FIB) (Boehm et al., 2009). Both indicator bacteria and viruses pose a barrier to safe discharge and non-potable use of stormwater as storm flows have been found to frequently exceed recreational water quality standards (Parker et al., 2010) and non-potable use regulations (Pitt and Clark, 2012).

Recently, green infrastructure (GI) and low impact development (LID) have been used for stormwater management to increase permeability in urban settings and reduce peak storm flows (Pitt and Clark, 2008; U.S. EPA, 2000). GI projects have also been recognized as having the potential to incorporate treatment technologies to meet water quality discharge limits (Clark and Pitt, 2012). Bioretention basins, a Best Management Practice (BMP) for GI, consist of a depressed trench to collect and infiltrate stormwater through filter media before discharging to the storm sewer (He and Davis, 2011). Bioretention basins typically contain a planted top layer, a treatment layer packed with conventional bioretention media (CBM) consisting of a mixture of soil, sand, and compost, and a gravel underdrain for water storage (Davis et al., 2009). In lab-controlled settings, CBM bioretention filters have been observed to be effective barriers for several classes of stormwater pollutants, including FIB (Davis et al., 2001). *Escherichia coli* (*E. coli*) removal has been observed between 1.1 – 3 log (Barrett et al., 2013; Bright et al., 2010; Chandrasena et al., 2012; Chandrasena et al., 2014; Kim et al., 2012; Li et al., 2012; Rusciano and Obropta, 2007; Zhang et al., 2011), and F-RNA coliphage removal has been reported around 4.3 log (Li et al., 2012). Media aging and low infiltration rates were associated with higher *E. coli* removal (Chandrasena et al., 2014; Zhang et al., 2011), and straining, adsorption, inactivation/decay, predation, and nutrient competition were cited as possible removal mechanisms (Chandrasena et al., 2014; Li et al., 2012; Zhang et al., 2011). Stormwater was typically delivered to columns at regular intervals, but extended dry periods were observed to increase infiltration rates and decrease *E. coli* and F-RNA coliphage removal (Chandrasena et al., 2014; Li et al., 2012).

In field evaluations of bioretention basins, however, researchers have not reported similar *E. coli* removals as observed in lab studies. A database pooling BMP performance reported an average of 0.5-log *E. coli* removal in field bioretention basins (International Stormwater BMP Database, 2014). Variable performance has been reported across field studies with indicator bacteria removal results ranging from 16% (Birch et al., 2006) to 95% (Passeport et al., 2009). Furthermore, effluent indicator bacteria concentrations have frequently surpassed recreational water quality standards (Birch et al., 2006; Passeport et al., 2009) and have even exceeded influent concentrations in one study (Hathaway et al., 2011). The study of bioretention basins is challenging because they are distributed systems that collect stormwater in varying quantity, frequency, and quality (Grebel et al., 2013). Without a better understanding of removal mechanisms, it is unclear what factors lead to poor field performance and high effluent concentrations.

Various amendments to the media used in bioretention basins also present an opportunity to improve indicator organism removal performance. Zero valent iron (ZVI) appears to be a promising filter amendment to increase removal of phosphate (PO_4^{3-}) (Erickson et al., 2007; Erickson et al., 2012) and heavy metals (Rangsivek and Jekel, 2005) from stormwater. ZVI-amended media also has the potential to increase removal of bacteria and viruses by bioretention basins. At neutral pH, CBM and most bacteria and viruses typically exhibit a net negative surface charge (Kosmulski, 2011; Michen and Graule, 2010), impeding bacteria and virus attachment by electrostatic repulsion (Dong et al., 2002). ZVI corrosion products, such as amorphous iron hydroxides (ferrihydrite) and the more stable iron oxides/oxyhydroxides (e.g. goethite, hematite, and magnetite) (Furukawa et al., 2002; Noubactep, 2010), exhibit a net positive surface charge at neutral pH (Kosmulski, 2011), which is expected to enhance bacteria and virus attachment by electrostatic attraction (Elimelech and Song, 1992; Elimelech, 1994).

In short-term column studies, researchers found ZVI-amended media to remove up to 5 logs of indicator viruses (You et al., 2005) and human viruses (Shi et al., 2012) from drinking water. These studies, however, were conducted over a short period and did not include other constituents found in stormwater. It is unclear how well ZVI amendments will perform in stormwater containing high concentrations of natural organic matter (NOM) and PO_4^{3-} , known to interfere with iron oxide binding sites (Foppen et al., 2008; Park et al., 2009). Short-term column studies with iron oxide coated sand have been conducted in synthetic stormwater and reported less than 1-log removal of fecal indicator bacteria (Mohanty et al., 2013; Zhang et al., 2010). ZVI amendments may perform better than static iron oxide coatings due to the continual corrosion process in the presence of water (Noubactep et al., 2009).

Part 2A aimed to increase our understanding of indicator organism removal in bioretention basins and inform better designs for more predictable performance. We had two objectives: (1) investigate the possible mechanisms of indicator organism removal in aged CBM columns and (2) evaluate the effectiveness of ZVI-amended media for removing indicator organisms over several storms. The lab-based column studies were designed to capture several key features of field conditions. For example, feed water was selected to contain a natural microbial community, and column performance was followed over 46 weeks to allow biofilm development and media aging.

Materials and Methods

Before conducting long-term column studies, a short-term column experiment was conducted with synthetic stormwater to evaluate whether ZVI amendments improved indicator bacteria removal over silica sand. For the long-term studies, columns containing silica sand, conventional bioretention media (CBM), silica sand and ZVI, or CBM and ZVI were injected with stormwater once per week for 5.15 h over 46 weeks to evaluate indicator bacteria, indicator virus, and PO_4^{3-} removal. Hydraulic conductivity (HC) was measured throughout the experiment to track clogging. Silica sand and CBM columns were sacrificed at four time points to quantify biofilm changes on the media in the top, middle, and bottom column sections. In ZVI-amended columns, dissolved and particulate iron were monitored in the effluent to determine whether iron was leached out of the columns. For all media types, a longer rest period experiment was conducted to determine whether increased residence time further improved indicator organism removal. Finally, a sodium azide experiment in silica sand and CBM columns was conducted after 46 weeks to determine the impact of microbial activity on indicator organism removal.

Indicator *Escherichia coli* and MS2 Coliphage

Escherichia coli NCM 4236 (*E. coli*), kanamycin-resistant K12 strain, was provided by the late Professor Sydney Kustu (University of California-Berkeley) (Inwood et al., 2009). *E. coli* cultures were grown at 37 °C in tryptic soy broth containing 0.025 g/L of kanamycin. To prepare each batch of stormwater, a frozen *E. coli* culture was grown to stationary phase three times before harvesting. Cells were harvested by centrifugation at 8000 g for 5 minutes. The supernatant was discarded, and the pellet was resuspended in phosphate buffer solution (PBS). The rinsing process was repeated three times before adding the *E. coli* suspension to the column influent water. The *E. coli* concentration in influent and effluent samples, counted as colony forming units (CFU) per mL, was enumerated in duplicate via the spread plate technique on selective agar containing 0.025 g/L kanamycin. 100- μL inocula were added to each plate and incubated at 37 °C for 18 h before counting.

MS2 coliphage (MS2) (ATCC no. 15597-B1), a male specific F+ coliphage, was propagated using EPA Standard Method 1601 and *Escherichia coli* F_{amp} (ATCC no. 700891) as host (U.S. EPA, 2001). The MS2 concentration in influent and effluent samples was enumerated in duplicate using the double agar layer (DAL) technique in agar containing 0.015 g/L of ampicillin and streptomycin. 100- μL inocula were used to determine plaque forming units (PFU) per mL from each sample (U.S. EPA, 2001).

Media Preparation

Coarse Ottawa sand (0.6 – 0.85 mm, Fisher Scientific, NH) and a compost (American Soil and Stone, CA) were purchased from their suppliers and sieved to a size range between 20 – 30 mesh to ensure similar pore volumes in columns containing different media blends. The compost was produced from a mixture of plant materials and food waste. Prior to column packing, Ottawa sand was soaked in 12 N hydrochloric acid (HCl) overnight to dissolve metal impurities, which have been observed to influence the surface charge of supplier-delivered sand and may have

increased *E. coli* and MS2 attachment (Litton and Olson, 1993). The sand was then rinsed several times in deionized water to remove residual acid. The rinsed Ottawa sand was dried at 110 °C for 24 h and sterilized in an autoclave (120 °C, 20 psi, 15 min). The compost was rinsed with deionized water until the discarded water was clear and then dried at 110 °C for 24 h. To preserve the microbial community, the dried compost was not autoclaved prior to packing. Zero valent iron (ZVI) filings were obtained as cast iron aggregates (Peerless Metal Powders and Abrasives, MI), sieved to a size range between 20 – 30 mesh, and set aside without further preparation. The four media types were produced from the Ottawa sand, compost, and ZVI filings for this study. Plain sand (PS) solely contained the autoclaved Ottawa sand. CBM was prepared following the recommendation for bioretention soil from the Bay Area Stormwater Management Agencies Association (BASMAA), and contained 70% Ottawa sand and 30% compost by volume (BASMAA, 2010). Plain sand with a ZVI amendment (PS+ZVI) contained 90% Ottawa sand and 10% ZVI by weight, and CBM with a ZVI amendment (CBM+ZVI) contained 90% CBM and 10% ZVI by weight. Each media was mixed in a separate 2-L glass container for 1 h prior to packing in a column.

Short-Term Column Experiment with Synthetic Stormwater

The synthetic stormwater consisted of 0.75 mM of CaCl₂, 0.075 mM of MgCl₂, 0.33 mM of Na₂SO₄, 1 mM of NaHCO₃, 0.072 mM of NaNO₃, 0.072 mM of NH₄Cl, 0.016 mM of Na₂HPO₄, and 20 mg C/L Suwanee River natural organic matter (NOM) (International Humic Substances Society, MN) in deionized water. 10⁶ CFU/mL of *E. coli* were added to this matrix as indicated below. The final ionic strength and pH were 4.7 mM and 7.0, respectively.

PS and PS+ZVI were dry-packed into separate glass chromatography columns (Kontes, 2.5-cm diameter, 15-cm length), yielding a porosity of 0.39 and pore volume (PV) of 28 mL. After packing, deionized (DI) water was pumped upward through the column for 20 PVs to rinse out loose particles. 5 PVs of sterile synthetic stormwater were then pumped upward through the columns to flush DI from the columns. Finally, 3.5 PVs of lab-based synthetic stormwater with *E. coli* was injected upward into each column. Samples were collected after 1.5 PVs to allow sterile synthetic stormwater to exit the column. After 1.5 PV, 10-mL effluent samples were collected every 0.4 PV until 3.5 PVs had passed through the columns. An influent sample was taken at the start of the *E. coli*-amended stormwater injection. Influent and effluent samples were immediately plated to enumerate *E. coli*.

46-Week Column Experiment with Amended Creek Water

The stormwater matrix is a particular challenge in stormwater research because characteristics can be highly variable (Grebel et al., 2013). Stormwater is also only available during rain events. Therefore, we simulated stormwater in this study by collecting water from the North Fork of Strawberry Creek on the University of California, Berkeley campus immediately prior to weekly injections. Water was collected during dry periods to prevent large variability in influent characteristics between injections. Local creek water was selected to include an environmental microbial community in addition to indicator organisms. A natural organic matter (NOM) amendment, *E. coli* suspension, and MS2 suspension were added to reach concentrations around

10 mg/L total organic carbon (TOC), 10^5 CFU/mL, and 10^5 PFU/mL, respectively. The NOM amendment accounted for about 85% of the 10 mg/L TOC in the influent. The influent was allowed to mix for a minimum of 15 minutes on a stir plate before injecting into the columns and was continuously mixed throughout the injection.

PS, CBM, PS+ZVI, and CBM+ZVI were packed into custom-built columns (2.5-cm diameter, 22-cm length) with clear polyvinyl chloride (PVC) pipe (McMaster-Carr, IL). 40 columns were built at the onset of this study with 10 replicate columns packed with each media type. Media was dry-packed into columns in 2-cm increments to a final depth of 20 cm. A hand-held massager was placed on the column sides between media additions to apply vibrations and ensure tight packing. A 1-cm polyester fiber bed was placed at the top and bottom of the column to support the media bed and prevent media bleeding. A cross-section schematic of the columns is shown in Figure 3.1, and a summary of the media and column characteristics is provided in Table 3.1. Prior to the initial stormwater injection, DI water was injected into each column at flow velocities below 1 cm/h for 36 h for a final rinse. The PV and porosity were estimated by subtracting the weight of a dry-packed column from a saturated column. A photo of the 46-week experiment setup is included in Figure 3.2.

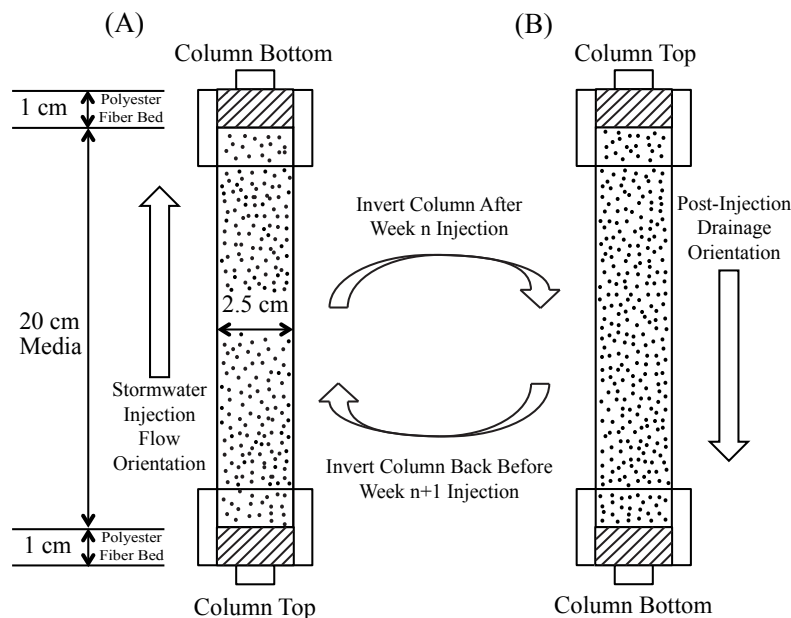


Figure 3.1 – Cross-section schematic of columns for this study. (A) Upward flow orientation used during the weekly 5.15-h stormwater injections. After each 5.15-h injection, the columns were inverted to the (B) orientation to allow drainage via gravity without reversing the direction of flow. The columns stayed in the (B) orientation for the remainder of the week. Immediately prior to the next injection, the columns were inverted back to the (A) orientation to again receive stormwater.

Table 3.1 – Column and Media Characteristics.

Column Characteristics	Average
Column Diameter	2.5 cm
Column Media Length	20 cm
Ottawa Sand, Compost, and ZVI Diameter	20 – 30 mesh or 0.6 – 0.85 mm
Porosity	0.34
Pore Volume	33 mL
PS Media Composition (% by volume)	100% Ottawa Sand
CBM Composition (% by volume)	70% Ottawa Sand, 30% Compost
PS+ZVI Composition (% by weight)	90% Ottawa Sand, 10% ZVI
CBM+ZVI Composition (% by weight)	90% CBM, 10% ZVI

Plain Sand (PS), Conventional Bioretention Media (CBM), Zero Valent Iron (ZVI)



Figure 3.2 – Photo of the experimental setup for the 46-week column experiment.

For 46 weeks, columns were injected once each week with amended creek water in an upward direction to ensure a constant saturated flow rate. Using an upward injection allowed the control of filtration velocity independent of the HC. This upward-flow orientation can be viewed in Figure 3.1A. During weekly injections, stormwater was injected into all columns at a flow velocity of about 10 cm/h for 5.15 h using a 20-channel Masterflex pump (Cole-Parmer[®], IL). This hydraulic loading was based on a 3.2-cm storm lasting 5.15 h and corresponds to a 1-year

storm in Berkeley, CA. Assuming a bioretention basin sized to 5% of the total drainage area, a runoff coefficient of 80% (percent of rain becoming runoff), and a runoff treatment goal of 100%, each column received about 250 mL of stormwater during each injection. This injection contains around 7.5 PVs. The calculated hydraulic residence time (HRT) in the 20-cm deep media was about 41 min. The observed column HRT, including the 2 cm of polyester fiber support, varied between media types but typically ranged between 45 – 55 min. Following an injection, all columns were inverted to allow for gravity drainage without reversing the direction of flow. The columns remained drained in this orientation, shown in Figure 3.1B, for the rest of the week until the next injection. Immediately prior to this next injection, the columns were inverted back to the upward-flow orientation, shown in Figure 3.1A, to again receive stormwater.

To evaluate *E. coli* and MS2 removal, column effluent was collected 3 h into each injection or after about 3.2 – 3.5 PVs of stormwater had exited the column. As shown in Figure 3.3, *E. coli* and MS2 removal was highest after 1 – 2 PVs had exited the column. Removal decreased after this point but stabilized after 3 PVs had exited the column. Samples taken after 3 PVs were therefore assumed to be representative of *E. coli* and MS2 removal throughout each 1-year storm. 50 mL of effluent sample were collected over 1 h and then analyzed for *E. coli* and MS2 concentrations, TOC, PO_4^{3-} , dissolved and particulate iron, and total cell concentrations (TCC). TCC analysis was conducted beginning in week 24. A 50-mL influent sample was collected at the same time and analyzed along with the effluent samples. Effluent samples were collected and analyzed from columns every 2 – 3 weeks. PS/PS+ZVI and CBM/CBM+ZVI column effluent samples were analyzed during the same weeks.

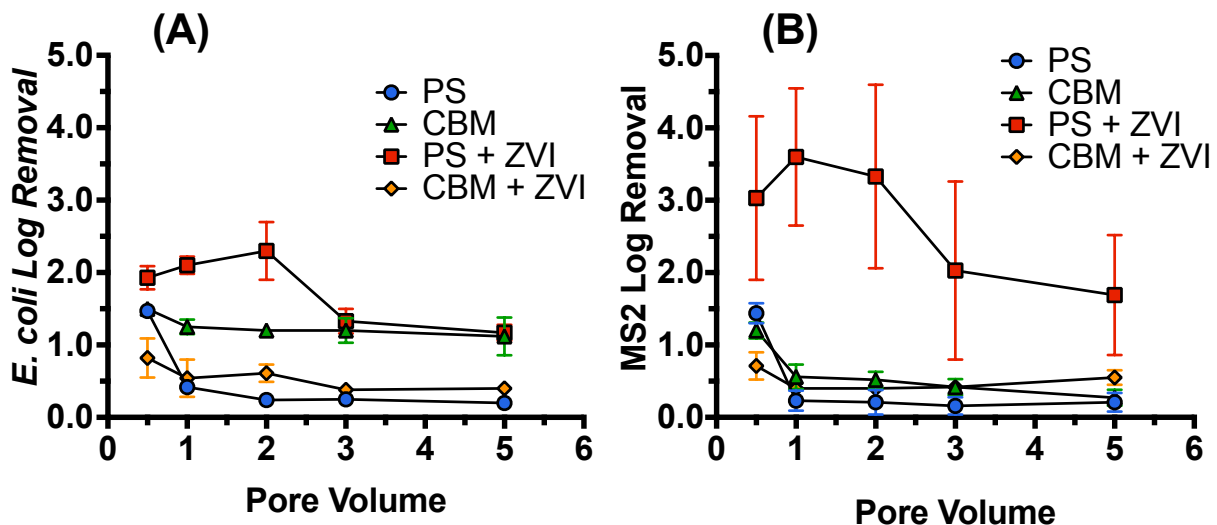


Figure 3.3 – Typical (A) *E. coli* and (B) MS2 removal changes in PS, CBM, PS+ZVI, and CBM+ZVI columns throughout a 1-year storm injection. For routine sample collection, a single sample was collected from each column after 3 pore volumes had been injected through the columns. Error bars represent one standard deviation.

To quantify clogging and biofilm changes with time, random PS, CBM, PS+ZVI, and CBM+ZVI

columns were selected at weeks 8, 18, 31, and 46. Duplicate columns of each media were chosen with a random number generator and injected with a 5.15-h storm. During the week 46 sacrifice, effluent samples were collected after 0.5 and 5 PVs passed through the columns and analyzed for *E. coli*, MS2, dissolved and particulate iron, PO_4^{3-} , and TCCs. Prior to draining the columns via gravity, the HC was measured using the ASTM E2396 Falling-Head Method with 20 cm of head (ASTM, 2015). (The initial HC was measured on separate freshly packed columns in triplicate.) Then, the columns were allowed to drain and rest for 24 h. PS and CBM columns were then sacrificed and media samples were taken from the top 3 cm, middle 3 cm, and bottom 3 cm of each column for biofilm characterization. ZVI interfered with the biofilm characterization method so PS+ZVI and CBM+ZVI columns were discarded after HC characterization. After the week 46 sacrifice, 2 replicate columns of each media type remained.

Rest Period and Sodium Azide Experiments

After the week 46 sacrifice, two experiments were conducted on the remaining columns to evaluate the effect of residence time and biological activity on *E. coli* and MS2 removal. First, a longer rest period experiment, in which stormwater was allowed to rest in the columns, was conducted to determine whether *E. coli* or MS2 increased with a 24-h residence time. In PS and CBM columns, a longer rest period was expected to increase *E. coli* and MS2 decay due to grazing and enzymatic activity of the microbial community as observed in biosand experiments (Elliott et al., 2011). In PS+ZVI and CBM+ZVI columns, a longer rest period was expected to increase *E. coli* and MS2 removal due to extended exposure to iron oxide corrosion products. Duplicate columns of each media blend were saturated with 1 PV of stormwater and allowed to rest for 24 h. Afterwards, 1 PV of stormwater was injected into the columns and the initial 0.5 PV of effluent was collected for *E. coli* and MS2 enumeration. The *E. coli* and MS2 removal observed after the 24-h rest period was compared to the removal observed during the week 46 injection when stormwater was injected into a different set of columns without a rest period. These data, referred to as 0-h rest period, were collected after 3 PVs of stormwater had passed through the columns.

Second, an experiment in which a microbial inhibitor was added to the influent feed was conducted to determine whether microbial activity had any effect on *E. coli* and MS2 removal in the PS and CBM columns. PS+ZVI and CBM+ZVI columns were not included in this experiment due to safety concerns with iron and sodium azide reactions. Sodium azide (NaN_3) is a microbial inhibitor known to prevent oxidative phosphorylation and the respiration of aerobic and denitrifying bacteria and eukaryotes (Elliott et al., 2011; Weber-Shirk and Dick, 1997). Concentrations up to 50 mM have not been observed to reduce bacteria viability or virus infectivity (Elliott et al., 2011), and sodium azide does not alter pre-formed substances, including extracellular polymeric substances (EPS), on the filter media (Weber-Shirk and Dick, 1997). Thus, the sodium azide feed was intended to determine whether microbial respiration had any impact on *E. coli* and MS2 removal in aged media. The sodium azide feed was created by adding 6 mM NaN_3 to the same influent water used in the previous 46 weeks. The 6 mM NaN_3 addition increased the influent's ionic strength from around 3 mM to 9 mM (Hans and Maranzana, 2006) but was not expected to change the results. Chen and Walker (2012) observed no change in *E. coli* removal in porous media when the ionic strength increased from 1 mM to 100 mM, and Yuan et al. (2008) reported MS2 attachment efficiencies below the detection limit on silica sand

coated with organic matter at an ionic strength of 10 mM. One PS and CBM column were injected with this feed for 5.15 h on 3 consecutive days. Samples were taken for *E. coli* and MS2 after 0.5, 1, and 5 PVs passed through the columns on the 3rd day. Data from this experiment were compared to the removal data in the week 46 sacrifice experiment.

Water Chemistry

NOM, PO₄³⁻, turbidity, pH, and TCCs were monitored throughout the 46 weeks. NOM was measured on a TOC analyzer (TOC-5000A, Shimadzu Co., Japan). PO₄³⁻ was measured using the ascorbic acid method (EPA Standard Method 365.2) with a detection limit of 0.02 mg/L (U.S. EPA, 1983). Turbidity was measured as nephelometric turbidity units (NTU) on a Hach[®] 2100N turbidity meter (Hach[®], CO), and pH was measured using a Beckman-Coulter Φ [™] 200 Series meter (Beckman-Coulter, CA). Assimilable organic carbon (AOC) was measured in the influent on two separate days. AOC and TCCs were measured with flow cytometry (FCM) and are described in a subsequent section. Influent characteristics are summarized in Table 3.2.

Iron samples, analyzed for dissolved ferrous iron (Fe[II]), total dissolved iron, and total iron (Tot Fe), were measured using the ferrozine colorimetric method developed by Viollier et al. (2000) with a detection limit of 0.05 mg/L. Fe[II] and total dissolved iron samples were filtered through a 0.45- μ m filter prior to the addition of reagents. Dissolved ferric iron (Fe[III]) was then calculated as the difference between total dissolved iron and Fe[II]. Tot Fe samples were not filtered and included both particulate and dissolved species in the analysis. 2 mL of a Tot Fe sample was mixed with 1 mL of 2 N HCl overnight to dissolve particulates prior to reagent addition. All colorimetric analysis was completed on a UV-vis spectrophotometer at 562 nm (UV-2600, Shimadzu, Japan).

Table 3.2 – Influent Characteristics. *E. coli*, MS2, and TOC added to creek water 15 minutes prior to every injection. Dissolved oxygen (DO) and alkalinity were not measured directly, but historical monitoring values of Strawberry Creek are reported here (Hans and Maranzana, 2006).

Influent Characteristics	Average \pm Standard Deviation
TOC	9.31 \pm 1.84 mg/L
AOC	0.25 \pm 0.07 mg/L
PO ₄ ³⁻	1.98 \pm 0.89 mg/L
Turbidity	0.80 \pm 0.54 NTU
DO	8 mg/L
Alkalinity (as CaCO ₃)	120 mg/L
pH	8.31 \pm 0.13
TSS	4.17 \pm 1.44 mg/L
Fe[II]	0.00 \pm 0.00 mg/L
Fe[III]	0.03 \pm 0.04 mg/L
Tot Fe	0.07 \pm 0.08 mg/L
Total Cell Concentration	3.2 \times 10 ⁶ \pm 3.2 \times 10 ⁶ cells/mL
<i>E. coli</i>	10 ⁵ CFU/mL
MS2	10 ⁵ PFU/mL

The NOM amendment was created prior to the start of column injections because the NOM concentration in Strawberry Creek (between 1 – 2 mg/L) was lower than typical stormwater (Grebel et al., 2013). The amendment was created from Strawberry Creek water to increase the influent NOM concentration without providing a labile carbon source for artificially high biofilm growth. To create the amendment, 15 L of Strawberry Creek water was collected in a 20-L bucket from the same North Fork site where the column influent water was collected. 150 g of wood chips (collected near the creek), 100 g of maple leaves (collected near the creek), and 500 g of plant-based compost were added to the water and mixed well. The 20-L bucket was covered with a fabric mesh and set outside for 2 weeks. After 2 weeks, the mixture was filtered through a 25- μm filter followed by a 3- μm filter to remove solids. Finally, the suspension was concentrated using a tangential flow filter with a molecular weight cut off (MWCO) of 1 kDa. The final concentration in this suspension was around 265 mg/L TOC. Two batches of this amendment were created and used throughout this experiment. The adsorption spectrum, specific ultraviolet absorbance (SUVA), peak wavelength, and peak absorbance of this NOM amendment is included in Figure 3.4 and Table 3.3.

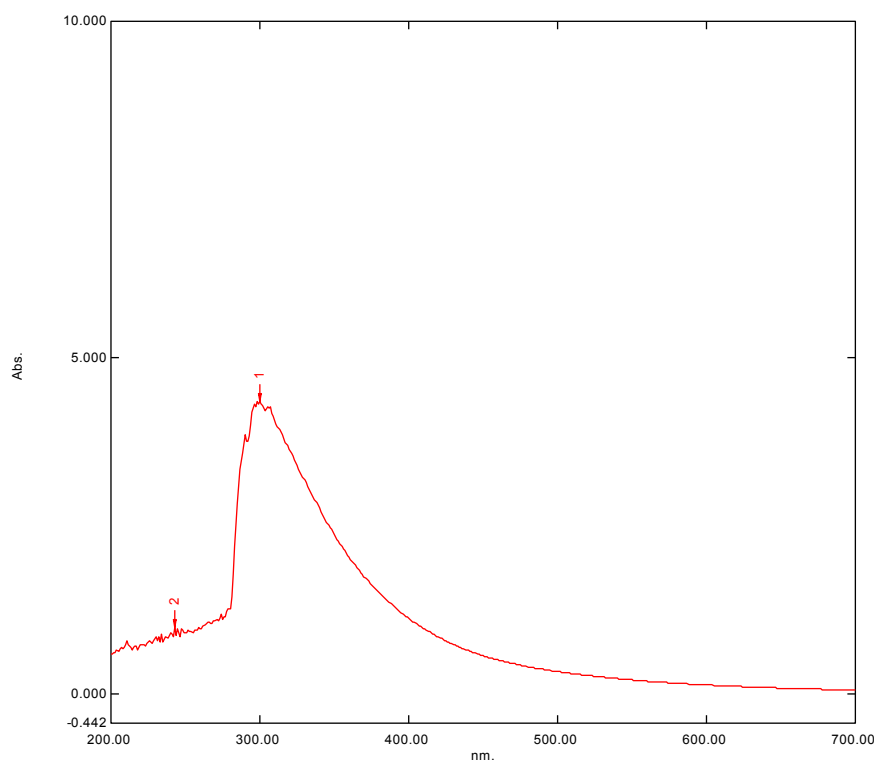


Figure 3.4 – Absorption spectrum of NOM amendment created from Strawberry Creek water, wood chips, maple leaves, and American Soil and Stone compost.

Table 3.3 – Specific Ultraviolet Absorbance (SUVA), Peak Wavelength, and Peak Absorbance for NOM amendment.

UV Wavelength	UVA	TOC	SUVA	Peak Wavelength	Peak Absorbance
254 nm	0.929	265 mg/L	0.35 L/mg-M	300 nm	4.347

Clogging Model

The Mays and Hunt clogging model was used to convert the HC changes in PS and CBM columns to specific deposit (volume of particles per bed volume) to track changes as the media aged (2005). Clean bed HC was measured on freshly packed columns that had been conditioned with DI water for 24 h. The following is a brief description of the model derivation.

1. The ratio of head loss to clean bed head loss is related to permeability, hydraulic conductivity, and specific area:

$$\frac{\Delta H}{\Delta H_0} = \frac{k_0}{k} = \frac{HC_0}{HC} = \left(\frac{M}{M_0} \right)^2 \quad \text{Equation 1}$$

where ΔH is the head loss, ΔH_0 is the clean bed head loss, k is the permeability, k_0 is the clean bed permeability, HC is the hydraulic conductivity, HC_0 is the clean bed hydraulic conductivity, M is the specific area for a clogging filter, and M_0 is the specific area for a clean bed filter.

2. The specific deposit, σ , is the volume of particles collected per bed volume and is proportional to the number of particles attached:

$$\sigma = \frac{\# \text{ Particles}}{\text{Collector}} \times \text{Volume Particle} \times \frac{\# \text{ Collectors}}{\text{Bed Volume}}$$

$$\sigma = N \times V_p \times \frac{6(1-\varepsilon)}{\pi d_c^3} \quad \text{Equation 2}$$

3. Rearranging Equation 2 for N :

$$N = \frac{\sigma \pi d_c^3}{6V_p(1-\varepsilon)} \quad \text{Equation 3}$$

where N is the # particles/collector, V_p is the particle volume, ε is the porosity, and d_c is the collector diameter.

4. The specific area for a clean bed filter, M_0 , is the surface area per bed volume:

$$M_0 = \frac{\text{Surface Area}}{\text{Collector}} \times \frac{\# \text{ Collectors}}{\text{Bed Volume}}$$

$$M_0 = \pi d_c^2 \times \frac{6(1-\varepsilon)}{\pi d_c^3} = \frac{6(1-\varepsilon)}{d_c} \quad \text{Equation 4}$$

5. The specific area for a clogging filter, M , increases as more particles are deposited on collectors:

$$M = \left(\frac{\text{Surface Area}}{\text{Collector}} + \frac{\text{Surface Area Deposited Particles}}{\text{Collector}} \right) \times \left(\frac{\# \text{ Collectors}}{\text{Bed Volume}} \right)$$

$$M = \left(\pi d_c^2 + \beta' N A_p^2 \right) \times \frac{6(1-\varepsilon)}{\pi d_c^3} \quad \text{Equation 5}$$

where A_p is the surface area per particle and β' is an empirical parameter representing the deposited particles increasing the filter's specific area.

6. Combining Equation 3 and 5 yields:

$$M = \left(\pi d_c^2 + \beta' \frac{\sigma \pi d_c^3}{6 V_p (1-\varepsilon)} A_p^2 \right) \times \frac{6(1-\varepsilon)}{\pi d_c^3} \quad \text{Equation 6}$$

7. Simplifying Equation 6 yields:

$$M = \left(1 + \frac{\beta' \sigma A_p^2}{6 V_p (1-\varepsilon)} \right) \times \frac{6(1-\varepsilon)}{\pi d_c^3} \quad \text{Equation 7}$$

8. Combining Equations 3, 4, and 6 yields:

$$\frac{\Delta H}{\Delta H_0} = \frac{HC_0}{HC} = \left(\frac{M}{M_0} \right)^2 = \left(\frac{\left(1 + \frac{\beta' \sigma A_p^2}{6 V_p (1-\varepsilon)} \right) \times \frac{6(1-\varepsilon)}{\pi d_c^3}}{\frac{6(1-\varepsilon)}{d_c}} \right)^2 \quad \text{Equation 8}$$

$$\frac{HC_0}{HC} = (1 + \gamma \sigma)^2 \quad \text{Equation 9}$$

$$\text{where } \gamma = \frac{\beta' d_c A_p}{6(1-\varepsilon) V_p}$$

9. γ is a clogging parameter that was empirically derived as a function of the Peclet Number:

$$\gamma = 1 * 10^6 * Pe^{-0.55} \quad \text{Equation 10}$$

$$\text{where } Pe = \frac{U d_c}{D_p} \text{ and } D_p = \frac{\kappa T}{3 \pi \mu d_p}$$

where Pe is the Peclet Number, U is the approach velocity, D_p is particle diffusivity, κ is Boltzmann's Constant = $1.38 \times 10^{-16} \text{ gm}^2 \text{K}^{-1} \text{s}^{-1}$, and μ is dynamic viscosity.

10. Combining Equations 9 and 10:

$$\frac{HC_0}{HC} = (1 + 10^6 Pe^{-0.55} \sigma)^2 \quad \text{Equation 11}$$

11. Solving for σ :

$$\sigma = \frac{\left(\sqrt{\frac{HC_0}{HC}} - 1 \right)}{10^6 Pe^{-0.55}} \quad \text{Equation 12}$$

12. Equation 12 was used to convert HC changes throughout the experiment to specific deposit. Parameters and their assumed values are included in Table 3.4.

Table 3.4 – Parameters used in the clogging model to track HC changes (Mays and Hunt, 2005).

Description	Symbol	Units	Value
Particle Diameter	d_p	cm	0.0001
Collector Diameter	d_c	cm	0.06
Temperature	T	K	298
Boltzmann Constant	k	J/k	1.38×10^{-23}
Dynamic Viscosity	μ	Ns/m ²	0.001002
Diffusion Coefficient	D_p	cm ² /h	1.76×10^{-5}
Approach Velocity	U	cm/h	9.8
Peclet Number	Pe	-	33284
Clogging Parameter	Υ	-	3256

Biofilm Characterization

The biofilm characterization method was conducted based on the procedure developed in Velten et al. (2007). The method was conducted on PS and CBM media only because the ZVI amendment in PS+ZVI and CBM+ZVI media interfered with the ATP measurement. This method produced data on the ATP concentration per unit of media (ng ATP/g media), ATP concentration per cell (ng ATP/cell), and number of cells per unit of media (cells/g media). For ng ATP/g media, 5 g samples of media from PS and CBM columns were collected from the top, middle, and bottom 3 cm and then rinsed three times in a 1 mM NaCl solution that had previously been autoclaved and filtered through a 0.1- μ m filter. From the washed media, a 200 mg wet weight (WW) sample was collected in pre-weighed, 1.5-mL centrifuge tubes. 500 μ L of 1 mM NaCl was added to this same centrifuge tube and then placed in a 38 °C water bath for 3 min. Concurrently, 55 μ L of BacTiter-Glo™ reagent (Promega Corporation, WI) was added to a separate centrifuge tube and incubated in the same water bath. After 3 min, 50 μ L of the BacTiter-Glo™ reagent was added to the other centrifuge tube with the media sample and 1 mM NaCl solution. After gently vortexing, this centrifuge tube was placed back into the water bath for 20 s. After 20 s, 200 μ L of the supernatant was extracted and placed into an unused centrifuge tube, and the relative light units (RLU) were measured immediately on a Glomax® 20/20 Luminometer (Promega Corporation, WI). The RLUs were converted into adenosine triphosphate (ATP) concentrations using a standard curve. Afterwards, the centrifuge tube containing the media was dried at 100 °C for 48 h to determine the media's dry weight (DW).

The ATP/g media value was calculated by dividing the ATP concentration by the media DW. The data were then reported as ng ATP/g media. Media from each column section was measured in duplicate.

Standard curves were created using excess media from column sections not sampled for ATP measurement. Prior to rinsing, the excess media was autoclaved and dried to sterilize the microbial community. The autoclaved media was then prepared for ATP analysis in the same procedure as the media samples. However, instead of 1 mM NaCl, 500 μ L of a known ATP standard solution, ranging from 10 – 10,000 ng/L ATP, was added to separate media samples. The RLUs were then measured on a Luminometer as described previously. A linear curve was created relating RLUs to ATP concentrations. Sample ATP standard curves for PS and CBM media are included in Figure 3.5. Different standard curves were created for every sacrifice to account for changes to the media's physical characteristics.

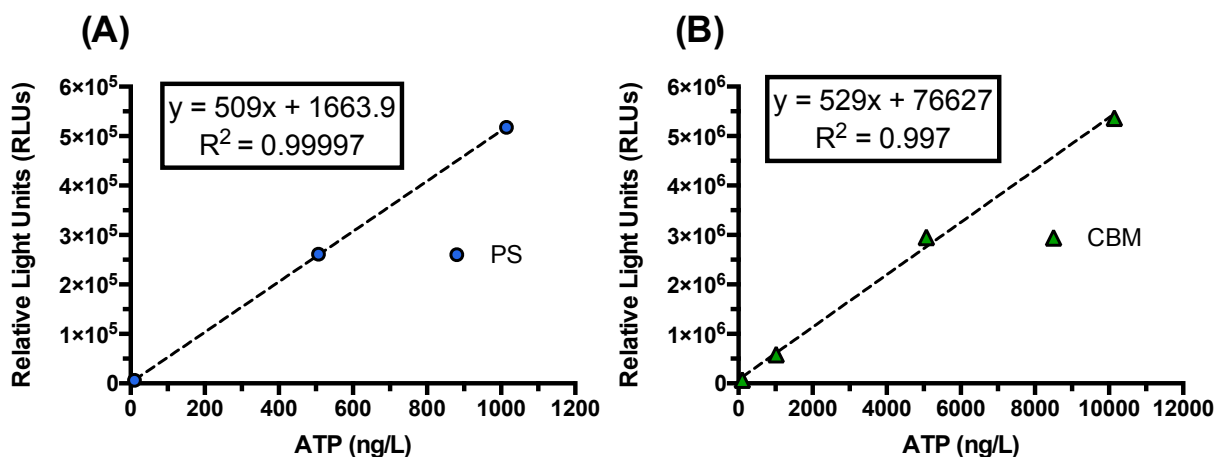


Figure 3.5 – Sample ATP standard curves for (A) PS and (B) CBM media.

ATP/cell was determined by taking a 1 g subsample from the rinsed, 5-g media sample of each column section and placing it in a 15-mL centrifuge tube with 10 mL of 1 mM NaCl. The centrifuge tube was then gently rotated for 10 min, and duplicate 500 μ L samples were taken to determine the ATP concentration on the Luminometer as previously described. Separate duplicate 500 μ L samples were also collected and analyzed on a flow cytometer to determine the total number of cells. FCM analysis is described in the subsequent section. The ATP/cell value was calculated by dividing the ATP concentration by the total number of cells. The data were then reported as ng ATP/cell. The cells/g media value was calculated by dividing the ng ATP/g media value by the ng ATP/cell value. The data were then reported as number of cells/g media. The standard deviation for all reported values was calculated using error propagation.

Flow Cytometry and Assimilable Organic Carbon

Total Cell Concentration (TCC) and the fraction of low nucleic acid (LNA) and high nucleic acid (HNA) bacteria were determined using a BD Accuri™ C6 flow cytometer (BD Biosciences, CA)

with a 488-nm blue laser and volumetric counting hardware. The FCM analysis was conducted based on procedures described previously (Hammes et al., 2008; Hammes and Egli, 2010; Prest et al., 2013). Briefly, a working solution was made from SYBR[®] Green I nucleic acid gel stain (SG) (Life Technologies, NY) and propidium iodide (PI) (30 mM, Life Technologies, NY). SG was diluted 100x in anhydrous dimethyl sulfoxide (DMSO) to which PI was added to make the final PI concentration 0.6 mM. 5 mL of this working solution was produced, allotted into separate vials (each with 0.25 mL), and stored at -20 °C until needed. Prior to FCM analysis, influent and effluent samples were filtered through a 0.7- μ m filter to prevent large solids from clogging the flow cytometer. 5 μ L of the working solution was mixed with 0.5 mL of a sample, placed in an incubator at 37 °C for 15 min, and then immediately analyzed on the flow cytometer. FCM measurements were collected on the flow cytometer at the pre-set slow flow rate of 14 μ L/min. 10 – 50 μ L of a sample were typically used to count the number of cells.

Electronic gates were drawn with the BD Accuri CFlow[®] software to distinguish between cells and non-living particles. The gating strategy was based on the procedure developed previously for evaluating drinking water treatment, and pre-drawn templates were provided with the BD Accuri[™] C6 flow cytometer (Hammes et al., 2008; Prest et al., 2013). SG has an excitation and emission maxima at 494 and 521 nm, respectively, whereas PI has an excitation and emission maxima of 535 and 617 nm, respectively. Fluorescence emissions were therefore collected on a green fluorescence channel (FL1; 533 \pm 30 nm) and red fluorescence channel (FL3; > 670 nm) to distinguish between SG-stained microbial cells and PI-stained particles. An acquisition threshold of 800 was set on the FL1 channel. TCCs were selected on a FL3 vs. FL1 graph using a lower gate limit drawn at 2,000 on the FL1 channel. HNA/LNA bacteria were counted using a histogram plot of the FL1 channel where the two-cluster fluorescent pattern of HNA and LNA bacteria were observed. Gates were drawn between these peaks to denote the HNA and LNA bacteria communities. Example gates for TCC, HNA/LNA bacteria, and forward/side scatter plots are included in Figure 3.6.

AOC was measured based on the procedure developed by Hammes and Egli (2005). Prior to collecting samples, 20-mL glass vials were washed and then baked at 600 °C for 6 h to remove any organic carbon contamination. To measure the AOC in the column influent, 15-mL samples of fresh influent (Strawberry Creek water with the NOM amendment) were collected and then immediately autoclaved for 25 min. To remove any particles, the autoclaved sample was allowed to cool and then filtered through a 0.2- μ m filter into a pre-baked glass vial. 10 μ L of a stock microbial inoculum was added to the 15-mL influent sample, and this mixture was incubated in a water bath at 30 °C for 3 d. After 3 d, the TCC was measured on the BD Accuri[™] C6 flow cytometer. The AOC concentration was then calculated using a conversion factor of 1×10^7 cells per 1 μ g of AOC. The influent AOC concentration was measured in triplicate on two separate days. Store-purchased Evian water was used as the stock microbial inoculum solution.

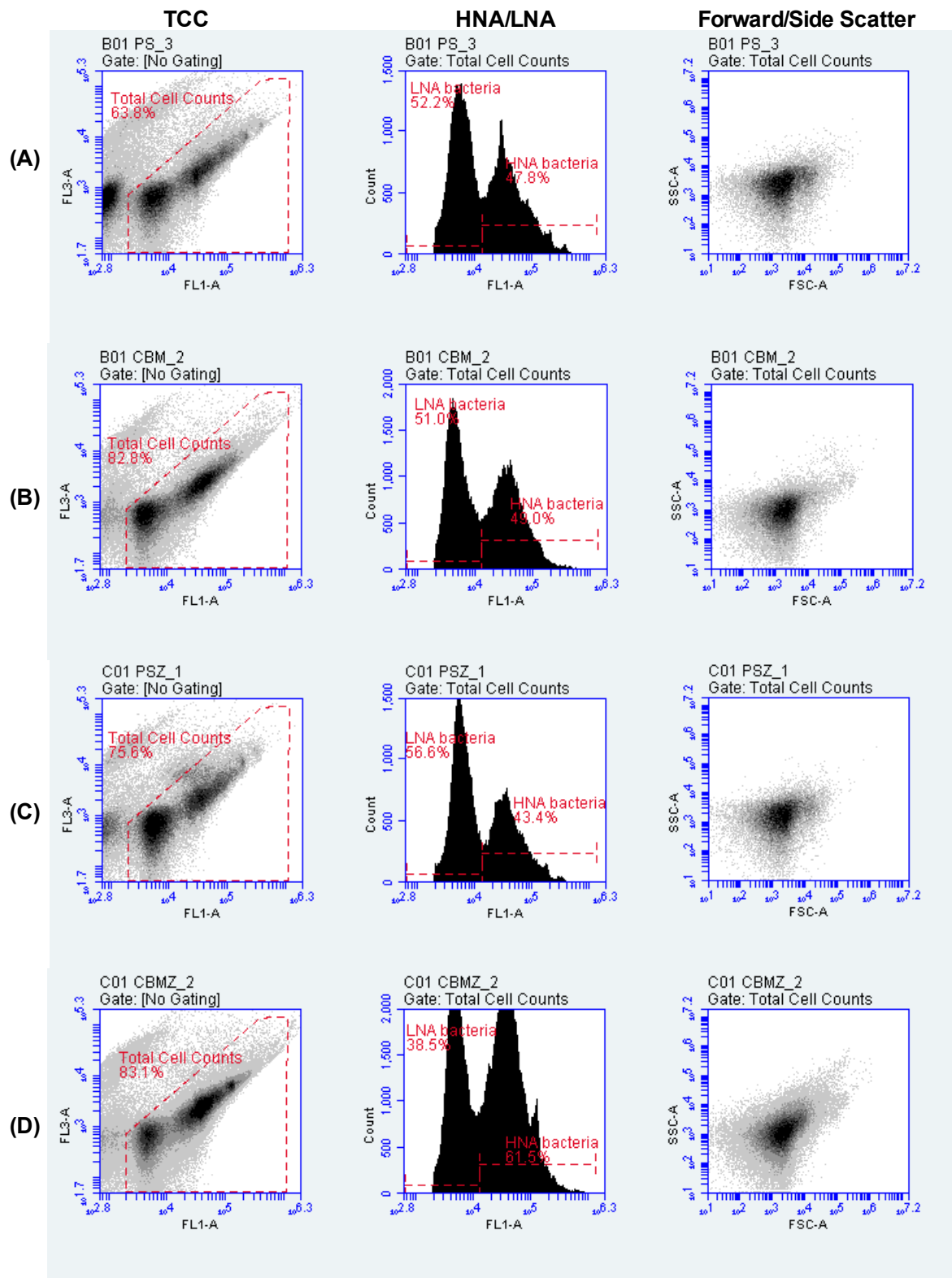


Figure 3.6 – Flow cytometry plots displaying the gates drawn for TCCs and HNA and LNA bacteria concentrations for effluent from (A) PS, (B) CBM, (C) PS+ZVI, and (D) CBM+ZVI columns. The forward and side scatter plots are also included.

Data Analysis

Indicator organism log removal was calculated as the difference between the logarithmic (base 10) influent concentration and logarithmic (base 10) effluent concentration. All standard deviations were calculated using error propagation based on the influent and effluent samples from the replicate columns throughout the study. Statistically significant differences were calculated using a two-sample t-Test on R Statistical Software (version 3.1.3, Austria) and were considered significant at $p < 0.05$. Figures were produced using GraphPad Prism Software (version 6, CA).

Part 2A Cont. – Stormwater Treatment Unsaturated Column Experiment

Chapter 4: Results and Discussion for Intermittently Fed, Unsaturated Stormwater Columns with Conventional Bioretention Media

Results

Removal of *E. coli*, MS2, Total Organic Carbon, and Phosphate

Escherichia coli (*E. coli*) and MS2 removal in plain sand (PS) and conventional bioretention media (CBM) columns is presented in Figure 4.1. *E. coli* removal by PS columns was poor; week 1 removal averaged 0.2 log and remained similar throughout the 46-week study. Removal of *E. coli* in CBM columns, however, increased over time. Removal through week 22 was about 0.5 log, then increased gradually and stabilized at nearly 1.5 log. During the last three sampling points (weeks 38, 41, and 46), average removal in CBM columns was significantly higher than in PS columns ($p = 0.005, 0.01, \text{ and } 0.007$, respectively).

MS2 removal in PS columns was low (-0.05-log average) and remained negligible throughout the experiment. In CBM columns, initial average MS2 removal was 0.0 log and remained below 0.5 log throughout the study.

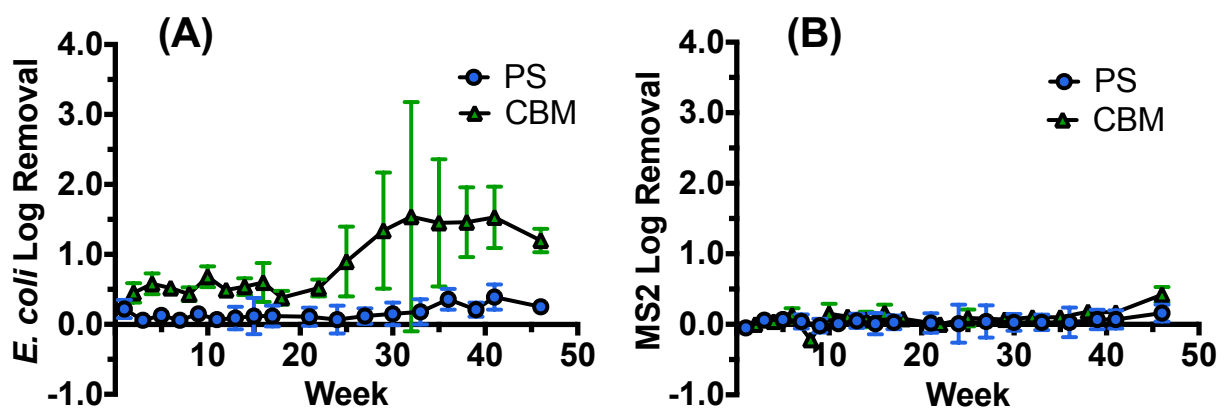


Figure 4.1 – Removal of (A) *E. coli* and (B) MS2 in PS and CBM columns during weekly stormwater injections. Stormwater was injected weekly for 5 h and samples were taken after 3 pore volumes of stormwater passed through the columns. Error bars represent one standard deviation.

Normalized effluent (C_{out}/C_{in}) total organic carbon (TOC) and phosphate (PO_4^{3-}) results are presented in Figure 4.2. In PS columns throughout the experiment, TOC removal was minimal, averaging -0.05% removal, while PO_4^{3-} removal averaged 29%. In CBM columns, effluent TOC and PO_4^{3-} concentrations were higher than influent concentrations. A similar increase in effluent TOC and PO_4^{3-} was reported in Bratieres et al. (2008) with a compost-amended loamy sand media. Increased organic matter was attributed to the compost dissolving in the stormwater. This organic matter also likely contained phosphorous and may account for the increased PO_4^{3-} concentration in the effluent (Bratieres et al., 2008).

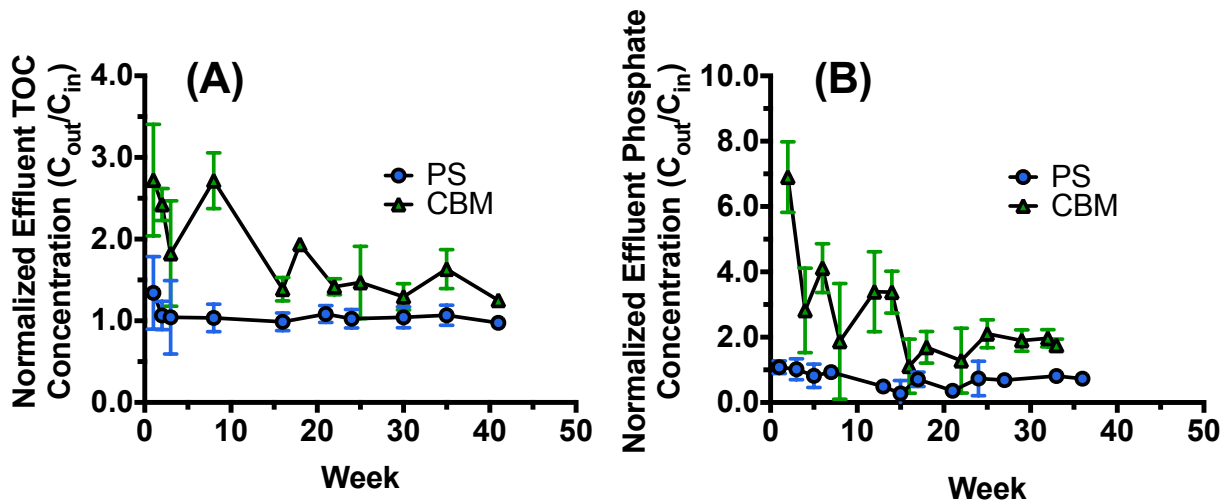


Figure 4.2 – Normalized effluent (A) TOC and (B) phosphate concentrations from PS and CBM columns. Samples were collected after 3 pore volumes of stormwater passed through the columns. Error bars represent one standard deviation.

Hydraulic Conductivity and Clogging Model

The average hydraulic conductivity (HC) for PS and CBM columns is reported in Figure 4.3. The initial HC was higher in PS than CBM columns by a factor of 1.6, but there was no significant difference between the media types in subsequent weeks. At week 8, HC in PS columns had decreased by a factor of 1.8 from the initial value to an average of 334 cm/h. Afterwards, there was no further significant decrease. HC in CBM columns decreased slower than in PS columns but reached a lower final value (254 cm/h) at week 46. While trending down, the HC at week 46 in CBM columns was not significantly different than week 1 ($p = 0.16$).

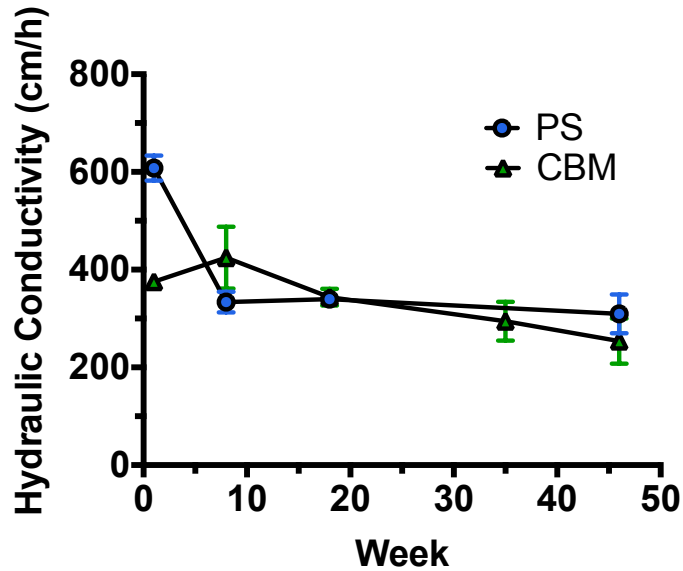


Figure 4.3 – Hydraulic conductivity (cm/h) of PS and CBM columns during weeks 1, 8, 18, 35, and 46. Hydraulic conductivity was measured via the falling head method from duplicated columns immediately following a 5-h stormwater injection. Error bars represent one standard deviation.

The relationship between the specific deposit from the Mays et al. clogging model (2005) and indicator organism log removal is displayed in Figure 4.4. In PS columns, no correlation was observed between specific deposit and *E. coli* or MS2 log removal. In CBM columns, the specific deposit remained below values observed in PS columns, but an increase in specific deposit was correlated with an increase in *E. coli* removal. For MS2, no correlation was observed between specific deposit and log removal.

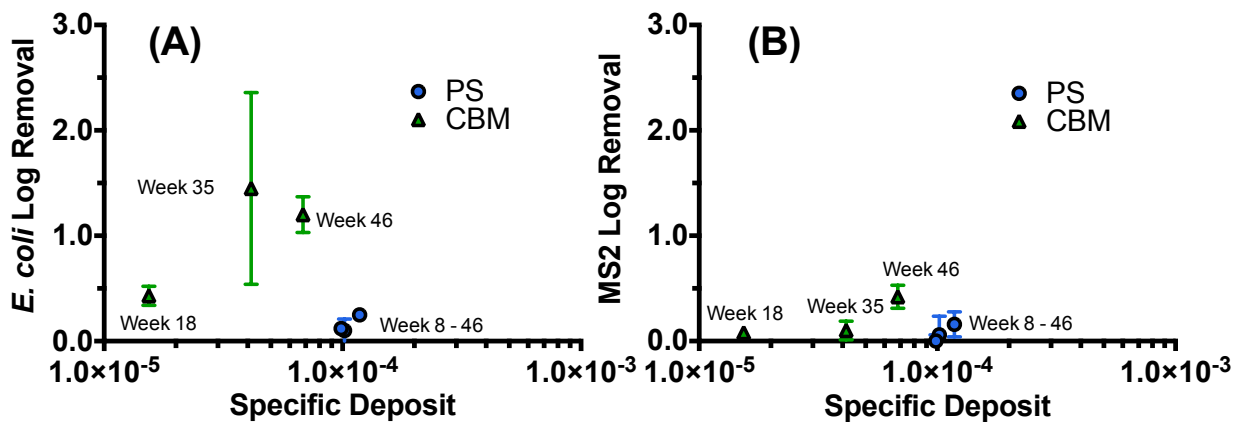


Figure 4.4 – Correlation between specific deposit and log removal of (A) *E. coli* and (B) MS2 for PS and CBM columns. Specific deposit was calculated using the Mays et al. clogging model

(2005). The week 8 specific deposit for CBM columns could not be calculated since HC remained unchanged from the initial HC. Error bars represent one standard deviation.

Effect Biological Activity on Indicator Removal

The effect of biological activity on *E. coli* and MS2 removal is reported in Figure 4.5. In PS columns, the sodium azide feed did not have a significant effect on removal of either *E. coli* or MS2. In CBM columns, the sodium azide feed had a significant effect on *E. coli* removal after 1 and 5 pore volumes (PV), reducing removal from 1.2 log to 0.6 log (p-value = 0.02) and 1.1 log to 0.4 log (p-value = 0.007), respectively. MS2 removal was not significantly different for the sodium azide feed.

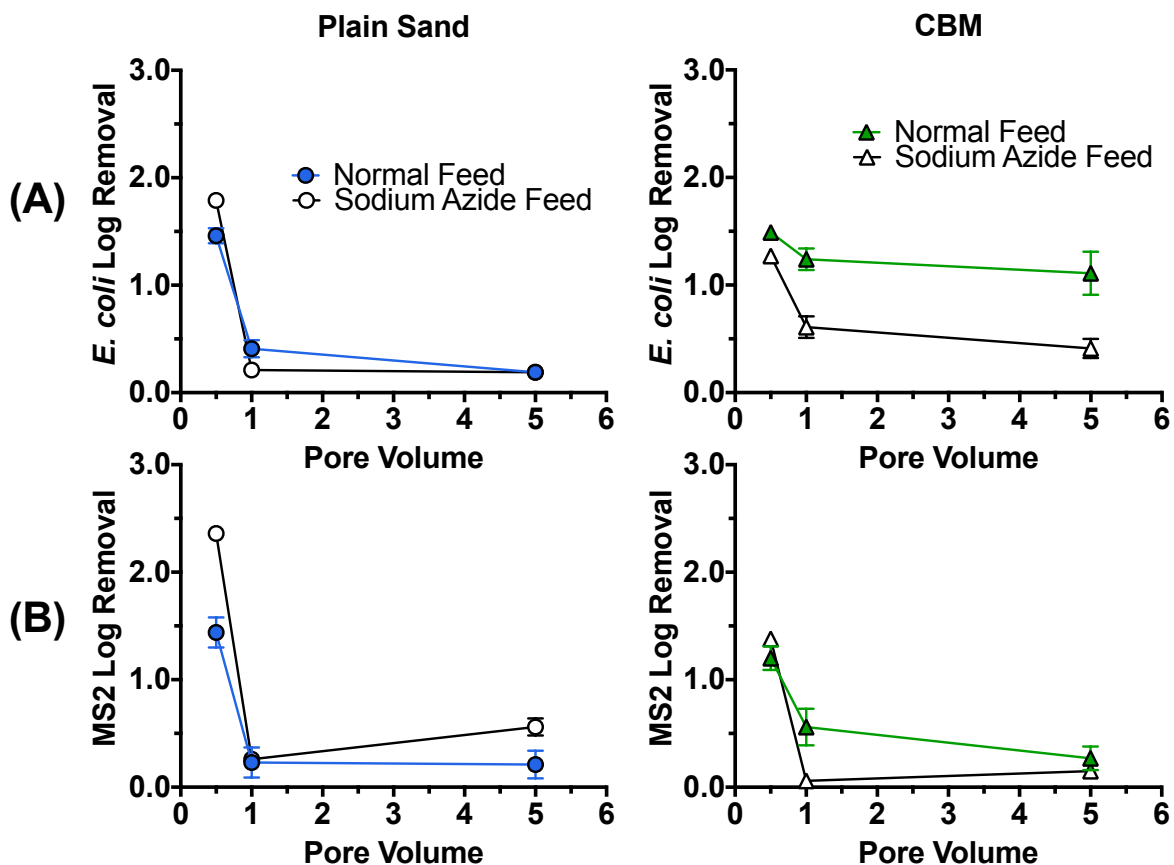


Figure 4.5 – (A) *E. coli* and (B) MS2 removal in PS and CBM columns fed with or without sodium azide feed. The normal feed was the same stormwater recipe used throughout the 46-week experiment. These data were collected during the week 46 regular feed. The sodium azide feed contained the stormwater recipe with 6 mM of sodium azide and was conducted on a different replicate column. The sodium azide feed was injected for 5 h on three consecutive days. Samples were analyzed for indicators on the 3rd day. Error bars represent one standard deviation.

Effect of Rest Period on Indicator Removal

The effect of a rest period on *E. coli* and MS2 removal is presented in Figure 4.6. In PS and CBM columns, the 24-h rest periods did not improve *E. coli* or MS2 removal above a 0-h rest period.

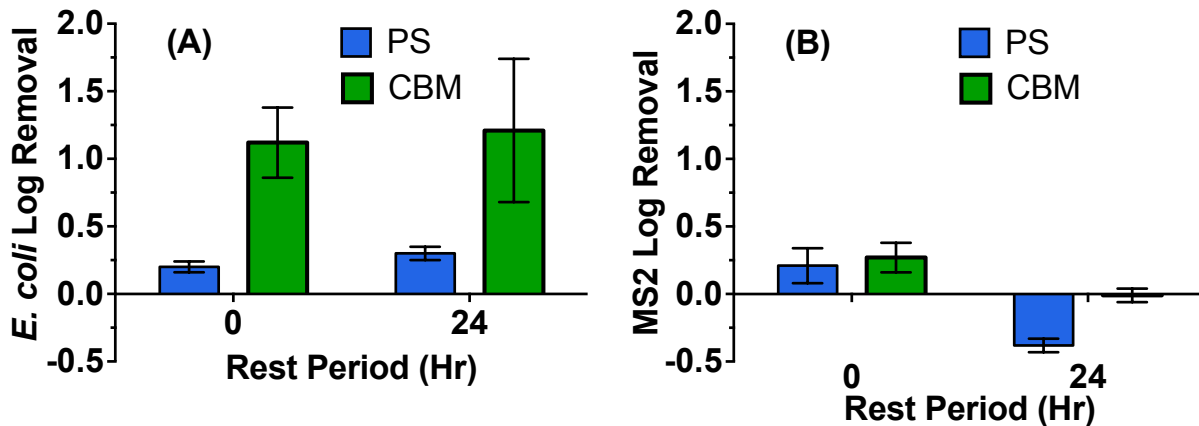


Figure 4.6 – (A) *E. coli* and (B) MS2 removal in PS and CBM columns after rest periods. Duplicate columns were first saturated with stormwater. After 24 h, stormwater was again injected, and the effluent was collected for analysis. The 0-h rest period removal data were collected from the week 46 injection in which stormwater was injected at a constant flow rate without a rest period. Error bars represent one standard deviation.

Biofilm Characterization on Media

The biofilm characterization results from the PS and CBM columns are shown in Figure 4.7. In PS and CBM columns, the ATP/cell concentration exhibited a similar trend throughout the experiment. It should be noted that the ATP/cell measured at week 8 in PS may not be accurate, because the cell counts were very low. ATP/cell generally increased over time to values between $1 \times 10^{-7} - 2 \times 10^{-7}$ ng ATP/cell, falling within the range observed in bacteria on drinking water granular media filters ($1.9 \times 10^{-8} - 7.3 \times 10^{-7}$ ng ATP/cell) (Lautenschlager et al., 2014; Magic-Knezev and van der Kooij, 2004; Vital et al., 2012). The increase in ATP content in cells over the initial 31 weeks suggests that attached cells increased in size and/or activity and then stabilized for the experiment's remaining duration (Karl, 1980).

The ATP/g and cells/g results exhibited different trends in PS and CBM columns. In PS columns, the ATP/g and cells/g results from the top media section increased throughout the experiment. In the final sacrifice, ATP/g and cells/g values in the top section were higher than values in the middle and bottom media sections by a factor of 3. These differences may reflect the formation of a *Schmutzdecke*, the biologically active cake layer documented in previous slow sand filter (SSF) studies (Huisman and Wood, 1974; Fox et al., 1984).

In CBM columns, significant differences in ATP/g or cells/g results between column sections were not observed, and the results have been combined in Figure 4.7. These results suggest that a more uniform microbial community was maintained throughout the column and that a *Schmutzdecke* was not formed in the top media section. In general, the ATP/g and cells/g results were an order of magnitude higher than corresponding values in PS columns. These values agreed well with ATP/g (100 – 30,000 ng ATP/g) (Lehtokari et al., 1983; Tiquia et al., 2002; Tseng et al., 1996) and cells/g (about 1×10^{11} cells/g) ranges (Czaczyk et al., 2001) from previous compost studies, indicating that the compost amendment supported a robust microbial community that was likely present in the initial compost used to prepare the column media. Between weeks 18 and 46, the cells/g values decreased significantly (p-value = 0.0004), but the ATP/g values did not (p-value = 0.2). When combined with the ATP/cell values, these results suggest that the cell number on the media may have decreased but the remaining cells were probably larger and more active.

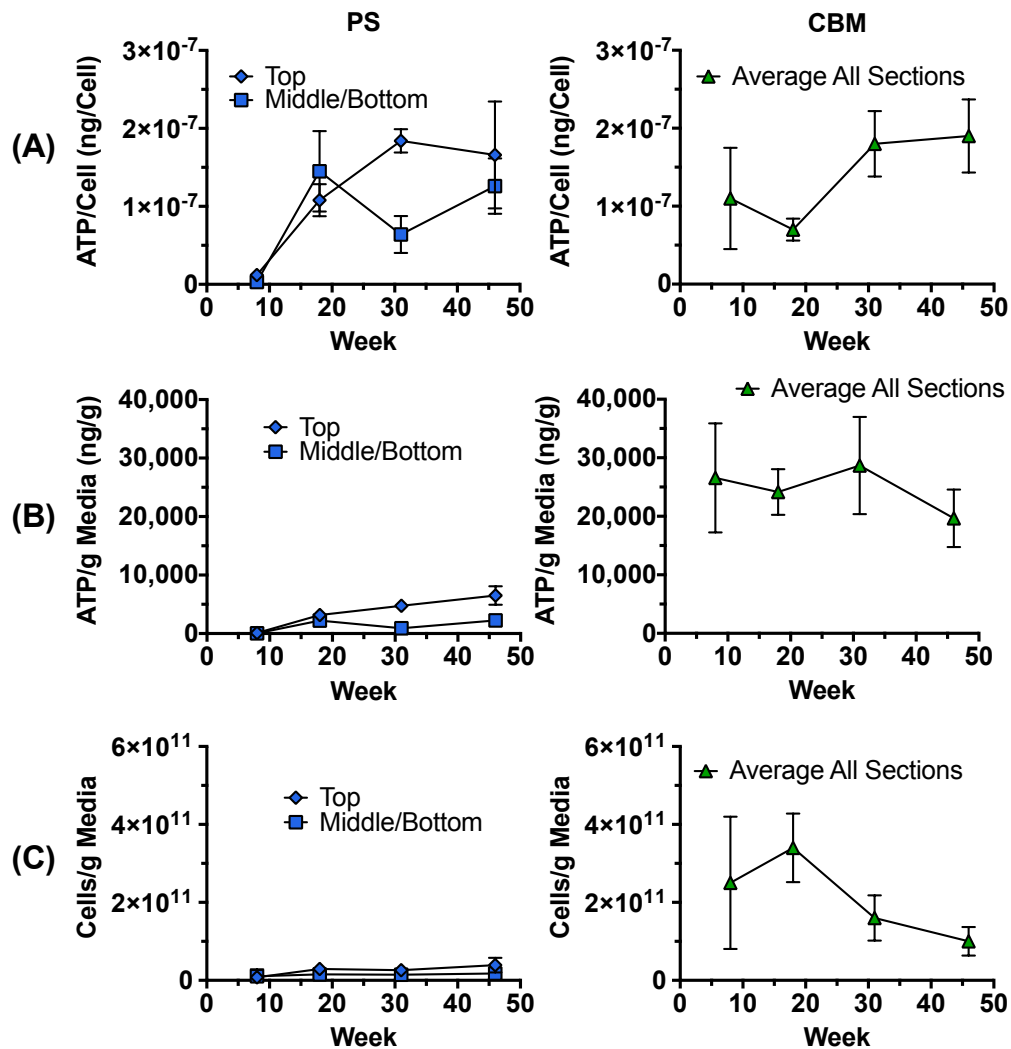


Figure 4.7 – Biofilm characterization in PS and CBM columns reported as (A) ATP/cell, (B) ATP/g Media, and (C) Cells/g Media. Columns were sacrificed during weeks 8, 18, 31, and 46,

and samples were taken from the top, middle, and bottom 3 cm of duplicate columns. PS data from the middle and bottom sections and CBM data from all sections were averaged due to statistical similarity ($p > 0.05$). Error bars represent one standard deviation.

Flow Cytometry Counts of Influent and Effluent Samples

The total cell counts (TCC) in weekly influent and PS and CBM column effluent samples were analyzed beginning in week 24 and are presented in Figure 4.8. The influent TCC was variable but averaged $3.2 \times 10^6 \pm 3.2 \times 10^6$ cells/mL. In PS and CBM column effluent, the average TCC was higher than in the influent. CBM effluent contained the highest TCCs, exceeding the influent TCCs by a factor of 3.1 – 6.5.

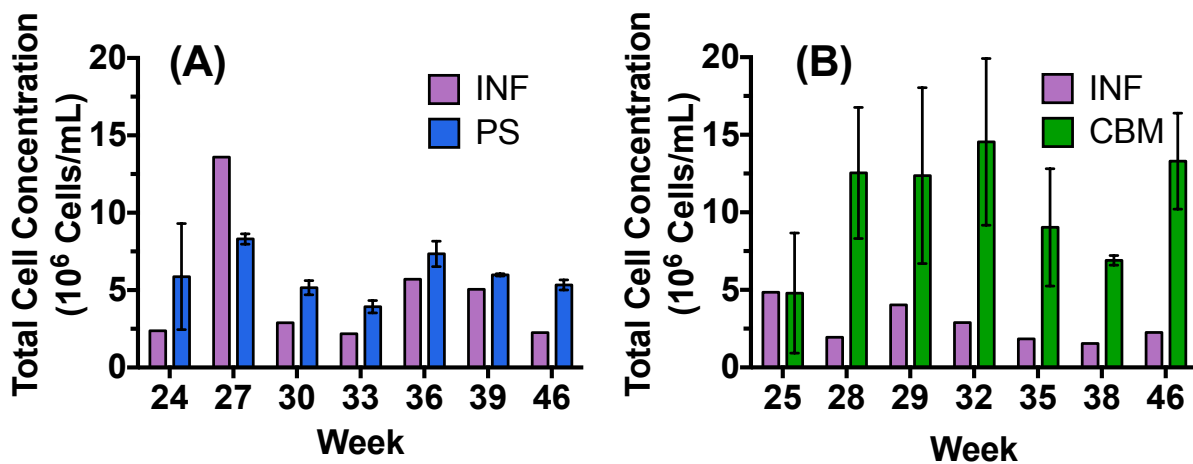


Figure 4.8 – TCCs in the influent and effluent of (A) PS and (B) CBM columns. Samples were taken after 3 pore volumes of stormwater had been injected and measured via flow cytometry. Error bars represent one standard deviation.

The TCC results from the week 46 injection experiment, divided into HNA and LNA bacteria concentrations, are presented in Figure 4.9. The influent was dominated by HNA bacteria, which accounted for approximately 65% of TCCs. In PS and CBM column effluent, the initial 0.5 PV contained the highest TCCs with values exceeding the influent by a factor of 5 – 12. The spike in effluent TCCs during the initial PV can be attributed to growth of bacteria in the columns during dry periods that were mobilized at the air-water interface as the wetting front progressed through the drained column (Auset et al., 2005). HNA and LNA effluent concentrations were both higher than the corresponding influent values; however, the samples collected at 0.5 PV were dominated by LNA bacteria (41% HNA). Similar changes in the HNA/LNA ratio toward LNA bacteria dominance have been observed in previous SSF studies (Lautenschlager et al., 2014; Vital et al., 2012), and there are at least two possible explanations: (1) there was a shift in the bacterial community during the intermittent period that favored the growth of LNA bacteria, possibly from a superior ability to grow during dry and low nutrient conditions (Wang et al., 2009); or, (2) the LNA bacteria were mobilized more readily than the HNA bacteria.

Unfortunately, we did not characterize HNA and LNA bacteria in the biofilm samples. After 5 PVs, the effluent TCC for both PS and CBM columns decreased to values observed during weekly monitoring in which samples were collected after 3 PVs, and HNA bacteria were again dominant (61% HNA).

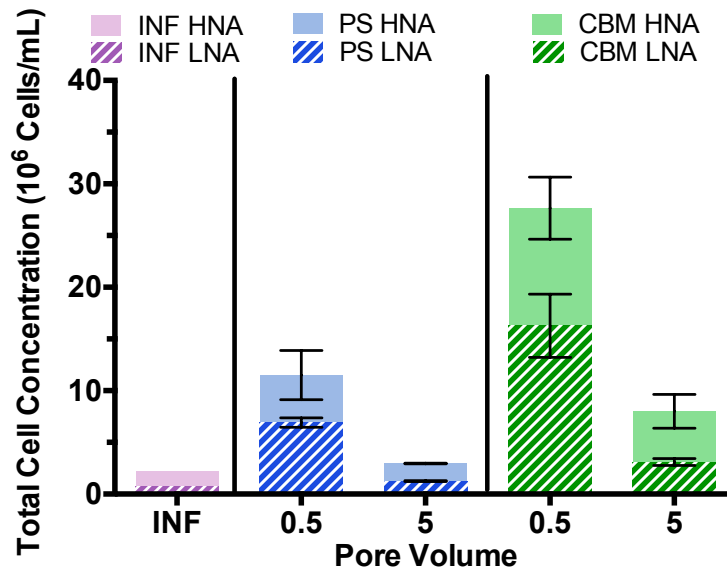


Figure 4.9 – Influent and PS and CBM effluent TCCs, reported as HNA and LNA bacteria concentrations, during the week 46 injection. The influent sample was taken at the beginning of the stormwater injection. Effluent samples were taken after 0.5 and 5 pore volumes of stormwater had been injected into the columns. Error bars represent one standard deviation.

Discussion

The results from this study demonstrated the importance of media aging, clogging, and biological activity to the removal of *E. coli* in stormwater columns filled with CBM.

E. coli and MS2 Removal

The *E. coli* removal, HC, and clogging results from PS and CBM columns exhibited different trends as the columns aged. In PS columns, the low, unchanged *E. coli* removal throughout the experiment likely stemmed from limited or incomplete *Schmutzdecke* and extracellular polymeric substance (EPS) formation. *E. coli* removal in a SSF, which operates under similar infiltration rates as the columns in this study, has been attributed to straining and adsorption in both the *Schmutzdecke* and underlying media (Huisman and Wood, 1974). Biological activity has been identified as having the strongest influence on removal efficiency (Bellamy et al., 1985), and EPS formation has been previously shown to increase colloid removal in porous media (Leon Morales et al., 2007). In this study, the ATP/g and cells/g data demonstrated clear

biological growth throughout the 46-week experiment, especially in the top column section where a *Schmutzdecke* was likely forming. However, the biofilm may have been heterogeneously distributed or incomplete as previous SSF studies found biological growth in both the *Schmutzdecke* and underlying media to be spatially and temporally variable (Campos et al., 2002; Vandevivere and Baveye, 1992). Moreover, EPS production has been less prevalent in previous studies with low substrate feeds (Kim et al., 2010; Vandevivere and Baveye, 1992). In our study, the influent, with an average AOC concentration of 250 µg/L, likely contained significantly less substrate than the lowest substrate feeds (5 mg/L glucose) used in these studies (Vandevivere and Baveye, 1992). Our PS columns were also fed intermittently, further limiting their substrate exposure. Thus, the *Schmutzdecke* and EPS formation may have been insufficient or incomplete for *E. coli* retention. The same reasoning likely explains why the initial HC decrease at week 8 was not followed by further HC reductions. A similar initial decrease in HC has been observed in a previous study on biofilm growth in flow cells and was found to be influenced by biofilm accumulation in pore spaces (Kim et al., 2010). Vandevivere and Baveye (1992) previously observed biomass concentrations as low as 1.7×10^9 cells/cm³ to significantly decrease HC, a concentration surpassed by PS column media at week 8 (2.3×10^{10} cells/cm³). These researchers showed that further HC reductions, however, were found to depend on the influent substrate concentration and EPS linkages between cells and sand grains. Without EPS formation, which was less prevalent in low substrate feeds, the HC was found to stabilize after the initial decrease (Kim et al., 2010; Vandevivere and Baveye, 1992). EPS formation may have been limited in our PS columns and may account for the limited HC reductions after the initial decrease.

In CBM columns, the compost amendment in the media likely influenced the initial HC and *E. coli* removal results. Compared to sand, compost has a lower HC (by a factor of 25) and a higher specific surface area, cation exchange capacity (CEC), and hydrophobicity (Grebel et al., 2013). Thus, these properties led to the lower initial HC in CBM but also provided more adsorption sites for the slightly higher initial *E. coli* removal (Lawrence and Hendry, 1996). In the aged columns, several mechanisms were likely occurring that were responsible for the steady increase in clogging and *E. coli* removal. Increased clogging in aged filters has been attributed in previous filtration studies to both abiotic and biotic processes. The abiotic process involves the accumulation of suspended solids in pore spaces (Siegrist and Boyle, 1987; Le Coustumer et al., 2009; Le Coustumer et al., 2012). The biotic process involves EPS layer formation, a microbial response to high substrate inputs and desiccation stress (Kim et al., 2010; Roberson and Firestone, 1992; Vandevivere and Baveye, 1992), and gas bubble production, a bi-product of microbial respiration (Ronen et al., 1989). The abiotic and biotic clogging processes fill pore spaces with material, cause more dispersive flow paths, and reduce HCs (Mattison et al., 2002; Or et al., 2007; Vandevivere and Baveye, 1992). More importantly, clogging causes changes in the filter pore spaces that likely led to the observed increase in *E. coli* removal, including increased contact time with filter media, reduced distance between bacteria and filter media (Yates and Yates, 1987), increased exposure to a biofilm and EPS layers (Bellamy et al., 1985), and increased exposure to air-water interfaces (Wan et al., 1994). Although *E. coli* removal increased after week 25, considerable variability in removal results was observed across replicates through week 38. A similar pattern for *E. coli* removal was observed previously by Zhang et al. (2011) in CBM columns monitored over 18 months. Variable initial removal efficiencies were followed by higher and more uniform removal results after 6 months. This observation was also attributed to clogging with a model correlating increased hydrodynamic

dispersion and decreased porosity with increased *E. coli* removal (Zhang et al., 2011). These results suggest clogging contributes to *E. coli* removal and that the clogging process can be variable between replicates.

An important finding in this study is the distinction between the effects of infiltration rate and HC on the removal of *E. coli*. Previous column studies were operated where the infiltration rate was determined by gravity flow through the media, such that lower HC was correlated with lower infiltration rate (Barrett et al., 2013; Bright et al., 2010; Chandrasena et al., 2012; Chandrasena et al., 2014; Kim et al., 2012; Li et al., 2012; Rusciano and Obropta, 2007). As expected from filtration models, these studies found that slower infiltration rates caused by lower HC were correlated with increased *E. coli* removal (Chandrasena et al., 2014; Tufenkji and Elimelech, 2004); however, it is unclear whether increased *E. coli* removal stems simply from the slower infiltration rate or from processes associated with clogging, including abiotic and biotic material accumulation. In this study, we maintained constant infiltration rates (10 cm/h) and residence times (41 min) throughout the study by injecting stormwater into columns with a pump in the upward direction. This setup allowed us to isolate the impact of changes in HC and enabled better identification of factors that contributed to different performance between the media types. We recommend that future studies should also attempt to separate HC from infiltration rate to aid better comparisons between media with different properties.

MS2 removal in both PS and CBM columns was low and exhibited little change throughout the 46-week experiment. Low initial removal in both column types was expected as repulsive electrostatic interactions between virus and media (Yuan et al., 2008) and high pH in the influent (Chu et al., 2003) all negatively impact virus attachment. However, it was unexpected that MS2 removal would not improve over time, as *E. coli* removal did. The low removal also contrasted sharply with the 4.3-log F-RNA coliphage removal observed in a previous study (Li et al., 2012). Several reasons may explain these different results. First, the Li et al. (2012) study used columns that were deeper by a factor of 3.5 and filled with different media (sandy loam). Previous results have indicated that removal scales with depth (Tufenkji and Elimelech, 2004; Yates and Yates, 1987), and the different media mixture may have increased surface area, CEC, and attachment sites to aid virus removal (Lawrence and Hendry, 1996). Second, F-RNA coliphage may behave differently in filtration studies than lab-grown MS2. Different surface characteristics on viruses, including surface charge and hydrophobicity, can greatly influence removal in porous media (Redman et al., 1997). Third, the influent in the Li et al. (2012) study had a total suspended solids (TSS) concentration that was higher than this study by a factor of 4 – 60. Indicator viruses have been shown to associate with TSS in stormwater which can enhance removal by increasing transport to the media surface via sedimentation (Characklis et al., 2005; Cizek et al., 2008; Syngouna and Chrysikopoulos, 2015). Finally, further clogging and HC reductions may have been necessary to improve MS2 removal. Future research should focus on conditions that promote more reliable attachment of viruses, including column and media design, influent characteristics, and clogging levels.

Effect of Biological Community on Indicator Removal

Results from the sodium azide experiment suggest biological activity may have contributed to

the increased clogging and *E. coli* removal observed in aged CBM columns. In our study, sodium azide was used as a microbial inhibitor to suppress the respiration of both aerobic and denitrifying bacteria without disrupting the EPS layers formed by the biofilm (Weber-Shirk and Dick, 1997; Elliott et al., 2011). In the presence of sodium azide, *E. coli* removal in CBM columns was observed to significantly decrease after 1 and 5 PVs. In a similar experiment with an aged soil filter, Seki et al. (1998) observed a rapid increase in HC after column exposure to sodium azide, attributing the permeability increase to lower gas production from respiration and the opening of previously clogged pore spaces. Although HC in this study was not measured following the sodium azide experiment, the rapid decrease in *E. coli* removal to levels observed in fresh columns suggests microbial respiration and gas bubble production contributed to the increased clogging, reduced HCs, and increased *E. coli* removal in aged columns. In PS columns, the microbial community may have not have been numerous enough to produce enough gas bubbles to sufficiently reduce HC.

Previous filtration studies using sodium azide have observed a similar decrease and attributed it to suppression of predation or proteolytic enzyme production (Weber-Shirk and Dick, 1997; Elliott et al., 2011), but the results from the rest period experiments at week 46 indicate that decay from predation or enzymes were unlikely mechanisms for indicator organism removal. In a previous biosand study with significant grazing or enzyme production, Elliott et al. (2011) observed a first-order decay rate of MS2 during the rest period. MS2 log removal increased from less than 0.5 log at 6 h to over 1 log at 24 h. Elliott et al. (2011), however, operated biosand filters injected daily with influent that contained 2.5% by volume primary wastewater effluent. In contrast, we operated intermittent columns that were frequently drained and fed with influent once per week, exposing the microbial community to desiccation and starvation stresses. These conditions, typical for bioretention filters, and different influent sources (local creek versus primary wastewater) may not have been capable of supporting a microbial community capable of robust grazing or enzyme production, as indicator organism decay was not observed over 24 h. Thus, the increased *E. coli* removal observed in CBM columns likely relied on physical/chemical transport and attachment mechanisms related to clogging and reduced HC.

One limitation should be noted before expanding these findings. The influent TSS concentration in this study was an order of magnitude lower than average values found in stormwater (Grebel et al., 2013). Accumulation of TSS in pore spaces has been considered a main contributor to clogging in previous biofilter studies (Le Coustumer et al., 2012) and likely contributed less to this study due to the lower influent concentration. A similar experiment with higher TSS concentrations may help to understand the relative contribution of abiotic and biotic processes toward clogging and indicator organism removal.

Biofilm Characterization and Flow Cytometry Counts

Overall biofilm growth was monitored by tracking attached biomass and suspended bacteria concentrations. In PS and CBM columns, the attached biomass in week 46 averaged 1.8×10^{10} and 1.1×10^{11} cells/g, respectively. When multiplied by the total mass of media in PS and CBM columns, the total number of attached cells was 3.9×10^{12} and 1.7×10^{13} cells, respectively. The suspended bacteria concentrations in PS and CBM effluent during a 1-year storm averaged 5.0×10^6 and 1.3×10^7 cells/mL, respectively. When multiplied by a 1-year storm's volume, the

total number of cells in PS and CBM effluent was 1.3×10^9 and 3.2×10^9 cells, respectively. Thus, suspended bacteria lost in the effluent during each 1-year storm injection accounted for 0.03% and 0.01% of total attached cells in PS and CBM columns, respectively. This observation contrasts with biofilm results from a drinking water granular activated carbon (GAC) filter in which the majority of bacteria grown, nearly 84%, were lost in the effluent as suspended bacteria. These drinking water filters, however, were operated continuously at infiltration rates near 600 cm/h, likely scouring off new cells as they were produced (Velten et al., 2011). In our study, the PS and CBM columns were operated intermittently at infiltration rates below 10 cm/h. The combination of short, intermittent injections and lower infiltration rates may have limited the number of cells scoured off PS or CBM biofilms. Therefore, it seems likely that attached biomass changes in PS and CBM were not impacted heavily by cell loss in the effluent and were likely influenced by the influent substrate concentration (Kim et al., 2010) and microbial community in compost (Czaczyk et al., 2001).

Another interesting observation in the CBM columns is the contrast between the effluent TCCs and *E. coli* removal results. Effluent TCCs were consistently higher than the influent whereas *E. coli* removal was observed to increase to about 1.5 log with age. Previous drinking water SSF studies have observed similar high effluent TCCs and hypothesized the bacteria originated from the media biofilm (Hammes et al., 2010; Lautenschlager et al., 2014). *E. coli* removal may be occurring throughout the depth of the filter, but the other bacteria may be leaching from the compost and sand media into the effluent. Future research should focus on understanding the microbial makeup of this effluent to determine if there are risks of pathogen growth within the filter's bacterial community.

Conclusions

Overall, the results from this study provide insight into the removal mechanisms of *E. coli* in bioretention basins. In CBM columns, *E. coli* removal increased gradually with age and clogging, and some evidence suggested that biofilm growth and microbial respiration impacted performance. In PS columns, a similar increase in *E. coli* removal was not observed over the course of the experiment. The main benefit of the compost amendment to sand in CBM appears to be the addition of a microbial community to the media. This community may have led to a faster and more robust development of a biofilm over time that contributed to clogging and the retention of *E. coli*. PO_4^{3-} leaching, however, was observed in CBM columns throughout the experiment. Care should be exercised when selecting the type and proportion of compost to minimize PO_4^{3-} leaching while maintaining *E. coli* removal. The experimental setup in this study, in which infiltration rates were set by a pump, distinguished whether slower infiltration rates or other processes associated with clogging (buildup of solids or biofilm in pore spaces) were responsible for the observed *E. coli* removal. A similar setup should be considered in future studies to ensure better comparisons between results from different media types. Larger diameter media was used in this study to permit large changes in HC. This media, however, would likely result in extreme infiltration rates if operated under gravity flow, and smaller media should be used for gravity-fed bioretention basins.

Future research should focus on the biofilm, identifying conditions that optimize growth and

respiration during operation. First, varying stormwater matrices, based on street or lawn runoff, could give insight into characteristics, like AOC, that are important for biofilm growth. Second, microbial sequencing on attached biomass could provide valuable insight into whether indicator organisms are growing in the biofilm. Finally, future research should investigate conditions, including clogging, influent TSS concentrations, and media mixtures, which contribute to MS2 removal. These studies would provide additional insight into how to improve the predictability of indicator organism removal by bioinfiltration basins with CBM for stormwater treatment.

Part 2A Cont. – Stormwater Treatment Unsaturated Column Experiment

Chapter 5: Results and Discussion for Intermittently Fed, Unsaturated Stormwater Columns with Zero Valent Iron-Amended Media

Results

Short-term Column Studies

Escherichia coli (*E. coli*) removal in the short-term experiment with plain sand (PS) and 10% by weight ZVI-amended sand (PS+ZVI) columns is reported in Figure 5.1. Detection limit removal of *E. coli* was observed in the PS+ZVI column (5.1 log removal) through 2 pore volumes (PV) and removal remained above 4 log through 3.2 PVs. *E. coli* removal in PS columns remained below 0.5 log throughout the experiment.

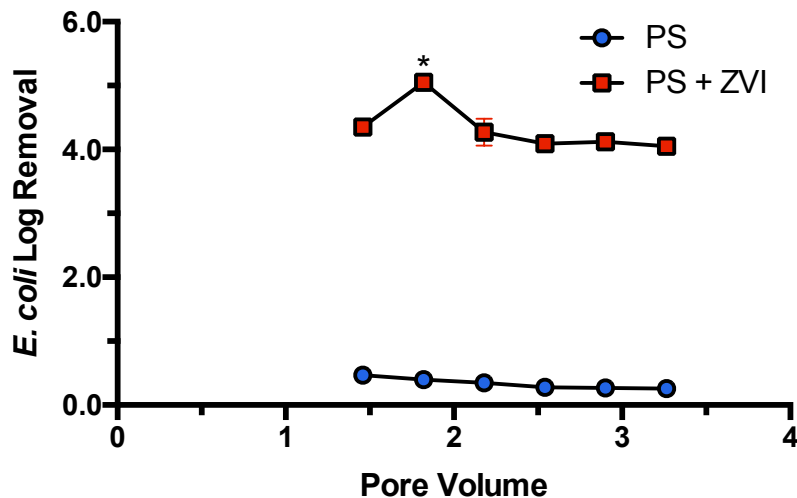


Figure 5.1 – *E. coli* removal through 3.2 pore volumes in PS and PS+ZVI columns. * denotes removal to the detection limit (10 CFU/mL). Error bars represent one standard deviation.

46-Week Removal of *E. coli* and MS2

E. coli and MS2 coliphage (MS2) removal in PS, PS+ZVI, and 10% by weight ZVI-amended conventional bioretention media (CBM+ZVI) columns in the 46-week experiment is shown in

Figure 5.2. *E. coli* removal in PS columns was below 0.5 log throughout the experiment. In PS+ZVI columns, *E. coli* removal was above 1 log through 9 weeks and decreased to about 0.5 log afterwards. In CBM+ZVI columns, *E. coli* removal was low (0.5 log) through week 24 and increased slightly to about 1 log by week 41.

MS2 removal in PS columns was low and unchanged throughout the study. In PS+ZVI columns, MS2 removal followed a similar trend as observed for *E. coli* removal: 1.4 log removal at week 11 was followed by a rapid decrease as the columns aged. In CBM+ZVI columns, MS2 removal was low and did not improve over the course of the experiment.

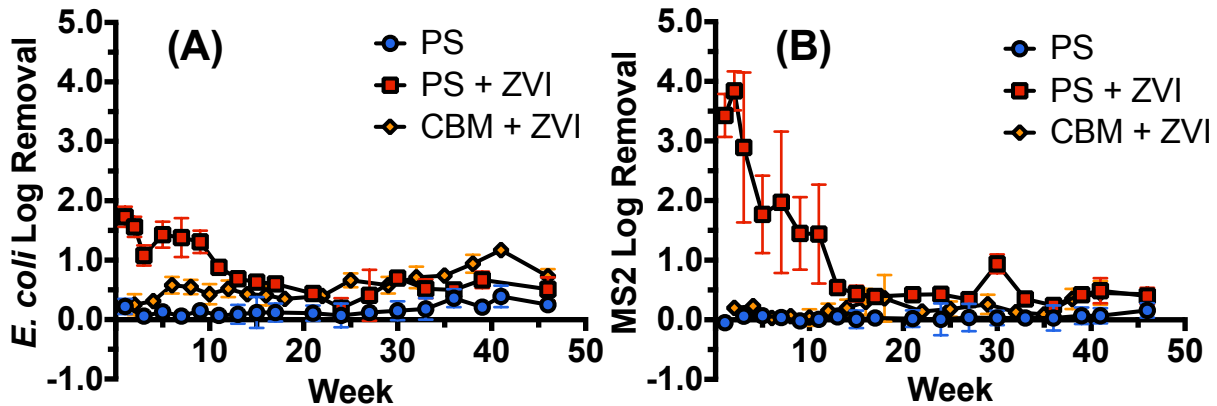


Figure 5.2 – Removal of (A) *E. coli* and (B) MS2 in PS, PS+ZVI, and CBM+ZVI columns. Stormwater was injected weekly for 5 h and samples were taken after 3.2 – 3.5 pore volumes of stormwater passed through the columns. Error bars represent one standard deviation.

Total Organic Carbon, Phosphate, and Flow Cytometry Counts

The normalized total organic carbon (TOC) and phosphate (PO_4^{3-}) concentrations from PS, PS+ZVI, and CBM+ZVI columns are presented in Figure 5.3. The average influent TOC concentration and standard deviation throughout the 46-week experiment was 9.3 ± 1.84 mg/L. In PS columns, the effluent TOC concentration closely tracked the influent concentration. In PS+ZVI columns, TOC removal averaged 30% between weeks 8 – 41. In CBM+ZVI columns, the initial effluent TOC concentration was higher than the influent (averaging 28 mg/L), likely due to the breakdown of compost in the media. After week 1, however, TOC removal increased, averaging 13% for weeks 8 – 41.

The average influent PO_4^{3-} concentration was high and variable, averaging 1.98 ± 0.89 mg/L. In PS columns, PO_4^{3-} removal was variable but stabilized after week 24 around 25%. PO_4^{3-} removal was higher in both PS+ZVI and CBM+ZVI columns, averaging 85% throughout the study.

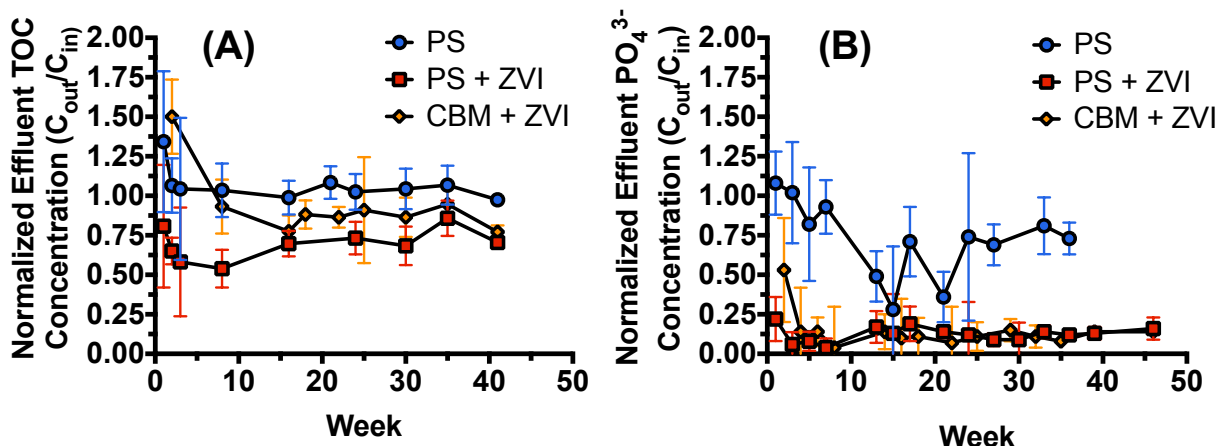


Figure 5.3 – Normalized (A) TOC and (B) PO₄³⁻ concentrations in PS, PS + ZVI, and CBM + ZVI effluent. Error bars represent one standard deviation.

Measurement of the total cell concentrations (TCC) began in week 24, and the results for the influent and PS+ZVI and CBM+ZVI effluents are reported in Figure 5.4. From week 24 – 46, the influent TCC averaged $3.2 \times 10^6 \pm 3.2 \times 10^6$ cells/mL. In PS+ZVI effluent, the TCC matched or slightly exceeded the influent TCC. In CBM+ZVI effluent, the TCC was nearly an order of magnitude higher than the PS+ZVI effluent TCC and exceeded the influent TCC by a factor of 1.4 – 9.8.

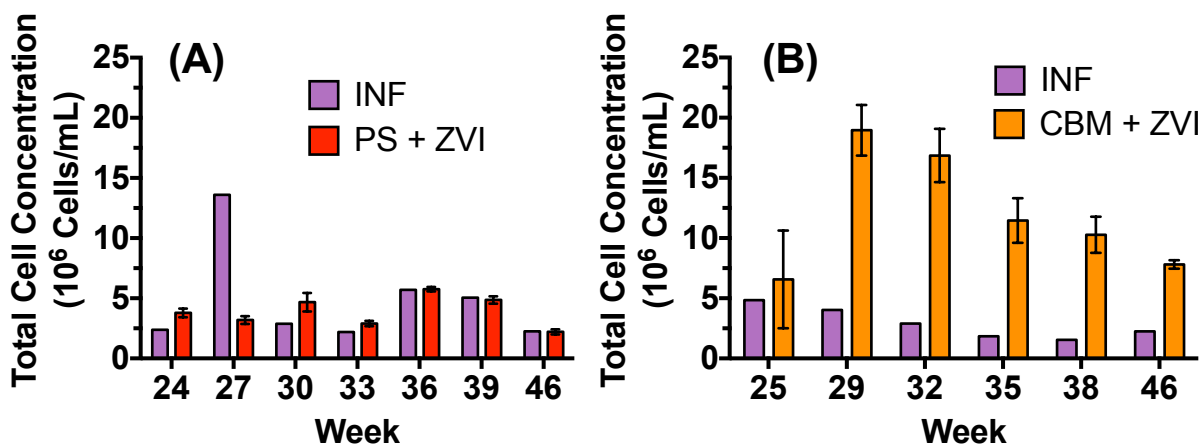


Figure 5.4 – TCCs in the influent and effluent of (A) PS + ZVI and (B) CBM + ZVI columns. Samples were taken during weekly stormwater injections after 3 pore volumes and analyzed via flow cytometry. Error bars represent one standard deviation.

TCCs, broken down into high nucleic acid (HNA) and low nucleic acid (LNA) bacteria concentrations, from the week 46 injection experiment are reported in Figure 5.5. The influent TCC averaged 1.8×10^6 cells/mL and contained a majority (66%) of HNA bacteria. In PS+ZVI

and CBM+ZVI effluent, the highest TCCs were observed in the initial 0.5 PV and likely occurred due to bacteria growth in the columns during dry periods and remobilization at the advancing wetting front (Auset et al., 2005; Mohanty et al., 2013). After 5 PVs, effluent TCC in both columns decreased to similar values observed in Figure 5.4. The HNA and LNA bacteria community in both PS+ZVI and CBM+ZVI effluent also mirrored the influent community with HNA bacteria accounting for about 60% of the TCCs throughout the week 46 storm.

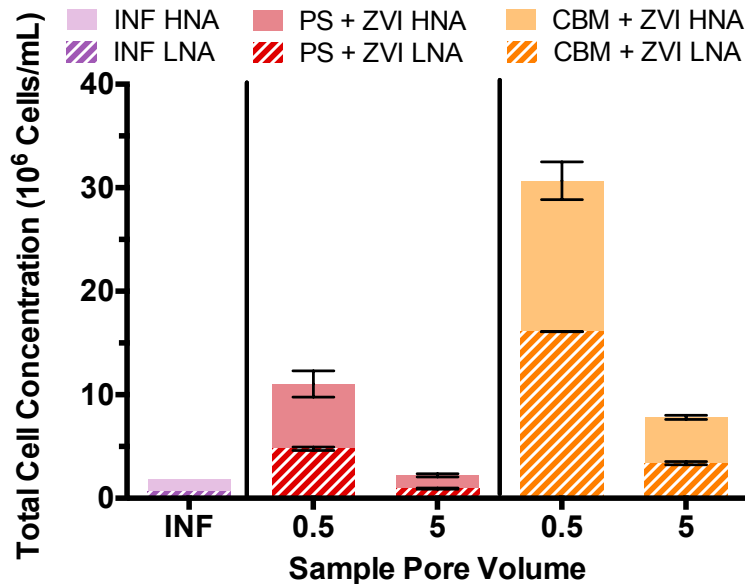


Figure 5.5 – TCC, broken down into LNA and HNA bacteria, in the influent and effluent of PS + ZVI and CBM + ZVI during the week 46 breakthrough experiment. The influent sample was taken at the beginning of the stormwater injection. Samples from the effluent were taken after 0.5 and 5 pore volumes of stormwater had been injected. Error bars represent one standard deviation.

Hydraulic Conductivity and Iron Leaching

Saturated hydraulic conductivity (HC) in PS, PS+ZVI, and CBM+ZVI columns is reported in Figure 5.6. The initial HC in PS and PS+ZVI columns was higher than in CBM+ZVI, likely due to the lower HC of compost in CBM. In PS columns, the HC at week 8 decreased by a factor of 1.8 from week 1 but then stabilized for the rest of the study. In PS+ZVI columns, the HC at week 8 decreased by a factor of 11 from week 1. At week 18, the HC decreased by a factor of 30 from week 1 before stabilizing for the remainder of the experiment. In CBM+ZVI columns, the HC decreased gradually throughout the experiment, reducing by a factor of 7 between week 1 and 46. The final HC in week 46 was lower in PS+ZVI columns (16 cm/h) than in CBM+ZVI columns (49 cm/h). Beginning in week 31, a high level of cementation, in which media grains were tightly bound together, was observed in both PS+ZVI and CBM+ZVI columns.

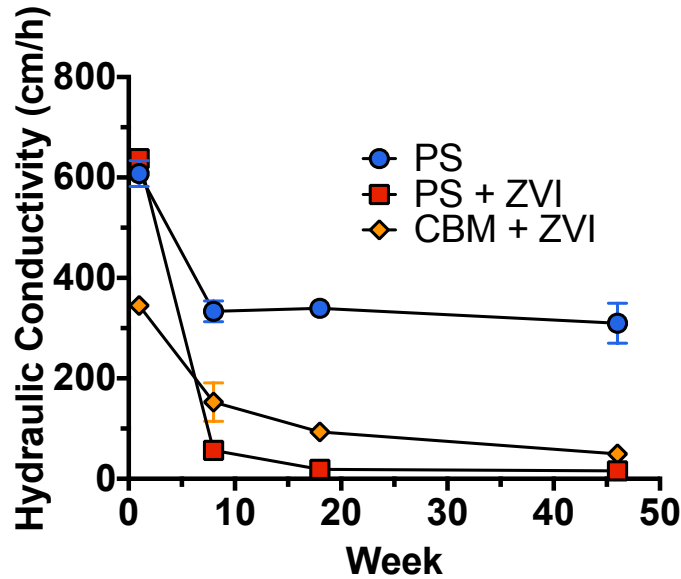


Figure 5.6 – Hydraulic conductivity (cm/h) of PS, PS + ZVI, and CBM + ZVI columns during weeks 1, 8, 18, and 46. Hydraulic conductivity was measured in duplicate columns via the falling head method immediately following a 5-h stormwater injection. Error bars represent one standard deviation.

Dissolved ferrous iron (Fe[II]), dissolved ferric iron (Fe[III]), and total iron (Tot Fe) concentrations in PS+ZVI and CBM+ZVI effluent during weekly stormwater injections are presented in Figure 5.7. In PS+ZVI columns, effluent Fe[II] and Fe[III] were below the detection limit (0.05 mg/L) throughout the experiment. Tot Fe was detected at week 21 and increased to 0.5 mg/L at week 36. In CBM+ZVI columns, Fe[III] and Tot Fe were measured in the effluent between weeks 1 – 3. Afterwards, the effluent contained highly variable concentrations of Fe[II] and Tot Fe. Interestingly, the effluent concentrations at week 46 were below the detection limit, suggesting leaching may have ceased.

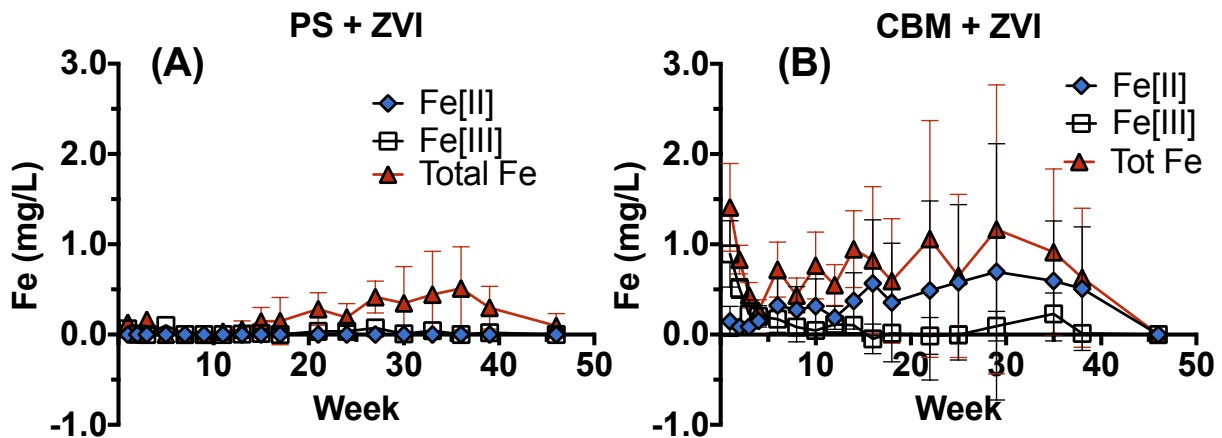


Figure 5.7 – Fe[II], Fe[III], Tot Fe concentrations in (A) PS + ZVI and (B) CBM + ZVI effluent during weekly stormwater injections. Samples were taken after 3 pore volumes of stormwater

had been injected into the columns. Error bars represent one standard deviation.

Effluent Fe[II], Fe[III], and Tot Fe concentrations throughout injections during weeks 8 and 46 are presented in Figure 5.8. In PS+ZVI columns, effluent Fe[II] and Fe[III] were below the detection limit throughout both injections, but effluent Tot Fe concentrations around 1 mg/L were observed in the initial 0.5 PV. In CBM+ZVI columns, effluent Fe[II], Fe[III], and Tot Fe concentrations throughout both injections were consistent with results in Figure 5.7. During week 8, effluent Fe[II] and Tot Fe concentrations were observed around 0.7 and 1 mg/L, respectively. During week 46, Fe[II], Fe[III], and Tot Fe concentrations were not observed in the effluent.

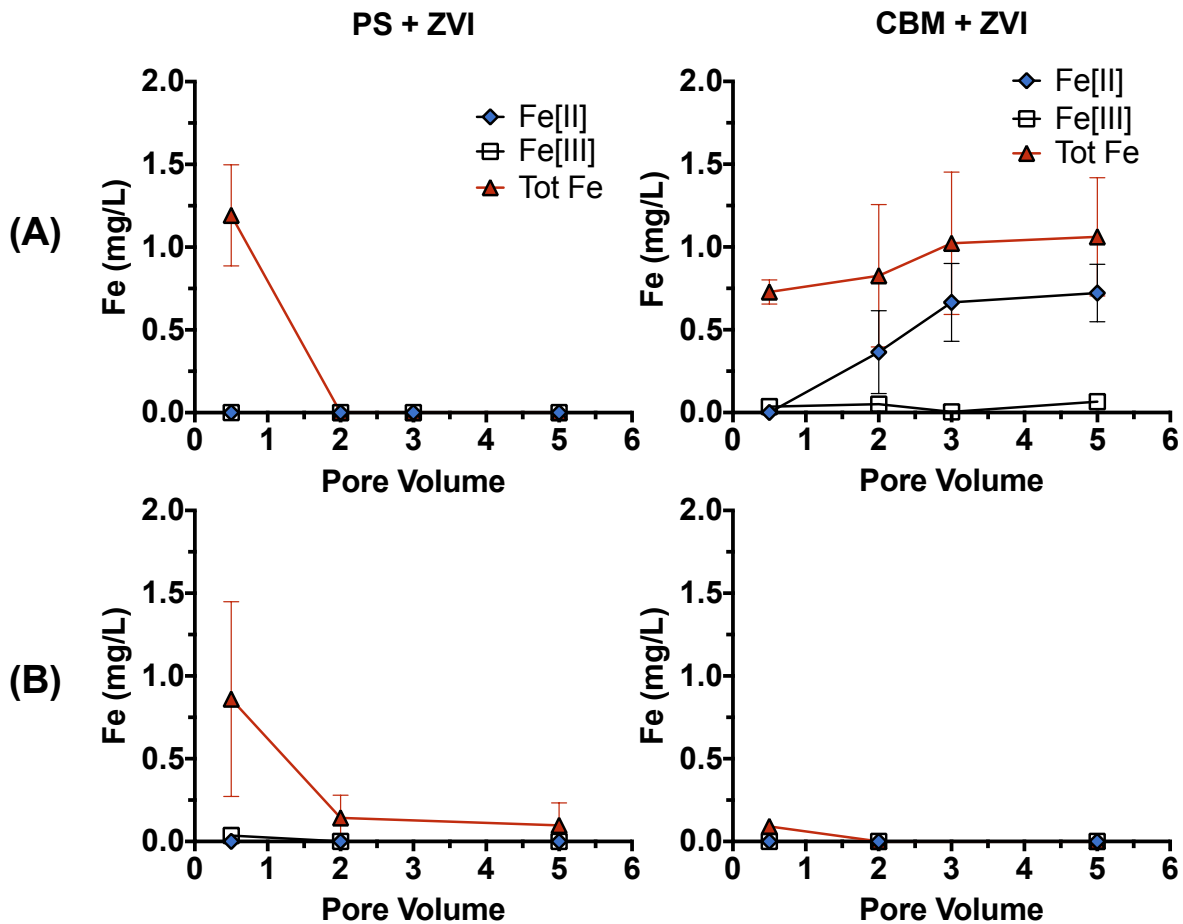


Figure 5.8 – Fe[II], Fe[III], Tot Fe concentrations in PS + ZVI and CBM + ZVI effluent during the (A) week 8 and (B) week 46 injections. Samples were taken at multiple points (0.5, 2, 4, and 5 pore volumes) throughout the 5-h stormwater injection. Error bars represent one standard deviation.

Effect of Rest Period on *E. coli* and MS2 Removal

The effect of a rest period on *E. coli* and MS2 removal in PS, PS+ZVI, and CBM+ZVI columns is presented in Figure 5.9. In PS columns, the 24-h rest periods had little effect on *E. coli* or MS2 removal. In PS+ZVI columns, the 24-h rest period had a significant effect on both *E. coli* and MS2 removal. In CBM+ZVI columns, the 24-h rest period significantly improved *E. coli* but not MS2 removal.

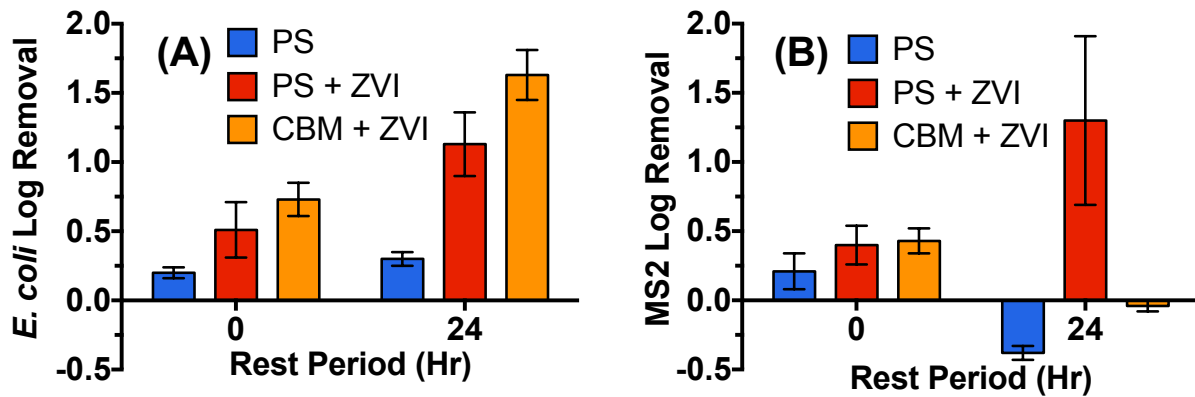


Figure 5.9 – (A) *E. coli* and (B) MS2 removal in PS, PS + ZVI, and CBM + ZVI columns after longer rest periods. For the 24-h rest period experiments, duplicate columns were saturated with stormwater and allowed to rest for the stated time period. Afterwards, stormwater was injected and the initial 0.5 pore volume of effluent was collected for indicator analysis. The 0-h rest period experiment is removal data from the week 46 injection in which stormwater was continually injected without a rest period. Error bars represent one standard deviation.

Discussion

Short-Term *E. coli* Removal in ZVI-Amended Column

In the short-term experiment, higher *E. coli* removal was observed in PS+ZVI columns as compared to PS columns, indicating the ZVI amendment contributed to the attachment of *E. coli*. These results are supported by several previous short-term ZVI studies conducted with bacteria (Ingram et al., 2012) and viruses (Bradley et al., 2011; Shi et al., 2012; You et al., 2005), and removal has been attributed to electrostatic attraction between the indicator organism and iron oxides on the ZVI filing (Bradley et al., 2011). The 4-log *E. coli* removal in our study also marked an improvement over previous short-term stormwater studies using an iron oxide-coated sand (IOCS). In experiments with similar setups (column size, media diameter, infiltration rate, duration, and influent water characteristics) as our study, Zhang et al. (2010) and Mohanty et al. (2013) evaluated *E. coli* removal by different IOCS and observed less than 1-log removal. ZVI amendments are potentially advantageous over IOCS for indicator organism removal because ZVI corrosion can continuously produce a mixture of iron oxides around the original iron filing

(Noubactep et al., 2009) whereas an IOCS has a pre-formed and limited quantity of a specific iron oxide bound to sand (Benjamin et al., 1996; Mills et al., 1994). The mixture of iron oxides also exhibits a range of point of zero charges (PZC) whereas the specific iron oxide on an IOCS exhibits a single PZC (Noubactep et al., 2009). At a similar pH, this mixture from ZVI corrosion may have a higher PZC than the IOCS, thereby exhibiting a more positive surface charge and enhancing electrostatic attraction between the iron oxides and indicator organisms (Brown and Sobsey, 2009). Although little corrosion likely occurred in our short-term study, the ZVI amendment (10% by weight) added more iron to the columns than in the previous IOCS studies (3% by weight) (Mohanty et al., 2013; Zhang et al., 2010). Thus, the ZVI amendment in the PS+ZVI columns may have provided more pre-formed adsorption sites (possibly due to ZVI filing corrosion prior to the experiment) for *E. coli* removal as compared to PS columns in our study and IOCS columns in previous studies (Mohanty et al., 2013; Zhang et al., 2010).

46-Week *E. coli* and MS2 Removal and Effect of Total Organic Carbon, Phosphate, and Background Microbial Community on Removal

Similar to the short-term experiment, the ZVI amendment in PS+ZVI columns was also observed to impact indicator organism removal in the 46-week experiment, as *E. coli* and MS2 removal was significantly higher in PS+ZVI columns than in PS columns through week 11. *E. coli* and MS2 adsorption again likely occurred due to favorable electrostatic interactions with the iron oxides on the ZVI filings (Bradley et al., 2011). However, unlike the short-term columns, repeated stormwater injections likely caused ZVI corrosion and the production of new iron oxides in the 46-week PS+ZVI columns. Direct analysis of iron oxides formed on the PS+ZVI media was not conducted, but significant HC reductions were observed at week 8. As ZVI corrodes, iron oxide products have been observed to expand in volume, reducing both porosity and HC (Noubactep, 2010). Ferrihydrite and hematite, for example, have been found to increase the volume occupied by the original ZVI filing by a factor of 6.4 and 2.1, respectively (Noubactep et al., 2009). Because similar HC reductions were not observed in PS columns, ZVI corrosion and iron oxide formation likely caused the observed HC reduction at week 8 in PS+ZVI columns.

For *E. coli* and MS2 removal in PS+ZVI from weeks 1 – 11, two observations from this period are worthy of comment. First, the magnitude of *E. coli* log removal during week 1 in the 46-week PS+ZVI columns was lower than the value observed in the short-term PS+ZVI columns by a factor of 3. The setup in both experiments (column size, iron amendment, media diameter, infiltration rate) was similar, but the synthetic stormwater influent had different characteristics. The short-term study used a stormwater spiked with a single *E. coli* strain and one interfering adsorbate (natural organic matter (NOM) at 20 mg/L TOC). While the amended creek water used for the 46-week experiment had lower TOC (about 10 mg/L), it had higher PO_4^{3-} (about 2 mg/L), higher pH (8.3), and an abundant and diverse microbial community. Higher pH and interfering adsorbates are known to reduce removal of *E. coli* in iron oxide media (Zhuang and Jin, 2008; Foppen et al., 2008) and likely reduced the week 1 *E. coli* removal in the 46-week columns as compared to the short-term columns. Second, during co-transport of two indicator organisms in the 46-week columns, the MS2 log removal value was observed to be nearly twice the *E. coli* log removal value from weeks 1 – 11. The favorable electrostatic interactions contributing to *E. coli* attachment to iron oxides may have been impacted more by the presence of competing ions

(NOM, PO_4^{3-}) and other microorganisms than the interactions for MS2 attachment. Furthermore, *E. coli*, with an average diameter about two orders of magnitude larger than MS2, may have been inhibited from accessing the iron oxides due to its size (Foppen et al., 2006; Foppen et al., 2008).

After week 11, the effectiveness of ZVI corrosion and iron oxide production for indicator organism removal in PS+ZVI columns may have decreased. ZVI corrosion likely continued as further HC reductions were observed after week 11 (HC at week 30 was lower than HC at week 8 by a factor of 3), but both *E. coli* and MS2 removal in PS+ZVI columns decreased from 1 log during week 11 to less than 0.5 log for the remaining weeks. Only two other filtration studies with ZVI amendments have reported removal of indicator organisms for operation over several months. Both of these studies mimicked household scale drinking water treatment by biosand filters, which are operated differently than typical stormwater bioretention basins. Bradley et al. (2011) did not observe a similar reduction in ZVI effectiveness over 36 weeks of daily operation, reporting greater than 6-log MS2 removal. However, their filters were kept constantly saturated and were deeper (40 cm), had higher ZVI content (14% by weight), higher residence times in ZVI-amended media (24 h), and lower influent NOM (3.1 mg/L TOC). In contrast, Chiew et al. (2009) reported a decrease in ZVI effectiveness for both *E. coli* and MS2 after 24 weeks. In that study, influent was poured through a ZVI diffuser before entering the biosand filter, limiting ZVI contact to a timeframe similar to our study. Higher ZVI content in the diffuser (100% by volume) likely contributed to slightly higher removal of both *E. coli* and MS2 in the aged filter compared to our PS+ZVI columns, but the reduction in removal over time was attributed to interference from NOM and PO_4^{3-} (Chiew et al., 2009). In our study, high influent pH and the presence of NOM, PO_4^{3-} , and a background microbial community were the likely reasons for decreased *E. coli* and MS2 removal after week 11. In CBM+ZVI columns, similar HC reduction at week 8 indicated that ZVI corrosion also occurred, but the ZVI amendment had little impact on *E. coli* and MS2 removal, as results were similar for PS columns. The breakdown of compost may have increased the concentration of NOM, PO_4^{3-} , and other microorganisms, greatly interfering with *E. coli* and MS2 removal throughout the experiment. The mechanisms of decreased *E. coli* and MS2 removal due to increased pH and interfering constituents (NOM, PO_4^{3-} , and microbial community) are discussed in more detail in the subsequent sections.

pH

Throughout the 46-week experiment, the influent pH (8.3) was higher than the PZC of several iron oxides (Kosmulski, 2011) and likely impacted indicator organism attachment. Previous studies have attributed bacteria and virus removal in ZVI-amended media to electrostatic attraction between the negatively charged indicator organisms and positively-charged iron oxides (Ingram et al., 2012; Shi et al., 2012; You et al., 2005). Iron oxides, produced in concentric layers extending outward from an iron filing (Noubactep et al., 2009), gain their net positive charge via pH-dependent protonation reactions (Cornell and Schwertmann, 2003). For typical iron oxides found in ZVI-amended columns (e.g., ferrihydrite, goethite, and hematite) the reported PZC values are above 7.5, resulting in a net positive charge at neutral pH (Kosmulski, 2011). At a pH above 8.0 however, ferrihydrite, hematite, and goethite have been reported to have either a negative or neutral surface charge (Hanna, 2007; Kosmulski, 2011; Rusch et al., 2010). In a previous column experiment with goethite-coated sand, MS2 removal was observed to decrease as pH increased. This result was attributed to lower electrostatic attraction between

goethite and MS2 (Zhuang and Jin, 2008). While not as high as the elevated pH (9.3) in Zhuang and Jin (2008), the influent pH (8.3) in our study was still near or above the PZC of likely iron oxides present in the PS+ZVI columns. Thus, electrostatic attraction between the iron oxides and *E. coli* and MS2 in our study may have been lower at a pH of 8.3 than at a pH closer to 7.0; however, it is unclear how a pH near 7.0 would combine with interfering ions and other microorganisms to influence *E. coli* and MS2 removal. Stormwater pH can range widely (Grebel et al., 2013), and future research should determine whether pH changes, in combination with interfering ions and microorganisms, impact indicator organism removal in ZVI-amended columns.

Natural Organic Matter

NOM, previously observed to inhibit attachment of indicator organisms to iron oxides (Foppen et al., 2006; Johnson and Logan, 1996), likely interfered with *E. coli* and MS2 removal in PS+ZVI and CBM+ZVI columns throughout the experiment. This inhibition has been attributed to numerous mechanisms, including a change in iron oxide net surface charge from NOM adsorption, competition for attachment sites, steric hindrance of attachment sites, and alteration of indicator organism surface characteristics such as hydrophobicity (Foppen et al., 2008; Yang et al., 2012). In this experiment, a change in iron oxide surface charge was the likely mechanism of *E. coli* and MS2 attachment. The TOC concentration in the weekly influent averaged 9.31 ± 1.84 mg/L, and removal of TOC by the PS+ZVI and CBM+ZVI columns averaged 30% and 13% from weeks 8 – 41, respectively. While ZVI corrosion produced new iron oxides, the influent NOM was well above the 1.9 mg/L TOC concentration observed to reverse a positive IOCS surface charge to negative (Abudalo et al., 2010). Thus, NOM likely adsorbed to new attachment sites produced by corrosion, reducing the electrostatically attractive force for indicator organisms (Yang et al., 2012). Similarly, the organic matter leaching from compost (as observed in Chapter 4) in CBM+ZVI media likely adsorbed to iron oxides from the beginning of the experiment, contributing to lower *E. coli* and MS2 removal as compared to PS+ZVI columns.

Phosphate

PO_4^{3-} removal in both PS+ZVI and CBM+ZVI columns was high throughout the 46-week experiment, averaging 87% and 89%, respectively. This high removal, also observed at an aged stormwater trench field site filled with iron-amended media (Erickson et al., 2012), was maintained despite the high TOC concentration in the influent and compost in the CBM+ZVI media. Competition for iron oxide binding sites and lower PO_4^{3-} removal was expected because NOM and PO_4^{3-} have been observed to adsorb via similar ligand exchange reactions with $\equiv\text{FeOH}$ groups on the surface of iron oxides (Borggaard et al., 2005; Chi and Amy, 2004; Parfitt et al., 1977). NOM's limited influence on PO_4^{3-} adsorption, however, has been observed previously (Borggaard et al., 2005) and can be explained in two ways. First, PO_4^{3-} may have been able to outcompete NOM for the adsorption sites. The type and specificity of the ligand exchange reaction between PO_4^{3-} and iron oxides can depend heavily on the type of iron oxide present. Goethite and magnetite, for example, has been observed to have the highest affinity for PO_4^{3-} , forming binuclear complexes and exhibiting a large number of adsorption sites with a strong PO_4^{3-} preference (Gimsing and Borggaard, 2007; Daou et al., 2007). If goethite and/or magnetite were present in the ZVI-amended media, its affinity for PO_4^{3-} likely contributed to the

high removal. Second, PO_4^{3-} may have been able to bind to iron oxides that had already adsorbed organic matter (Gerke and Hermann, 1992). PO_4^{3-} adsorption, in fact, has been reported to increase with exposure to humic-iron oxide complexes in comparison to uncoated iron oxides (Gerke, 1993). This phenomenon may have occurred in the CBM+ZVI columns as organic matter leaching from the compost did not negatively impact PO_4^{3-} removal.

The high influent PO_4^{3-} concentration may have negatively impacted indicator organism removal in the ZVI-amended columns. CBM+ZVI was particularly affected because PO_4^{3-} was observed to leach from the compost in Chapter 4. PO_4^{3-} has been observed to reduce *E. coli* (Park and Kim, 2009) and MS2 (Zhuang and Jin, 2008) attachment to IOCS and likely decreased removal in our columns via surface charge modification. Surface charge modification has been observed when mixing PO_4^{3-} with goethite. Without PO_4^{3-} , goethite particles have been measured with an isoelectric point (IEP) above pH 9. In the presence of 3 mg/L of PO_4^{3-} , however, these same particles were measured with an IEP around pH 1 due to the formation of a PO_4^{3-} coating (Appenzeller et al., 2002). Although Appenzeller et al. (2002) reported a PO_4^{3-} concentration higher than our 1.98 mg/L, a similar surface charge modification likely happened in both PS+ZVI and CBM+ZVI columns, lowering or eliminating the net positive charge on iron oxides formed and thus reducing indicator organism attachment.

Background Microbial Community

In the 46-week experiment, indicator *E. coli* and MS2 were spiked into an influent sourced from a local creek with a background microbial community averaging 3.2×10^6 cells/mL. *E. coli* cells constituted only 3% of the influent TCC, whereas MS2 accounted for less than 1% of typical total virus concentrations in surface waters (Hermes and Suttle, 1995). Thus, *E. coli* and MS2 had considerable competition for binding sites in ZVI-amended columns from other microbial organisms in the influent. This microbial community likely contained a diverse collection of bacteria and viruses that varied in size, morphology, and surface properties. As electrostatic forces, hydrophobic interactions, morphology, and size contribute to attachment of *E. coli* and MS2 to surfaces during saturated flow in porous media, other bacteria and virus strains may have had properties that led to better attachment (Chen and Walker, 2012; Redman et al., 1997). Most importantly, the high concentration of other organisms likely led to the fouling of iron oxide binding sites earlier than if the influent only contained indicator organisms. In weekly samples, effluent TCCs from both PS+ZVI and CBM+ZVI columns were equal to or greater than influent TCCs, suggesting that iron oxide fouling had occurred and that a robust microbial community had formed on the media. Furthermore, this observation also suggests a biofilm had formed on the ZVI-amended media, which can slow the corrosion process (Park et al., 2007).

Zero Valent Iron Corrosion, Hydraulic Conductivity, and Cementation

As noted previously, ZVI corrosion occurred throughout the 46-week experiment in PS+ZVI and CBM+ZVI columns and likely contributed to the observed HC reductions and media cementation. The PS+ZVI media was observed to change color from an original beige color at week 1 to a black color at week 46. The iron oxides formed in the ZVI-amended columns were not analyzed, but several previous studies of ZVI-amended filters have observed a similar color change and identified the iron oxides present as magnetite using X-ray diffraction (XRD) (Kohn

et al., 2005; Neumann et al., 2013). Magnetite formation is believed to occur after slow transformation of Fe[III] oxide phases with frequent exposure to Fe[II], produced either via abiotic corrosion or microbial processes (Neumann et al., 2013). PO_4^{3-} adsorption has also been shown to slow the transformation of ferrihydrite and preferentially lead to magnetite formation (Borch et al., 2007). Magnetite formation, previously observed to have low porosity (Cornell and Schwertmann, 2003), likely filled the pore spaces in the ZVI-amended columns and thus led to the observed HC reductions. A calculation can illustrate this decrease in porosity in the PS+ZVI columns. In a previous study, Leupin et al. (2005) estimated that 2.5 g of ZVI produced 4.8 g of ferrihydrite. Applying this ratio to our columns, 22 g of ZVI produced 42 g of ferrihydrite. Ferrihydrite is an amorphous iron oxide that has been shown to transform with age into various types of iron oxides, including hematite, goethite, and magnetite. In aged filters, however, magnetite has been found to be very common (Neumann et al., 2013). If all iron oxides are assumed to be magnetite, the 42 g of iron oxides increases the volume of the original ZVI filing by 8.1 cm^3 . This volume expansion would then decrease the PV from 33 cm^3 to 25 cm^3 and the porosity from 0.34 to 0.26.

In addition to HC reductions, both PS+ZVI and CBM+ZVI media were observed by week 46 to exhibit high levels of cementation. The cementation may have been due to the formation of iron carbonate precipitates between media grains, previously observed to cement together ZVI filings (Phillips et al., 2000; Westerhoff and James, 2003). A simple calculation can demonstrate the degree of supersaturation for iron carbonate. Assuming the dissolved oxygen was at saturation (8 mg/L), the ferrous iron concentration produced from oxidic corrosion was 0.5 mM. At the influent pH and alkalinity, the carbonate concentration was calculated assuming an open system and estimated at 0.012 mM. The saturation index (SI) could then be calculated from the ion activity product (IAP) and iron carbonate solubility constant (K_{SO}):

$$\text{IAP} = [\text{Fe}^{2+}][\text{CO}_3^{2-}] = (0.5 \times 10^{-3})(1.2 \times 10^{-5}) = 6 \times 10^{-9}$$

$$K_{\text{SO}} = 10^{-10.55}$$

$$\text{SI} = \frac{\text{IAP}}{K_{\text{SO}}} = 212$$

With an SI above one, iron carbonate precipitates were clearly forming in the PS+ZVI columns. Similar HC reductions and media cementation issues have been observed in previous studies on bioretention basins with 10% by weight ZVI-amended sand (Erickson et al., 2012; Rangsvivek and Jekel, 2005), presenting a considerable challenge for the long-term feasibility of the media. Higher ZVI weight fractions than 10% by weight may be inadvisable since the week 46 HC in PS+ZVI columns (16 cm/h) was close to the lower limit for bioretention regulations in Alameda County (12 cm/h) (BASMAA, 2010).

Iron in Effluent of ZVI-Amended Columns

Another major issue for ZVI-amended columns is the release of iron in the effluent. In PS+ZVI columns, dissolved iron was consistently below the detection limit throughout the experiment.

Tot Fe, likely consisting of particulate iron, increased slightly in the final half of the experiment, but the concentration remained below the U.S. EPA aquatic life criteria threshold of 1 mg/L (U.S. EPA). Samples taken within the initial 0.5 PV of an injection, however, contained Tot Fe concentrations above 1 mg/L. The wetting front in unsaturated columns has been observed to remobilize colloids and bacteria at the air-water interface (Auset et al., 2005; Mohanty et al., 2013) and likely contributed to the remobilization of iron colloids as well. Future research should investigate whether an additional filter section (without ZVI) installed below the ZVI-amended section is capable of retaining iron colloids that are mobilized at the start of wetting events to prevent elevated concentrations in the effluent.

In CBM+ZVI columns, dissolved Fe[II] was released in the effluent at concentrations near or above the 1 mg/L aquatic life criteria threshold (U.S. EPA). During the week 8 injection, Fe[II] and Tot Fe concentrations increased in later PVs, and Fe[II] was observed to account for nearly 75% of Tot Fe. Fe[III], however, was not observed in the effluent during most injections. NOM, observed to leach from CBM in Chapter 4, has a well known affinity for Fe[III] oxides, forming Fe[III]-NOM complexes via ligand exchange and aiding transport of Fe[III] oxides (Jones et al., 2009; Gu et al., 1999; Senesi et al., 1977). Fe[II] is much more selective in forming NOM complexes, making our results difficult to explain. Iron reduction mediated by microorganisms, in which organic matter is used as an electron donor and Fe[III] oxides are used as an electron acceptor, has been previously observed in anaerobic sediments (Lovley and Phillips, 1986; Lovley, 1997) and could explain our results. However, iron reduction requires nutrient rich growth media (Kostka et al., 1996) and the exhaustion of nitrate as an electron acceptor (Weber et al., 2006). It is unclear whether the stormwater provided the needed nutrients or anaerobic conditions for microbial iron reduction. Furthermore, if iron reduction occurred between weekly injections, we would have expected high Fe[II] concentrations to be measured within the initial 0.5 PVs. Instead, the Fe[II] concentration was low at 0.5 PVs and increased with each PV.

The microbial community and NOM in CBM+ZVI media, however, may still have contributed to the observed effluent Fe[II] concentrations. Effluent TCCs from the CBM+ZVI columns were consistently higher than the influent and PS+ZVI effluent, indicating the CBM+ZVI media had a larger microbial community from the compost amendment. Microbial activity, particularly of aerobic bacteria, has been observed to significantly slow corrosion rates by limiting oxygen exposure through respiration (Little and Ray, 2002; Park et al., 2007). In air-saturated batch systems, ZVI corrosion has been observed to produce low Fe[II] concentrations since the majority of Fe[II] is quickly oxidized to Fe[III] oxides. However, in oxygen-limited batch systems, Fe[II] concentrations increased with time since Fe[III] oxide production was negligible (Triszczyk et al., 2009). Thus, Fe[II] concentrations may have been present in the CBM+ZVI columns due to depressed corrosion rates and oxygen exposure from microbial respiration. NOM, released from the compost in the CBM+ZVI media, may have then formed Fe[II] complexes. Even though there are fewer ligands capable of exchange, complexes have been observed between Fe[II] and specific types of organic matter, including oxalate (Kim et al., 2010), tannic acid (Theis and Singer, 1974), and humic acid (Liu et al., 2008). Similar Fe[II]-organic matter complexes may then have prevented formation of ferric oxides (including ferrihydrite, hematite, and goethite) (Liu et al., 2008) and aided mobilization in the effluent. Thus, ZVI amendments to CBM media is inadvisable as the majority of iron may be lost due to organic matter complexation, dissolution, and transport.

Effect of Rest Period on Indicator Organism Removal

Despite *E. coli* and MS2 removal below 0.5 log in PS+ZVI columns after week 11, results from the rest period experiment indicated that 24-h rest periods in the column may extend the effectiveness of ZVI-amended media. In PS+ZVI columns, *E. coli* and MS2 removal remained around 0.5 log from weeks 12 – 46. After the week 46 injection, the columns were saturated and allowed to rest for 24 h, and significantly higher *E. coli* and MS2 removal was observed after this rest period as compared to during the week 46 injection (0-h rest period). The 24-h rest period may have exposed *E. coli* and MS2 to the electrostatically attractive binding sites not yet covered by NOM, PO_4^{3-} , or other organisms. In a previous ZVI-amended biosand filter study with 24-h rest periods, 6-log MS2 removal was observed after 36 weeks of daily operation, suggesting that MS2 removal can be sustained over repeated injections. Further study of stormwater columns should focus on whether rest periods of 24 h can sustain a *E. coli* and MS2 removal during timeframes longer than the scope of our study.

Conclusions

Our study was the first known evaluation of ZVI-amended media for *E. coli* and MS2 removal from stormwater. Results from our study demonstrated the short-term effectiveness of PS+ZVI for indicator organism removal; however, the presence of NOM, PO_4^{3-} , and other organisms quickly decreased removal to levels observed in PS after 11, 1-year storms. Rest periods up to 24 h in previously fouled PS+ZVI columns significantly increased removal of both *E. coli* and MS2 as compared to the week 46 injection and should be considered for longer-term operation. While still removing 90% of PO_4^{3-} , CBM+ZVI columns were not observed to enhance removal of either *E. coli* or MS2, and iron leaching in the effluent in Fe-NOM complexes should limit the media's use. HC reductions and cementation issues present a major limitation to ZVI amendments left unsaturated between storms. Future research should focus on higher residence times and saturated conditions in PS+ZVI media to determine whether *E. coli* and MS2 removal and media permeability can be sustained over the long-term.

Part 2B – Stormwater Treatment

Saturated Column Experiment

Chapter 6: A Novel Design for Stormwater Bioretention with Pulsed Feed and Saturated Bed: Evaluation of *E. coli* and MS2 Removal in Aged Columns with Different Media Amendments

Introduction

High stormwater flows, sourced from impermeable urban environments (U.S. EPA, 2009), can lead to scouring (Booth and Jackson, 1997) and contamination (Hatt et al., 2004) of local aquatic ecosystems. Human pathogens and indicator organisms, including bacteria and viruses, have been detected in stormwater and are a public health concern (Grebel et al., 2013). Pathogenic bacteria and human viruses, however, are difficult to measure in stormwater and monitoring studies typically quantify fecal indicator organisms (Olivieri et al., 2007), including *Escherichia coli* (*E. coli*) and MS2 coliphage (MS2), which are frequently found to exceed recreational water quality standards (Parker et al., 2010). Fecal indicator bacteria (FIB) present a barrier to nonpotable use of stormwater (Pitt and Clark, 2012), and indicator viruses increase the risk of groundwater contamination during stormwater infiltration (Pitt et al., 1999).

In response, municipalities have increasingly adopted green infrastructure (GI) to increase urban landscape permeability (U.S. EPA, 2000). Water quality concerns have also prompted GI design to maximize contaminant removal to meet discharge limits (Clark and Pitt, 2012; Davis et al., 2009). In bioretention basins, a depressed trench collects and infiltrates stormwater through a sand and compost media layer, called conventional bioretention media (CBM), reducing the peak flow rate and some contaminants in the process (Hipp et al., 2006). Results from laboratory column studies have indicated *E. coli* removal can range from 1.1 – 3 (Barrett et al., 2013; Chandrasena et al., 2014; Kim et al., 2012; Li et al., 2012; Zhang et al., 2011) and F-RNA coliphage removal exceeds 4 log (Li et al., 2012); however, results from field studies have indicated that *E. coli* removal is lower and more variable, possibly due to low media contact time, variable infiltration rates, and preferential flow pathways (International Stormwater BMP Database, 2014; Birch et al., 2006; Hathaway et al., 2011; Passeport et al., 2009). It is likely that longer and more uniform contact times with media can make bioretention basins more effective barriers for indicator organisms and pathogens.

In the traditional bioretention design, increased *E. coli* removal has been correlated with aging, increased clogging, slower infiltration rates, decreased porosity, and increased hydrodynamic dispersion (Chandrasena et al., 2014; Zhang et al., 2011). This design, therefore, requires the basin to clog and reduce infiltration rates enough to increase *E. coli* removal (but not enough to violate local regulations on minimum infiltration rates); however, clogging is an unpredictable process and most systems operate passively, without opportunities to manage the infiltration rate.

Introducing flow controls to bioinfiltration basins has the potential to address several factors that contribute to highly variable indicator organism removal. One option for flow control is an effluent valve that cycles between open and closed positions, allowing stormwater pulses to rest in the bioretention media for a set period of time before discharge. This type of design allows for longer and more uniform media contact times. It is also simpler to operate than a flow-restricting valve attempting to maintain a low, steady, continuous flow rate, which would require constant adjustments as the elevation head decreases during drainage. By decoupling the infiltration rate from the hydraulic conductivity, this design also allows the use of larger media to overcome the challenges presented by severe clogging in passive systems (insufficient filtration rates or the formation of preferential flow paths).

Research on biosand filters for treating drinking water, which are operated with intermittent flow and a saturated bed, provide evidence that indicator organism removal can be high, achieving above 4-log removal of *E. coli* and MS2 (Elliott et al., 2008; Wang et al., 2014). In the traditional design, bioretention basins infiltrate stormwater through media at velocities between 12 – 25 cm/h, offering one opportunity (filtration) to capture indicator organisms before discharge (Davis et al., 2009). With an effluent control valve, a bioretention basin could mimic a biosand filter and hold stormwater in the treatment media for a defined interval before discharge, offering three opportunities for capture (Elliott et al., 2008). First, the initial infiltration exposes indicator organisms to physical removal mechanisms like attachment via depth filtration and straining via the *Schmutzdecke* (Bellamy et al., 1985). Second, the rest period in the media increases the likelihood of attachment and exposes indicator organisms to decay from grazing and enzymatic stresses (Elliott et al., 2011). Third, the final infiltration before exiting the media adds a second exposure to depth filtration and straining (Young-Rojanschi and Madramootoo, 2014).

Media amendments, such as zero valent iron (ZVI) and biochar, also offer the potential to increase removal of indicator organisms. ZVI may improve removal by producing surfaces with net positive charge through corrosion and iron oxide production (Noubactep, 2010), thereby enhancing the attachment of indicator organisms by electrostatic attraction (Elimelech and Song, 1992). Biochar may improve removal through hydrophobic interactions (Abit et al., 2012) and its higher surface area than sand or soil (Xie et al., 2015). A ZVI-amended biosand filter was reported to achieve 6-log MS2 removal from drinking water over 300 d (Bradley et al., 2011), but stormwater has higher concentrations of organic matter and phosphate that may interfere with performance. Biochar amendments have shown promise in stormwater for removing indicator bacteria (Mohanty et al., 2014; Mohanty and Boehm, 2014), but long-term effectiveness and indicator virus removal remain unclear.

The objective of this study was to evaluate indicator bacteria (*E. coli*) and virus (MS2) removal in an effluent controlled, saturated bed, bioretention basin with ZVI and biochar amendments. Four different media types were compared: plain sand (PS), CBM, plain sand with ZVI (PS+ZVI), and plain sand with biochar (PS+BC). The columns were fed stormwater (amended creek water) in 24-h pulses, and performance was evaluated for 75-d to provide insight into the effects of biofilm growth and media aging.

Material and Methods

Indicator *E. coli* and MS2 Coliphage

Indicator *E. coli* NCM 4236, a gram-negative, kanamycin-resistant strain, was used as the indicator bacteria. Original cultures were obtained from the late Professor Sydney Kustu (University of California-Berkeley) (Inwood et al., 2009) and stored in frozen aliquots at -80 °C. *E. coli* cultures were grown in tryptic soy broth with 0.025 g/L kanamycin to stationary phase 3x at 37 °C before harvesting. Cells were harvested via centrifugation at 8000 g for 5 minutes, after which the supernatant was discarded. The pellet was washed three times in phosphate buffer solution and then diluted in the influent to the desired concentration. *E. coli* concentrations, counted as colony forming units (CFU) per mL, were enumerated using the spread plate technique on selective Luria Broth (LB) agar containing 0.025 g/L kanamycin. Samples were plated in duplicate with 100- μ L inocula and incubated at 37 °C for 18 h before counting.

Indicator MS2 coliphage (MS2) (ATCC 15597-B1), a male-specific F+ coliphage, was used as the indicator virus for this experiment. MS2 was propagated following the EPA Standard Method 1601 with *Escherichia coli* F_{amp} (ATCC 700981) as host (U.S. EPA, 2001). Sample enumeration, reported as plaque forming units (PFUs) per mL, was conducted in duplicate using the double agar layer technique with 100- μ L inocula in LB agar containing 0.015 g/L ampicillin and streptomycin.

Media and Column Preparation

Silica sand (40 – 100 mesh, Fisher Scientific, MO), a plant-based compost (Wonder Grow Compost, American Soil and Stone, CA), zero valent iron (ZVI) filings (Peerless Metal Powders and Abrasives, MI), and biochar (Sonoma Compost Company, CA) were obtained from their suppliers and sieved to a size range between 40 – 100 mesh. The silica sand was soaked overnight in 12 N hydrochloric acid, rinsed in deionized (DI) water, dried at 110 °C, and then autoclaved. The compost was rinsed in DI water until the rinsate was clear and then dried at 110 °C. The ZVI filings and biochar were set aside in separate containers after sieving without further preparation. The biochar was produced from wood chips and has been characterized previously (Mohanty et al., 2014; Ulrich et al., 2015). Details on the biochar source, feedstock, surface area, and composition are included in Tables 6.1 and 6.2. Media types were prepared in separate 2-L containers and mixed for 1 h prior to column packing. Recipes, ZVI and biochar weight fractions, and characteristics of the media types are provided in Table 6.3.

Table 6.1 – Biochar Source, Process Description, Feedstock, Peak Temperature (T), Surface Area (SA), and Micropore Volume ($V_{\mu\text{pore}}$) (Ulrich et al., 2015).

Source	Process Type	Feedstock	Peak T (°C)	SA (m ² /g)	$V_{\mu\text{pore}}$ (cm ³ /g)
Sonoma Compost Co. Petaluma, CA	Fast Pyrolysis, Composted	Mixed Soft Wood	1500	326 ± 5.9	0.161 ± 0.001

Table 6.2 – Physical and Chemical Composition of Sonoma Compost Co. Biochar (Mohanty et al., 2014).

Elemental Composition (% oven-dry weight basis)						Atomic Ratios		
Ash	C	H	O	N	S	H/C	O/C	(O+N)/C
12.2	78.9	0.69	7.77	0.4	0.043	0.009	0.098	0.105

The media was packed into columns (2.5-cm diameter, 62-cm length) built from clear polyvinyl chloride pipe (McMaster-Carr, IL). Two replicate columns were produced for each media type, yielding eight total columns. Media was dry-packed into the columns in 5-cm increments, and a massager was applied to the column between increments. The final media depth was 50 cm, not including 6 cm above and below the media for support media. The 6-cm support contained 1 cm of polyester fiber, 2.5 cm of gravel (20 – 30 mesh), and 2.5 cm of Ottawa sand (20 – 30 mesh). A photo of the experimental setup is included in Figure 6.1, and the cross-section schematic of the columns is shown in Figure 6.2. A summary of the column characteristics is provided in Table 6.3. Porosity and pore volume (PV) were measured by subtracting the dry weight of a packed column from the weight of a saturated column. Columns were kept saturated for 24 h before measuring the porosity and PV. PS+BC columns had a lower porosity and PV than other media types, which may have arisen from the biochar not reaching full saturation in 24 h. Before injecting stormwater, DI water was pumped upwards into each packed column at flow velocities below 1 cm/h for 36 h. All injections were operated in the upward direction to prevent short-circuiting and ensure plug flow conditions.



Figure 6.1 – Experimental setup including eight columns total.

Table 6.3 – Column and Media Type Characteristics.

Column Characteristics		Dimension	
Column Diameter		2.5 cm	
Total Column Depth		62 cm	
Column Media Depth		50 cm	
Media Diameter		40 – 100 mesh, 0.15 – 0.42 mm	
Media Type	Composition	Porosity	PV
PS	100% Sand (% by volume)	0.39	118 mL
CBM	70% Sand, 30% Compost (% by volume)	0.37	113 mL
PS+ZVI	95% Sand, 5% ZVI (% by weight)	0.36	111 mL
PS+BC	95% Sand, 5% Biochar (% by weight)	0.31	96 mL

Plain Sand (PS), Conventional Bioretention Media (CBM), Zero Valent Iron (ZVI), Biochar (BC)

75-Day Column Experiment

After the 36-h rinse, the columns were inverted 180° from their regular position for an initial HC measurement. HC was measured using the ASTM E2396 Falling-Head Method (ASTM, 2015), and the column inversion allowed gravity drainage without reversing the direction of flow. For the 75-d experiment, columns were returned to their regular position and were operated in a daily,

two-phase pattern consisting of (1) a 0.75-h stormwater injection phase and (2) a 23.25-h rest phase. The daily stormwater injection phase on Day N began at 9 AM, pumping about 90 mL of stormwater into the columns for 0.75 h (Figure 6.2.A). Stormwater was injected at a flow velocity of 25 cm/h, following recommended infiltration rates in bioretention basins (BASMAA, 2010). This volume was chosen to treat a 3.2-cm storm over 3 d, meeting the 5-d drawdown limit in Alameda County (Alameda Countywide Clean Water Program, 2012). Assuming a bioretention sized to 5% of the drainage area, a runoff coefficient of 80%, and a runoff treatment goal of 100%, the 3.2-cm storm corresponded to approximately 250 mL of stormwater. Due to different porosities, the stormwater injection phase resulted in pumping 0.8 PV into the PS, CBM, and PS+ZVI columns and 0.9 PV into PS+BC columns. Next, the columns began the rest phase, remaining saturated for 23.25 h (Figure 6.2.B). The next injection phase began at 9 AM on Day N+1 when stormwater was again injected for 0.75 h, expelling stormwater already in the columns (Figure 6.2.C). The expelled stormwater exiting the columns was analyzed as effluent from Day N. In PS, CBM, and PS+ZVI columns, effluent contained a mixture of 0.6 PVs of Day N stormwater and 0.2 PVs of Day N–1 stormwater. In PS+BC columns, effluent contained a mixture of 0.8 PVs of Day N injection stormwater and 0.1 PVs of Day N–1 stormwater. The columns then began the rest phase for the next 23.25 h (Figure 6.2.D), and this pattern was repeated daily for 75 d.

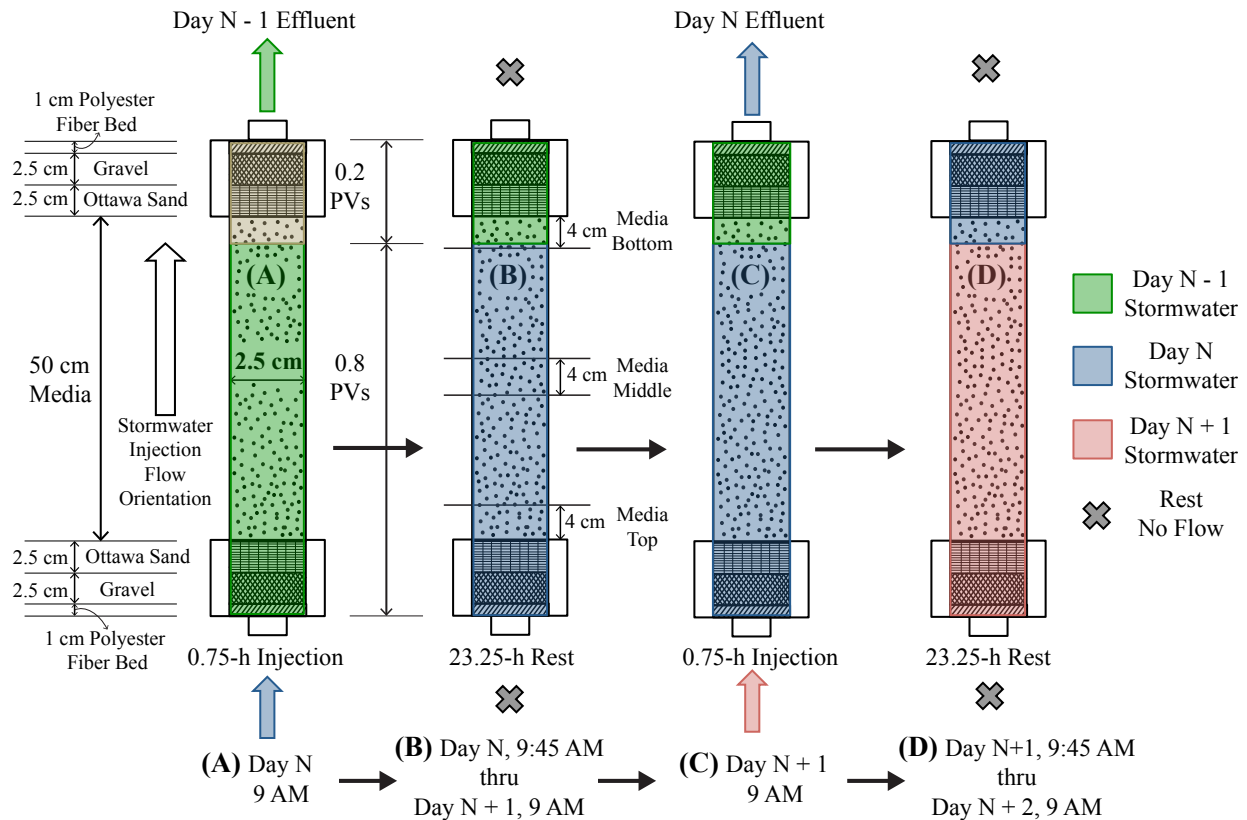


Figure 6.2 – Cross-section schematic and injection/sampling regimen for columns in this study. At 9 AM on Day N, columns were injected for 0.75 h (A). After the injection, the columns rested for the next 23.25 h until 9 AM on Day N+1 (B). The columns were then injected again for 0.75 h, displacing a mixture of Day N stormwater and Day N–1 stormwater (C). This effluent was

analyzed to evaluate removal performance for Day N. Afterward, the columns were allowed to rest for 23.25 h until the next injection (D). Due to differences in porosities, PS, CBM, and PS+ZVI columns received 0.8 PVs and PS+BC columns received 0.9 PVs during injections.

Effluent samples were collected from each column type at varying intervals. On sample days, fresh stormwater was produced for the injection phase. After the rest phase, a 90-mL composite sample of effluent was collected and analyzed for *E. coli*, MS2, total organic carbon (TOC), phosphate (PO_4^{3-}), pH, total cell concentrations (TCC), and low nucleic acid (LNA) and high nucleic acid (HNA) bacteria concentrations. A 50-mL influent sample was taken after the rest phase and analyzed for the same parameters to assess microbial loss from overnight storage. The average die-off in the influent after 24 h for *E. coli* and MS2 was 0.3 log and 0.9 log, respectively, and was accounted for in the final log removal calculations.

After day 75, the columns were inverted 180° for a final HC measurement. Duplicate PS and CBM columns and a single PS+BC column were then drained overnight and sacrificed to collect media samples for a biofilm characterization. Media samples were collected from the top, middle, and bottom 4 cm of the 50-cm media section. The biofilm was characterized by measuring the adenosine triphosphate (ATP) concentrations per cell, ATP per g of media, and number of cells per g media, following a procedure developed previously (Velten et al., 2007) that was described in Chapter 3. The procedure was not conducted on the PS+ZVI columns because ZVI interfered with ATP measurement.

Hydrophobic Interactions and Biochar

After day 75, one PS+BC column was injected with stormwater amended with 0.1% by volume Tween[®] 20. Log removal values in the 0.1% Tween[®] 20 feed were compared to day 75 results to determine if hydrophobic interactions contributed to *E. coli* and MS2 removal. Tween[®] 20 (Fisher Scientific, MO) is a non-ionic, hydrophobic surfactant that creates micelle structures capable of shielding hydrophobic interactions between indicator organisms and filter media (Lukasik et al., 1999).

Source Water

The influent water quality was designed to mimic stormwater with a diverse background microbial community. Column influent was collected from the North Fork of Strawberry Creek on the University of California-Berkeley campus and augmented with a NOM amendment, *E. coli* suspension, and MS2 suspension to reach concentrations of 10 mg/L total organic carbon (TOC), 10⁵ CFU/mL, and 10⁴ PFU/mL, respectively. Details on the NOM amendment, including the procedure and characterization, were included in Chapter 3. The influent was mixed for 15 min before injections and mixing continued until the injection ended. The influent was kept at room temperature between injections and replaced weekly. *E. coli*, MS2, NOM, PO_4^{3-} , pH, TCCs, and HNA/LNA bacteria were monitored roughly every 10 days. Total suspended solids (TSS) and assimilable organic carbon (AOC) were measured on two separate days in triplicate. TOC was measured on a TOC analyzer (TOC-5000A, Shimadzu Co., Japan). PO_4^{3-} was measured

using the ascorbic acid method (EPA Standard Method 365.2) with a detection limit of 0.02 mg/L (U.S. EPA, 1983). pH was measured using a Beckman-Coulter Φ^{TM} 200 Series meter (Beckman-Coulter, CA). TSS was measured using ASTM method D5907-13 (ASTM, 2013). AOC, TCCs, %HNA bacteria, and %LNA bacteria were measured with flow cytometry (FCM) and are described in a subsequent section. Influent characteristics are summarized in Table 6.4.

Table 6.4 – Influent characteristics during 75-d study. DO was not measured directly, but historical monitoring values of Strawberry Creek indicate that levels are typically near saturation (Hans and Maranzana, 2006).

Influent Characteristics	Average \pm Standard Deviation
TOC	10.5 \pm 2.34 mg/L
AOC	0.25 \pm 0.07 mg/L
PO ₄ ³⁻	1.58 \pm 0.23 mg/L
pH	8.25 \pm 0.15
TSS	4.17 \pm 1.44 mg/L
DO	8 mg/L
Total Cell Concentration	3.94 $\times 10^6 \pm 0.91 \times 10^6$ cells/mL
<i>E. coli</i>	10 ⁵ CFU/mL
MS2	10 ⁴ PFU/mL

Flow Cytometry and Assimilable Organic Carbon

TCC, AOC, and LNA and HNA bacteria concentrations were determined using a BD AccuriTM C6 flow cytometer (BD Biosciences, CA) with a 488-nm blue laser. The FCM analysis was conducted following the procedure described previously (Prest et al., 2013). Details on the staining, sample preparation, and gating strategy were included in Chapter 3. The AOC method followed a procedure developed previously and was described in Chapter 3 (Hammes and Egli, 2005). Two categories of bacteria, LNA and HNA, are often mentioned due to their distinct fluorescence signal. In general, LNA bacteria are smaller, contain less ATP/cell, grow slower, and are less susceptible to predation than HNA bacteria (Wang et al., 2009).

Data Analysis

Indicator organism log removal was calculated as the difference between the logarithmic (base 10) influent concentration and logarithmic (base 10) effluent concentration. All standard deviations were calculated using error propagation based on the influent and effluent samples from the replicate columns throughout the study. Statistically significant differences were calculated using a two-sample t-Test on R Statistical Software (version 3.1.3, Austria) and were considered significant at $p < 0.05$. Figures were produced using GraphPad Prism Software (version 6, CA).

Results

E. coli and MS2 Removal and Hydraulic Conductivity

E. coli and MS2 removal by all media types is presented in Figure 6.3. The PS+BC columns greatly outperformed the other three media types. Effluent *E. coli* concentrations were under the detection limit throughout the 75-d experiment. Although *E. coli* removal was initially high by PS+ZVI, it decreased to 1.2 log by day 45. Removal by CBM increased as the media aged, averaging 2.5 log on day 75. Removal in PS columns was similar throughout the study period, averaging about 1.5 log.

MS2 removal in PS+ZVI columns was greater than 2 log throughout the experiment. In PS+BC columns, effluent MS2 concentrations were below the detection limit through day 38, but MS2 removal decreased afterwards to 1.3 log on day 75. MS2 removal in PS and CBM columns did not exceed 0.5 log through day 75. Higher day 1 removals likely stemmed from residue iron oxides on the PS and CBM media (about 0.5% by weight Fe) in the underdrain, which was not cleaned prior to column packing.

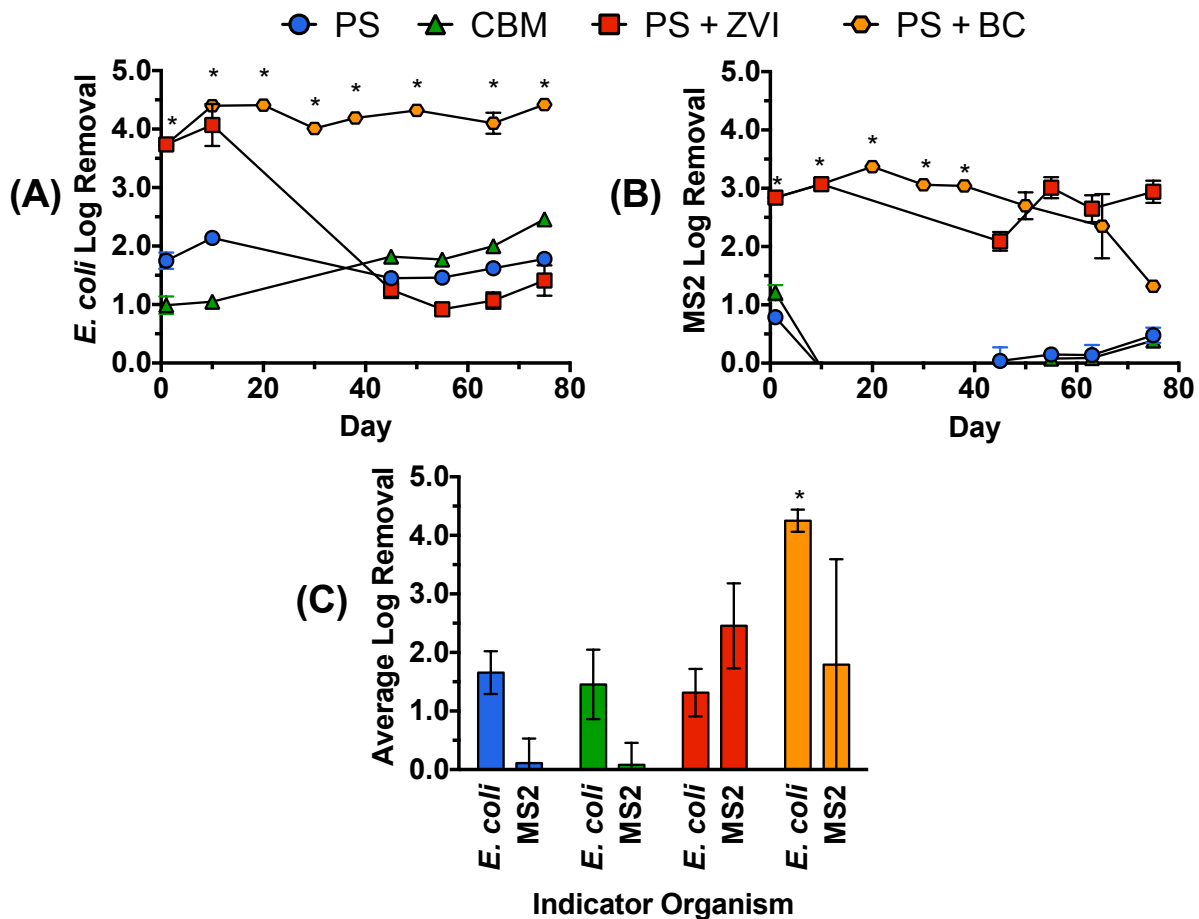


Figure 6.3 – Removal of (A) *E. coli* and (B) MS2 in each media type during the 75-d experiment. (C) Average *E. coli* and MS2 removal in each media type over entire 75-d experiment. Error bars

represent one standard deviation. * denotes concentrations were below the detection limit (10 CFU/mL or PFU/mL).

The HC changes in each media type are reported in Figure 6.4. The lowest initial HC was observed in PS+BC columns, presumably due to the high surface area and low HC of the biochar amendment (Barnes et al., 2014). Large HC decreases were not observed in any media type, and clogging to unacceptable levels (HC below the 12 cm/h minimum for bioretention basins (BASMAA, 2010)) was not observed in any column. The largest HC change over 75 d was observed in CBM columns, decreasing by a factor of 1.3 to 66 cm/h. A similar decrease in HC after 75 d was observed in PS, PS+ZVI, and PS+BC columns.

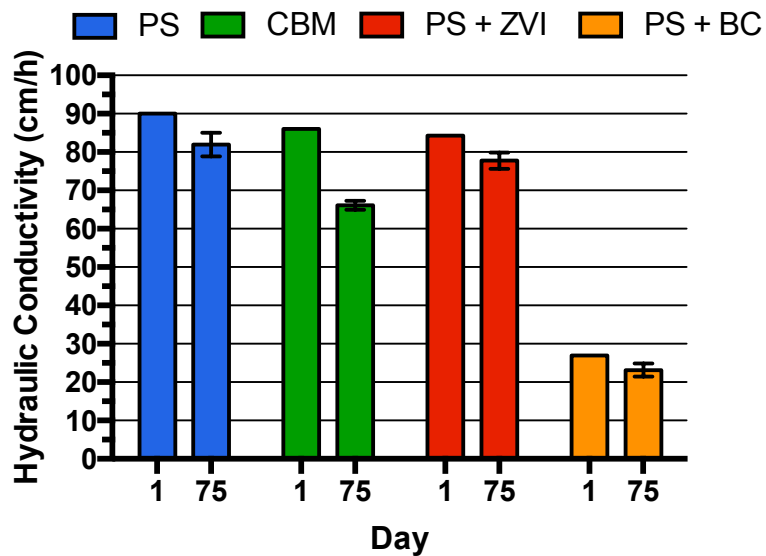


Figure 6.4 – Saturated hydraulic conductivity (cm/h) of PS, CBM, PS+ZVI, and PS+BC columns on day 1 and 75 of the experiment. Error bars represent one standard deviation.

Effect of Hydrophobic Interactions on Indicator Removal in PS+BC

The effect of hydrophobic interactions on *E. coli* and MS2 removal in a PS+BC column is presented in Figure 6.5. In comparison to the normal feed, significantly lower *E. coli* and MS2 removal was observed in the Tween[®] feed ($p < 0.05$). The effluent MS2 concentration was higher than the influent by an order or magnitude, suggesting viruses that attached to media surfaces during previous injections were eluted by Tween[®].

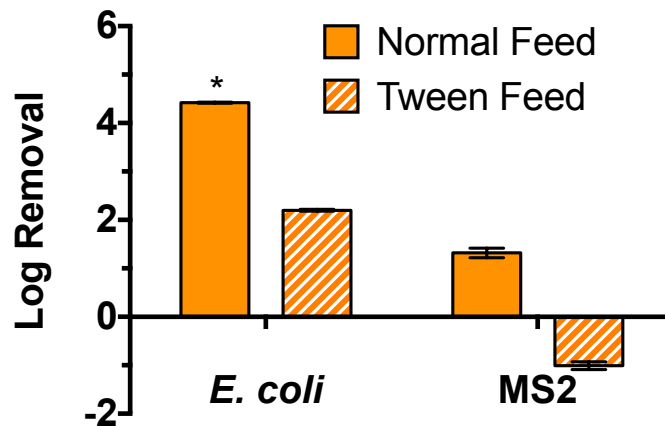


Figure 6.5 – Indicator *E. coli* and MS2 removal in PS+BC column with a normal and 0.1% Tween[®] 20 feed. * denotes removal to the detection limit (10 CFU/mL or PFU/mL). Error bars represent one standard deviation.

Total Organic Carbon and Phosphate

The normalized TOC and PO₄³⁻ effluent concentrations for all media types are presented in Figure 6.6. The highest TOC reduction was observed in PS+BC columns, reducing effluent concentrations to around 5 mg/L through day 75. Hydrophobic interactions, high surface area, and micropores were likely responsible for the observed TOC sorption to biochar (Kasozi et al., 2010). TOC was initially reduced by 50% in PS+ZVI columns, presumably from electrostatic attraction between iron oxides and TOC. Low removal was observed by day 10, however, as most bindings sites were likely occupied (Chi and Amy, 2004). In CBM columns, TOC concentrations exceeded the influent by a factor of 3 – 4, likely due to organic matter breakdown during the rest phase (Bratieres et al., 2008). In PS columns, TOC removal was low, largely matching or slightly exceeding the influent.

The highest PO₄³⁻ removal was observed in PS+ZVI columns, averaging above 73% through day 75. Although TOC breakthrough was observed by day 10, PO₄³⁻ removal was likely maintained since PO₄³⁻ has high affinities for specific iron oxides (Gimsing and Borggaard, 2007). PO₄³⁻ removal in PS+BC columns, in contrast, was below 20% through day 75. Periclase (≡MgO), previously suggested as PO₄³⁻ binding sites (Yao et al., 2011), could be lower in the biochar used in this study, which may account for the lower removal than the 50% removal reported in a previous study (Reddy et al., 2014). CBM columns discharged effluent with PO₄³⁻ concentrations averaging above 13 mg/L. The organic matter released by CBM columns may have contained phosphorus, accounting for the high effluent PO₄³⁻ concentration (Bratieres et al., 2008). This observation is a major limitation to the use of compost/sand in the field and may require alternate soil/sand mixtures. High initial PO₄³⁻ removal in PS was likely due to iron oxide residues on the gravel underdrain (about 0.5% by weight Fe), but later results largely matched PO₄³⁻ removal (about 10%) in previous studies (Erickson et al., 2012).

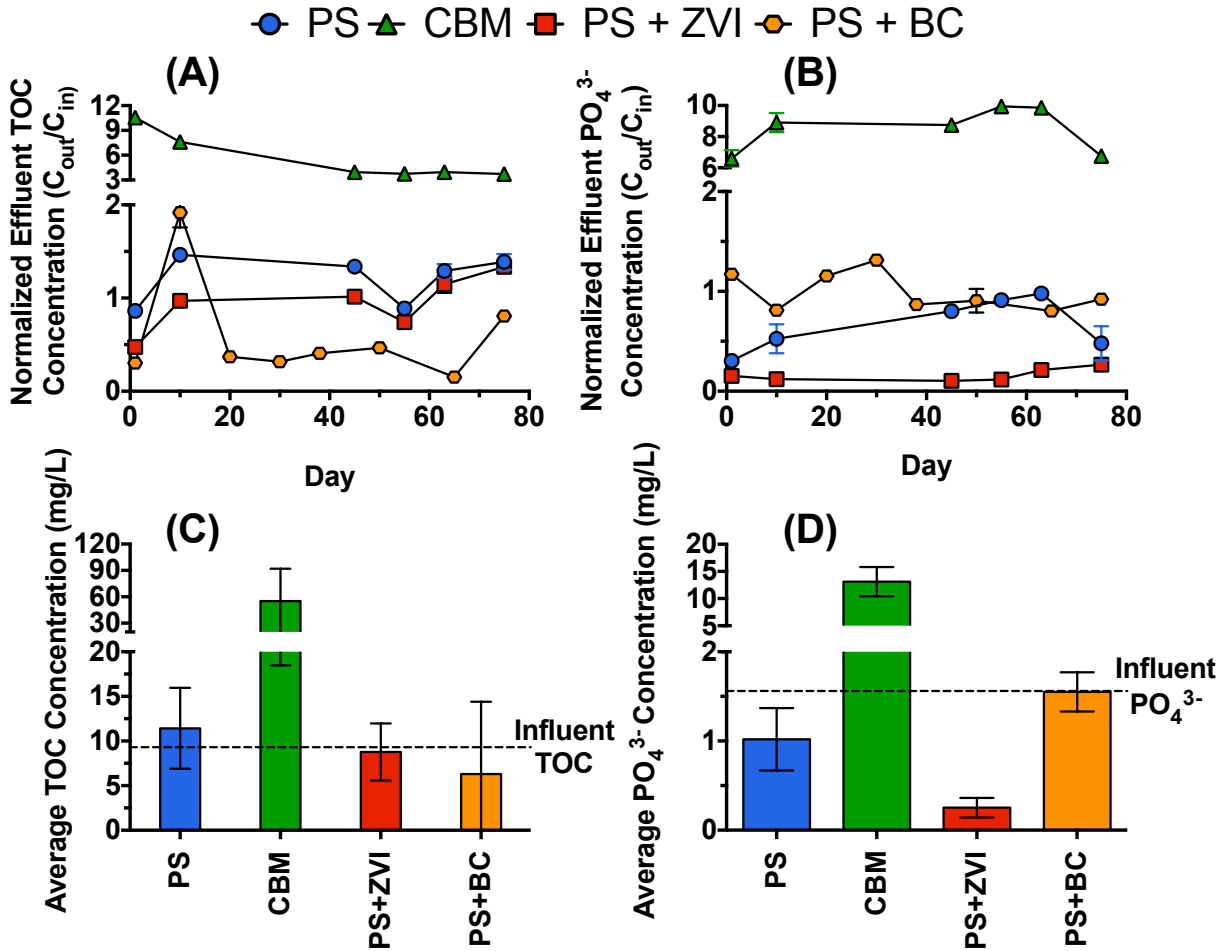


Figure 6.6 – Normalized (A) TOC and normalized (B) PO₄³⁻ concentrations in each media type effluent. Average effluent (C) TOC and (D) PO₄³⁻ concentration in each media type over entire 75-d experiment. Error bars represent one standard deviation.

Flow Cytometry Counts of Influent and Effluent Samples

TCC and HNA/LNA bacteria results in the influent and column effluent are presented in Figures 6.7 and 6.8. The average influent TCC was $3.9 \times 10^6 \pm 0.9 \times 10^6$ cells/mL. High TCC removal, above 90%, was observed in both PS+ZVI and PS+BC columns on day 1. In subsequent weeks, only the PS+BC columns achieved net removal of total bacterial cells, averaging 37% removal throughout the 75-d experiment. Growth of bacteria was observed in PS+ZVI columns as effluent TCCs exceeded the influent after day 45. In PS and CBM columns, effluent TCCs exceeded the influent throughout the entire 75-d experiment. Effluent from the CBM columns contained the highest TCCs of any media type, averaging 7.7×10^{11} cells/mL.

The influent TCC was dominated by HNA bacteria, accounting for roughly 70% of TCCs. In PS+BC columns, a significant shift towards LNA bacteria dominance was observed in the effluent between days 38 – 75. LNA bacteria accounted for 25% of effluent TCCs on day 38, but

this percentage increased to about 70% on day 75. Both HNA and LNA bacteria concentrations in PS+ZVI effluent increased with time, and the %HNA bacteria largely matched the influent. Between days 45 – 75, LNA bacteria concentrations in PS and CBM effluent doubled, but the effluent was still dominated by HNA bacteria, averaging about 60% of TCCs.

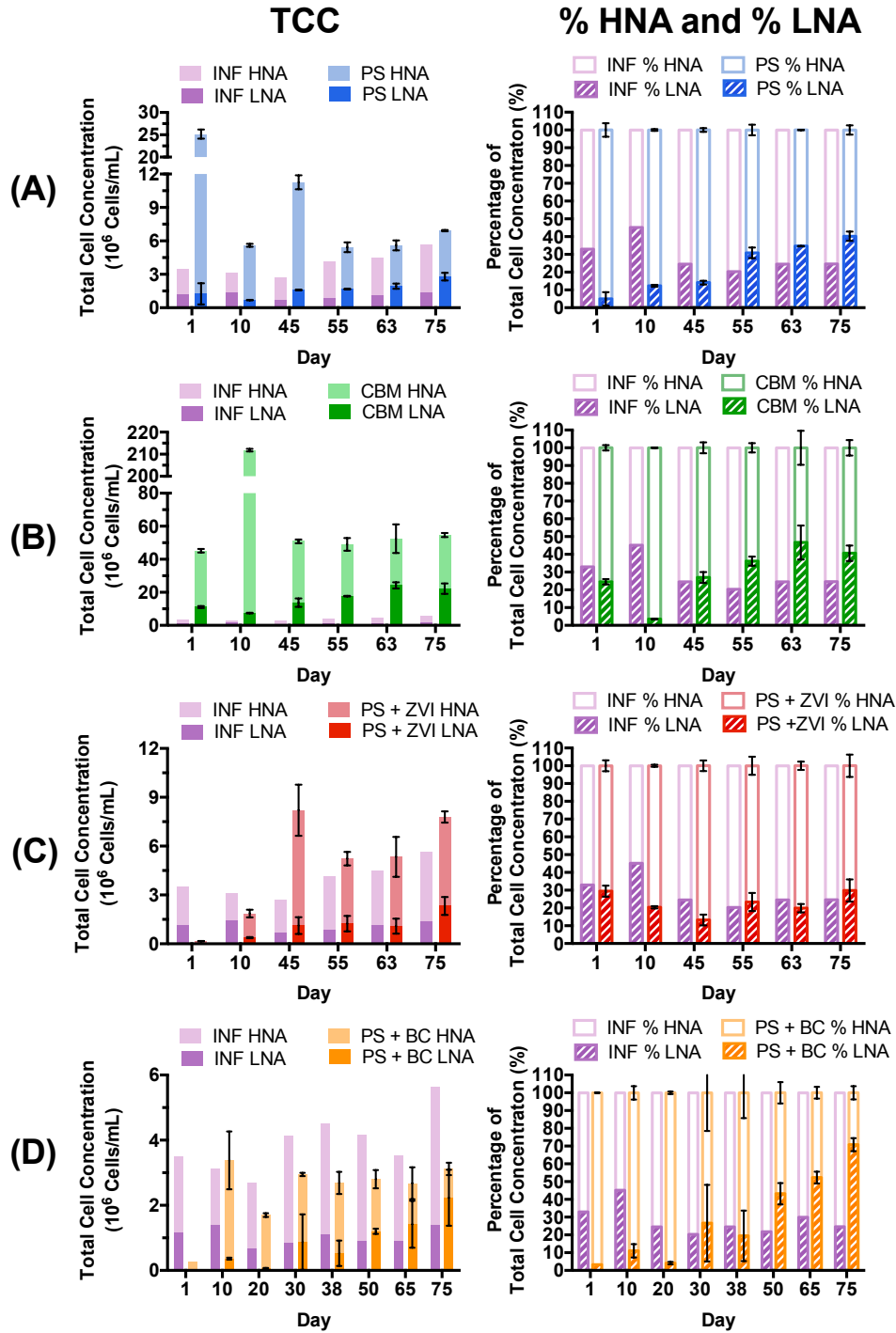


Figure 6.7 – TCCs, divided into HNA and LNA bacteria counts, and the % HNA and % LNA, reported as percentage of the TCC, in the influent and effluent of (A) PS, (B) CBM, (C) PS+ZVI,

and (D) PS+BC during the 75-d study. Error bars represent one standard deviation. Note the difference in scale for TCCs between media types.

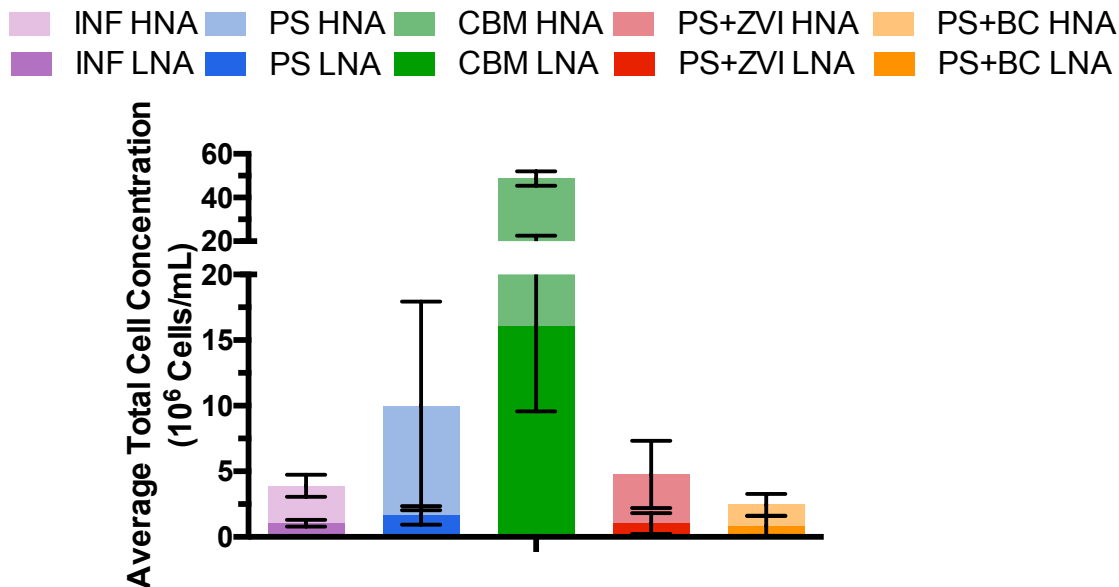


Figure 6.8 – Average TCC, broken down into HNA and LNA bacteria concentrations, in the influent and effluent of each media type over the entire 75-d experiment. Error bars are one standard deviation.

Biofilm Characterization

The biofilm characterization results from PS, CBM, and PS+BC are presented in Figure 6.9. PS+ZVI columns were excluded from this method because ZVI interfered with the ATP measurement. In PS and PS+BC columns, the highest biomass concentration (both ATP/g and cells/g) was measured in the top section. The most drastic decreases in biomass with depth occurred in the PS+BC columns (each section was an order of magnitude lower than the preceding section). The top media sections also contained the highest ATP/cell with averages indicative of HNA bacteria (greater than 1×10^{-7} ng ATP/cell) (Wang et al., 2009). The bottom media sections, in contrast, contained low ATP/cell values indicative of low activity and LNA bacteria (10^{-8} ng ATP/cell) (Wang et al., 2009). The top section received fresh stormwater daily with 250 $\mu\text{g/L}$ AOC, likely contributing to an environment conducive to higher activity HNA bacteria. The bottom section typically received influent water that had resided in preceding media sections for the previous 24 h (Figure 6.1). This extra residence time resulted in lower AOC concentrations, which is expected to select for LNA bacteria (Wang et al., 2009).

A different pattern was observed in the CBM columns. There was no clear trend in the biofilm biomass with depth (ATP/g and cells/g), and the media was characterized by higher ATP/g values (15,000 – 40,000 ng ATP/g), presumably due to the microbial community associated with

compost (Lehtokari et al., 1983). In addition, the highest ATP/cell values overall ($> 3 \times 10^{-7}$ ng ATP/cell) were observed in the top and middle sections as daily injections likely supported higher microbial activity.

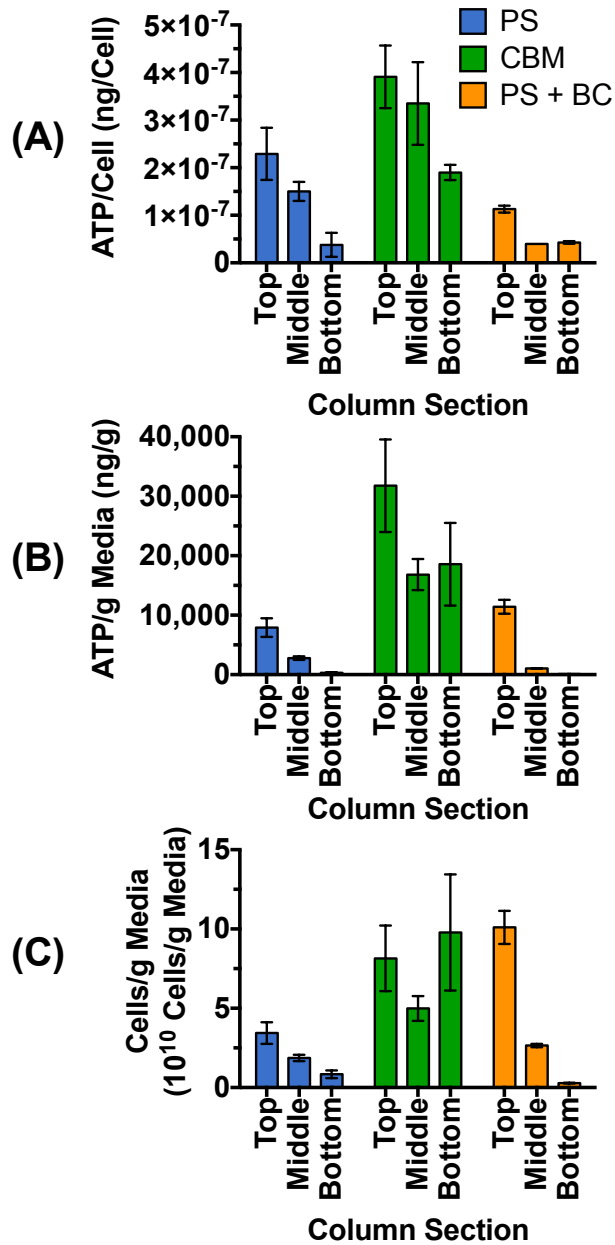


Figure 6.9 – Biofilm characterization in PS, CBM, and PS+BC columns reported as (A) ATP/Cell, (B) ATP/g Media, and (C) Cells/g Media. Duplicate columns were sacrificed after the day 75 injection, and samples were taken from the top, middle, and bottom 4 cm of the media section. Error bars represent one standard deviation.

Discussion

E. coli, MS2, and Phosphate Removal

E. coli removal in both PS and CBM columns was higher than removal observed in the unsaturated columns from Chapter 4, an expected result from filtration theory since this study used deeper columns, longer residence time, and finer media (Tufenkji and Elimelech, 2004). In PS columns, similar *E. coli* removal was observed as reported in previous biosand filter studies (Jenkins et al., 2011; Young-Rojanschi and Madramootoo, 2014), but removal did not increase over time as observed in other studies (Elliott et al., 2008). *E. coli* removal in biosand filters has been attributed to straining and attachment in the *Schmutzdeke*, a biologically active cake layer formed from trapped biomass and solids in the top 5 cm (Young-Rojanschi and Madramootoo, 2014). Elliott et al. (2008) observed filtration rates decrease by a factor of 7 after 50 d while *E. coli* removal increased. In slow sand filters, *Schmutzdeke* formation, including the ripening rate and spatial coverage, can be highly variable (Campos et al., 2002). In this study, the decrease in HC was minimal over 75 d, suggesting that ripening and formation of a *Schmutzdeke* occurred more slowly. Different influent sources could have also contributed to the slow *Schmutzdeke* formation in our columns. Elliott et al. (2011) augmented their influent with primary wastewater effluent, which may have provided more AOC to support *Schmutzdeke* growth than in our study. It should be noted that Young-Rojanschi and Madramootoo (2014) reported higher *E. coli* and MS2 removal in biosand filters operated under continuous, low flow conditions than intermittent, pulsed conditions. However, the difficulty of maintaining low, steady, and continuous flow rates in stormwater LID systems makes this design impractical. In CBM columns, *E. coli* removal increased with time, as observed in Chapter 4 and published laboratory bioretention studies (Zhang et al., 2011). Increased *E. coli* removal coincided with a decrease in HC over time, suggesting clogging may have contributed to improved retention. Clogging has been attributed to pore space accumulation of TSS (Siegrist and Boyle, 1987), biofilm growth (Vandevivere and Baveye, 1992), and gas bubble formation from microbial respiration (Seki et al., 1998). This accumulation of material can alter the hydrodynamic properties of a filter and improve *E. coli* retention through decreased infiltration rates (Huysman and Verstraete, 1993), increased contact with media grains (Yates and Yates, 1987) and increased exposure to biofilm surfaces and/or air-water interfaces (Bellamy et al., 1985; Wan et al., 1994). Straining efficiency may also increase if the resulting pore spaces are small enough to restrict *E. coli* passage (Bradford et al., 2002). The relative contribution of each mechanism is difficult to determine from this study, and future work, possibly involving microbial inhibitors, should aim to further characterize this mechanism.

MS2 removal in both PS and CBM columns was low and did not increase with time as observed in previous biosand filter studies (Elliott et al., 2011; Wang et al., 2014). In biosand filters, MS2 removal has been observed during the rest period at depths between 10 – 30 cm and attributed to adsorption and biological activity (Elliott et al., 2011; Young-Rojanschi and Madramootoo, 2014). Wang et al. (2014) likely observed higher MS2 removal due to the high divalent cation concentrations in their groundwater-based influent, which may improve adsorption by forming ionic bridges between carboxylate groups on NOM-coated media surfaces and MS2 capsids (Pham et al., 2009). In addition, the longer experimental timeframe of 300 d likely aided the biofilm development required for MS2 removal (Wang et al. 2014). Elliott et al. (2011) reported MS2 decay from biological activity in aged biosand filters, but the influent, amended with 2.5%

primary wastewater effluent, may have had characteristics more conducive to predation and enzyme activity by higher order organisms. It is unclear whether similar biological activity is likely in effluent controlled CBM filters fed with stormwater, and future work should focus on whether stormwater with different characteristics, including influent TSS and AOC, can impact MS2 removal.

Higher MS2 and PO_4^{3-} removal was observed in PS+ZVI columns than PS and CBM columns, and the results largely mirrored MS2 removal in a ZVI-amended biosand filter (Bradley et al., 2011) and PO_4^{3-} removal in a ZVI-amended bioretention basins (Erickson et al., 2012). *E. coli* removal, however, declined on day 45 to values observed in PS columns. The increasing effluent TCCs indicated that other microorganisms likely coated the ZVI surfaces quickly after the start of the experiment. In a previous study with an iron oxide-coated sand, *E. coli* removal decreased at an earlier point than MS2 removal (Lukasik et al., 1999). The factors that contribute to *E. coli* removal were likely affected more by interference from NOM (Foppen et al., 2008) and PO_4^{3-} (Park et al., 2009) than those that contribute to MS2 removal.

The small decrease in HC and lack of cementation in saturated PS+ZVI columns was encouraging for the practicality of using ZVI amendments in field applications. Large HC decreases (lower than the initial HC by a factor of 50) and cementation issues were observed previously in the unsaturated PS+ZVI columns in Chapter 5. Other stormwater bioretention studies have reported similar final HC values (Erickson et al., 2012) and cementation of media grains (Rangsvik and Jekel, 2005). This HC decrease in aged ZVI filters has been attributed to volume expansion as ZVI corrodes, forming low porosity iron oxides like magnetite (Noubactep, 2010) or precipitates like iron carbonate (Westerhoff and James, 2003). The columns in Chapter 5 and previous studies, however, were operated under unsaturated conditions, allowing the columns to drain between storms. The columns in this study, in contrast, were kept saturated between storms. Despite high influent DO, the small HC decrease observed in the PS+ZVI columns indicates the clogging and cementation issues likely stemmed from unsaturated conditions and not the DO concentration. Future research with ZVI-amended media in bioretention basins should focus on maintaining saturated conditions between storms to prevent clogging and cementation from ZVI corrosion. Future research should also determine whether iron reduction mediated by microorganisms could occur in ZVI-amended bioretention basins kept saturated for months between storms.

The highest *E. coli* removal in any media type was observed in PS+BC columns, demonstrating sustained detection limit removal (above 4 log) throughout the 75-d experiment. Other short-term column studies have also reported higher *E. coli* removal in biochar-amended media than sand, and several removal mechanisms have been proposed including high surface area, micropores, and hydrophobic interactions (Abit et al., 2012; Abit et al., 2014; Bolster and Abit, 2012; Mohanty et al., 2014). At a 5% by weight amendment, the Sonoma biochar used in this study has been reported to increase the surface area of sand by a factor of 1790 and the organic carbon content of sand by 4%. These properties expanded the number of bacteria attachment sites on the media and increased the likelihood of favorable interactions (Mohanty et al., 2014). Results from the Tween[®] feed experiment suggested *E. coli* removal was aided by hydrophobic interactions. NOM, a hydrophobic competitor, was also removed well by PS+BC columns. A previous study observed that NOM-amended stormwater decreased *E. coli* removal in a biochar

media as compared to stormwater without NOM (Mohanty et al., 2014). In this study, *E. coli* removal did not decrease over time in the presence of 10 mg/L TOC, suggesting the rest phase allowed both NOM and *E. coli* to be transported to suitable attachment sites on the biochar grains. The HC of PS+BC columns was also lower than the HC in the other media types by a factor of 3.5. Previous studies have not reported HC changes with biochar amendments, but the benefits of lower HC on indicator organism removal, including increased tortuosity, contact with media (Yates and Yates, 1987), and straining (Bradford et al., 2002), also likely contributed to the observed *E. coli* removal.

MS2 removal by PS+BC exceeded the detection limit through day 38 but declined quickly during the second half of the experiment. MS2 was reported to have a higher water contact angle than *E. coli*, suggesting the coliphage should be more susceptible to hydrophobic interactions (Chattopadhyay and Puls, 1999; Loosdrecht et al., 1987). The Tween[®] feed experiment further suggested hydrophobic interactions were important for MS2 removal and retention. Biochar, sand, and MS2, however, exhibit a net negative surface charge at the pH of stormwater, which likely also caused electrostatic repulsion (Mohanty et al., 2014). A possible explanation for the observed decrease in MS2 removal over time is that as hydrophobic attachment sites were exhausted, electrostatic repulsion between the biochar/sand media and MS2 led to lower attachment.

Promising *E. coli* and MS2/PO₄³⁻ removal results in pulsed, effluent controlled PS+BC and PS+ZVI columns motivate several future research questions to inform design. First, future work should focus on whether pulsed, effluent controlled columns with larger diameter grains (and higher HC) can achieve similar results as observed in this study. Second, it would be helpful to test different rest phases to determine how short they can be while still maintaining the removal results observed in this study. Applying information technology and real-time controls to the bioretention basin could allow the operator to change hold-up times in anticipation of predicted rainfall (Quigley et al., 2008). Third, storms should not be introduced consecutively, and larger gaps in time should be implemented between storms. Columns should be drained between 1-year storms to determine whether unsaturated conditions and remobilization is an issue. Finally, layered media, including both ZVI and biochar amendments, could lead to promising *E. coli*, MS2, and PO₄³⁻ removal.

Suspended and Attached Biomass

FCM analysis of column effluent and biofilm characterization of filtration media offered insight into the dynamics of the suspended and attached biomass, respectively. *E. coli* removal was observed by all media types even though *E. coli* accounted for less than 3% of influent TCC. Some media, PS and CBM, released more cells in the effluent than influent. The most interesting trend was observed in both the suspended and attached biomass results for PS+BC columns. The FCM and biofilm characterization results suggest there was a selection for LNA bacteria in the biochar-amended media. Throughout the 75-d experiment, the LNA bacteria concentration in the effluent increased by a factor of 260 while the HNA bacteria concentration remained fairly consistent. On day 75, effluent LNA bacteria concentrations exceeded the influent concentration by 60% whereas there was 80% removal of influent HNA. Several mechanisms may be driving this trend. First, smaller pore spaces may have increased the HNA straining efficiency in the top

section of the PS+BC columns. On the attached biomass, ATP/cell values in the top section (10^{-7} ng ATP/cell) were indicative of HNA bacteria whereas the ATP/cell values in the middle and bottom media sections (10^{-8} ng ATP/cell) were typical of LNA bacteria, suggesting more HNA bacteria were in the top section (Wang et al., 2009). Second, selective predation may have scavenged the suspended and attached HNA bacteria in the column (Boenigk et al., 2004). Finally, starvation stresses may have reduced the growth potential of HNA bacteria in the columns. High temperature biochar has been found to contain very low levels of biodegradable organic carbon and may even be toxic to certain types of bacteria (Luo et al., 2013). This low nutrient and high pH environment may only be suitable for growth of LNA bacteria. Future research should further classify these microbial community changes in more detail and determine whether attached indicator organisms are likely to persist in the biofilm or decay over time.

Conclusions

The purpose of this study was to evaluate the potential of a pulsed, effluent controlled bioretention basin to remove indicator organisms using higher HC media that prevent clogging issues reported in conventional bioretention basins. The results demonstrated the promise of this design paired with a ZVI amendment for MS2 and PO_4^{3-} removal and biochar amendment for *E. coli* and possibly MS2 removal. In the PS+ZVI columns, saturated conditions prevented clogging issues previously observed in ZVI-amended columns operated under unsaturated conditions between storms. A 5% by weight biochar amendment removed *E. coli* to the detection limit after 75 d. Previous research has found indicator bacteria removal to be influenced by hydrophobicity, suggesting the biochar amendment could also be effective against other more hydrophobic bacteria like *Enterococcus faecalis* (Abit et al., 2012). Media types including biochar and ZVI amendments could be an attractive option for indicator bacteria, virus, and phosphate removal, but careful consideration of saturation conditions is required to maintain HC in ZVI-amended media. The columns in this experiment were injected with 27 1-year storms consecutively and kept saturated throughout the 75-d experiment. Future research should add rest periods between 1-year storms and determine whether keeping the columns unsaturated or saturated between storms impacts indicator organism removal. Future research should also investigate community dynamics in the biochar media and determine whether indicator organism removal is impacted by larger diameter media, shorter rest phases, and lower biochar or ZVI weight fractions.

Chapter 7: Conclusions

The goal of this dissertation was to investigate the use of various media amendments to improve the removal of indicator bacteria and viruses from drinking water and stormwater. Throughout the course of this research, we evaluated a quaternary ammonium silane (QAS)-coated sand for treatment of drinking water in point-of-use filters (Chapter 2) and zero valent iron (ZVI) and biochar amendments for treatment of stormwater in bioretention basins (Chapters 3 – 6).

The findings from this research using media amendments (QAS, ZVI, and biochar) have led to a general observation: the effectiveness of media amendments is limited by the presence of other adsorbates. A weakness of several previous stormwater and drinking water filtration studies is their focus on short timeframes and simple water matrices with single microorganisms. Under similar conditions in this dissertation, the QAS-coated sand in Chapter 2 and ZVI-amended sand in Chapter 5 performed well, improving the removal of indicator bacteria and viruses as compared to plain sand controls either through electrostatic attraction, hydrophobic interactions, or both. These interactions, however, were limited by the interference of natural organic matter (NOM), phosphate (PO_4^{3-}), and other microorganisms. In water matrices with these competing adsorbates, indicator organism removal decreased in both QAS and ZVI-amended media. If we had only conducted short-term experiments in simple water matrices, such as low ionic strength MilliQ water, we would have missed this decreased in removal. For evaluating media amendments, it appears short-term experiments with simple water matrices have limited value for predicting performance under more realistic conditions. Before using any media amendment in the field, long-term lab experiments under realistic water matrices should be conducted to determine the expected fouling timeframe and sensitivity to specific competing adsorbates or biofilm growth. Predictable fouling timeframes would increase the desirability of using media amendments by helping operators know when to replace the media either in point-of-use filters or bioretention basins. Media regeneration would also increase the desirability of a media amendment if removal performance could be reliably restored once a fouling timeframe is approaching.

In addition to the general research finding, this dissertation has provided several contributions to the filtration literature, particularly in the bioretention and stormwater field. These contributions include the following:

1. A Bioretention Experimental Design That Mimics The Complexity In The Field

Research on bioretention basin treatment of stormwater is challenging because field installations are dynamic and exposed to variable local climates. Depending on their location, bioretention basins are likely to receive stormwater in different frequencies, quantities, and qualities. These differences can make it difficult to learn anything about what factors influence performance. Reductionist approaches are needed to understand removal mechanisms, but stormwater research has numerous factors to isolate, including water quality, flow regime, media types, and media aging. The experimental design in Chapter 3 sought to simulate the realistic conditions in the lab

while controlling for some variables like infiltration rate. This setup allowed us to gain some insights into removal mechanisms, but the ideas discussed in Chapter 4 will ultimately need to be tested again in the field.

2. Column Design Separating Infiltration Rate and Hydraulic Conductivity

An important insight that derived from the bioretention experimental design was the distinction between the effects of infiltration rate and hydraulic conductivity on the removal of *Escherichia coli* (*E. coli*). Previous column studies were operated where infiltration rate was driven by gravity and the media's hydraulic conductivity. Similar to our experiment, *E. coli* removal was observed to increase in conventional bioretention media (CBM) as the columns aged, but it was unclear whether the increased removal stemmed from lower infiltration rates (as predicted by filtration theory) or material accumulation in the pore spaces. In this study, we externally applied a constant infiltration rate with a pump. This setup allowed us to isolate the impact a hydraulic conductivity reduction had on removal from simply lowering the infiltration rate. Future studies should attempt a similar setup to gain further insight into removal mechanisms and aid better comparisons between studies.

3. Biofilm Characterization

This is the first known stormwater study to quantify the biomass in CBM and determine the influence of biological activity on indicator organism removal. Attached biomass was quantified by measuring adenosine triphosphate (ATP) on the media, and suspended biomass was tracked by measuring the total cell concentrations (TCC) in a flow cytometer. The results demonstrated that the biofilm in CBM had more microorganisms than the plain sand biofilm by an order of magnitude. *E. coli* removal in CBM increased with age whereas no increase was observed in plain sand, and some evidence suggested that the CBM biofilm had some role in the *E. coli* removal. Interestingly, *E. coli* removal was observed in CBM even though effluent TCCs exceed the influent by a factor of 6, suggesting *E. coli* removal occurred throughout the filter depth while other bacteria were leached from the biofilm.

4. Long-Term Study Of ZVI Filings

Previous short-term experiments have evaluated ZVI filings for indicator and human virus removal (Shi et al., 2012; You et al., 2005), and previous stormwater bioretention studies have evaluated ZVI amendments for PO_4^{3-} (Erickson et al., 2007; Erickson et al., 2012) and heavy metal removal. This is the first known experiment with ZVI amendments evaluating indicator bacteria and virus removal over a longer timeframe and in stormwater. In unsaturated columns, performance decreased due to the presence of interfering adsorbates, and extreme hydraulic conductivity reductions and cementation presented a major limitation to the long-term feasibility of ZVI amendments. ZVI amendments to CBM were also observed to leach iron in the effluent. Saturated conditions, however, did not observe a similar hydraulic conductivity reduction and could be an option for PO_4^{3-} and MS2 coliphage (MS2) removal.

5. Novel Effluent-Controlled Bioretention Design With Pulsed Feed

The most promising results were observed in Chapter 6 with a novel bioretention basin design that sought to maintain high media contact time. 24-h exposure to the favorable interactions and media amendments appears to have aided both *E. coli* and MS2 removal. Detection limit removal of *E. coli* was observed in a pulsed, effluent controlled filter with a biochar amendment after 27 1-year storms were injected over 75 days. Detection limit MS2 removal in the biochar-amended filter was also observed through day 40 and then decreased afterwards. This is the first known biochar filtration experiment to study long-term *E. coli* removal and MS2 removal over any timeframe.

Future research to build on the findings and contributions from this dissertation should consider the following suggestions:

1. Biofilm Contribution To Indicator Removal In CBM

The results in Chapter 4 suggested the biofilm in CBM columns contributed to the observed indicator removal. A net growth in biomass was not observed in CBM, but an increase in cell size and activity may have contributed to the increase in *E. coli* removal observed after week 22. Future research should focus on factors that contribute to the growth and activity of a biofilm in real systems, including assimilable organic carbon (AOC) concentrations, media type, time between storms, and dry periods. Other studies should further investigate the role the biofilm plays in indicator organism removal, including morphology changes. MS2 removal did not increase with time, and it is unclear what factors would contribute to indicator virus attachment. The total suspended solids (TSS) concentration was lower than average in our experiments, and it is unclear if a higher TSS concentration would lead to MS2 attachment either through clogging or particle association. Finally, it is unclear what microorganism communities populate the biofilm in CBM columns and whether pathogens could possibly grow after removal and pose a remobilization risk. This observation has already been reported in field bioretention basins in which effluent *E. coli* and *Enterococcus faecalis* concentrations exceeded the influent (Hathaway et al., 2011). Next-generation sequencing of media samples would allow us to better understand microbial community dynamics in bioretention basins and identify factors that lead to robust biofilm activity and minimal pathogen growth.

2. Pulsed, Effluent Controlled Bioretention Design With Biochar.

The experiments in Chapter 6 focused on a single configuration with a 24-h rest phase and 75 consecutive injections, and promising results were observed with a biochar amendment. Future studies should expand the scope of this experiment and determine whether *E. coli* and MS2 removal is impacted by larger media size, shorter rest phases, lower biochar weight fractions, and unsaturated periods between storms. Different bacteria and virus strains, including indicator organisms and pathogens, should be used to determine whether microorganism surface characteristics may interfere with attachment. A biochar and ZVI mixture should also be considered to improve *E. coli*, PO_4^{3-} , and MS2 removal. A similar mixture for drinking water treatment could also be applied in a field biosand filter for both indicator bacteria and virus removal. Finally, the microbial community dynamics in the biochar-amended columns, as

observed with the increase in suspended low nucleic acid (LNA) bacteria concentrations, should be studied further. Next-generation sequencing of media samples over time could yield valuable insights into the microbial communities growing in the biochar-amended media and determine whether attached pathogens could persist in the biofilm, posing a remobilization risk.

In conclusion, the goal of this dissertation was to identify and evaluate opportunities for using filtration to remove waterborne pathogens in distributed systems. The research focused on the removal of indicator bacteria and viruses from drinking water in point-of-use filters and stormwater in bioretention basins. The results have provided insights into the realistic limitations of media amendments, further characterized removal mechanisms in bioretention media, and demonstrated the promise of a pulsed, effluent controlled feed with increased rest periods and media amendments for long-term removal of indicator organisms. Numerous future research questions remain, but the strategies identified here may help lead to more robust barriers between waterborne pathogens, illness, and local communities.

References

- Abbaszadegan, M., Mayer, B. K., Ryu, H., and Nwachuku, N. (2007) Efficacy of removal of CCL viruses under enhanced coagulation conditions. *Environmental Science & Technology*, 41(3), 971–977.
- Abbaszadegan, M., Monteiro, P., Nwachuku, N., Alum, A., and Ryu, H. (2008) Removal of Adenovirus, Calicivirus, and bacteriophages by conventional drinking water treatment. *Journal of Environmental Science & Health, Part A: Toxic/Hazardous Substances & Environmental Engineering*, 43(2), 171–177.
- Abbaszadegan, M., Monteiro, P., Ouwens, R., Ryu, H., and Alum, A. (2006) Removal and inactivation of *Cryptosporidium* and microbial indicators by a quaternary ammonium chloride (QAC)-treated zeolite in pilot filters. *Journal of Environmental Science & Health, Part A: Toxic/Hazardous Substances & Environmental Engineering*, 41(6), 1201–1210.
- Abit, S. M., Bolster, C. H., Cai, P., and Walker, S. L. (2012) Influence of feedstock and pyrolysis temperature of biochar amendments on transport of *Escherichia coli* in saturated and unsaturated soil. *Environmental Science & Technology*, 46(15), 8097–8105.
- Abit, S. M., Bolster, C. H., Cantrell, K. B., Flores, J. Q., and Walker, S. L. (2014) Transport of *Escherichia coli*, *Salmonella typhimurium*, and microspheres in biochar-amended soils with different textures. *Journal of Environmental Quality*, 43(1), 371–378.
- Abudalo, R. A., Bogatsu, Y. G., Ryan, J. N., Harvey, R. W., Metge, D. W., and Elimelech, M. (2005) Effect of ferric oxyhydroxide grain coatings on the transport of bacteriophage PRD1 and *Cryptosporidium parvum* oocysts in saturated porous media. *Environmental Science & Technology*, 39(17), 6412–6419.
- Abudalo, R. A., Ryan, J. N., Harvey, R. W., Metge, D. W., and Landkamer, L. (2010) Influence of organic matter on the transport of *Cryptosporidium parvum* oocysts in a ferric oxyhydroxide-coated quartz sand saturated porous medium. *Water Research*, 44(4), 1104–1113.
- Alameda Countywide Clean Water Program (2012) *C.3 Stormwater Technical Guidance*, Alameda County.
- Alper, J. P. (2010) Optimization and Antimicrobial Testing of Quaternary Ammonium Silane Coatings, Masters Thesis, Department of Chemical Engineering, University of California at Berkeley.
- Appenzeller, B. M. R., Duval, Y. B., Thomas, F., and Block, J. C. (2002) Influence of phosphate on bacterial adhesion onto iron oxyhydroxide in drinking water. *Environmental Science & Technology*, 36(4), 646–652.
- Arnold, B. F. and Colford, J. M. (2007) Treating water with chlorine at point-of-use to improve water quality and reduce child diarrhea in developing countries: A systematic review and

- meta-analysis. *The American Journal of Tropical Medicine and Hygiene*, 76(2), 354–364.
- ASTM (2015) *Standard Test Method for Saturated Water Permeability of Granular Drainage Media (Falling-Head Method) for Vegetative (Green) Roof Systems*, American Society for Testing and Materials.
- ASTM (2013) *Standard Test Methods for Filterable Matter (Total Dissolved Solids) and Nonfilterable Matter (Total Suspended Solids) in Water*, American Society for Testing and Materials.
- Auset, M., Keller, A. A., Brissaud, F., and Lazarova, V. (2005) Intermittent filtration of bacteria and colloids in porous media. *Water Resources Research*, 41(9), W09408.
- Barnes, R. T., Gallagher, M. E., Masiello, C. A., Liu, Z., and Dugan, B. (2014) Biochar-induced changes in soil hydraulic conductivity and dissolved nutrient fluxes constrained by laboratory experiments. *PLoS ONE*, 9(9), e108340.
- Barrett, M. E., Limouzin, M., and Lawler, D. F. (2013) Effects of media and plant selection on biofiltration performance. *Journal of Environmental Engineering*, 139(4), 462–470.
- BASMAA (2010) *Technical Memorandum: Regional Bioretention Soil Guidance & Model Specification*, Bay Area Stormwater Management Agencies Association.
- Baur, W. H. (1977) Silicon–oxygen bond lengths, bridging angles Si–O–Si and synthetic low tridymite. *Acta Crystallographica Section B*, 33(8), 2615–2619.
- Bellamy, W., Hendricks, D., and Logsdon, G. (1985) Slow sand filtration - Influences of selected process variables. *Journal American Water Works Association*, 77(12), 62–66.
- Benjamin, M. M. (2002) *Water Chemistry*, New York, McGraw-Hill.
- Benjamin, M. M. and Lawler, D. F. (2013) *Water Quality Engineering: Physical / Chemical Treatment Processes*, Wiley.
- Benjamin, M. M., Sletten, R. S., Bailey, R. P., and Bennett, T. (1996) Sorption and filtration of metals using iron-oxide-coated sand. *Water Research*, 30(11), 2609–2620.
- Birch, G. F., Matthai, C., and Fazeli, M. S. (2006) Efficiency of a retention/detention basin to remove contaminants from urban stormwater. *Urban Water Journal*, 3(2), 69–77.
- Blott, S. J., Al-Dousari, A. M., Pye, K., and Saye, S. E. (2004) Three-dimensional characterization of sand grain shape and surface texture using nitrogen gas adsorption technique. *Journal of Sedimentary Research*, 74(1), 156–159.
- Boehm, A. B., Ashbolt, N. J., Colford, J. M., Dunbar, L. E., Fleming, L. E., Gold, M. A., et al. (2009) A sea change ahead for recreational water quality criteria. *Journal of Water and Health*, 7(1), 9–20.

- Boenigk, J., Stadler, P., Wiedroither, A., and Hahn, M. W. (2004) Strain-specific differences in the grazing sensitivities of closely related ultramicrobacteria affiliated with the *Polynucleobacter* cluster. *Applied and Environmental Microbiology*, 70(10), 5787–5793.
- Bolster, C. H. and Abit, S. M. (2012) Biochar pyrolyzed at two temperatures affects *Escherichia coli* transport through a sandy soil. *Journal of Environmental Quality*, 41(1), 124–133.
- Booth, D. B. and Jackson, C. R. (1997) Urbanization of aquatic systems: Degradation thresholds, stormwater detection, and the limits of mitigation. *JAWRA Journal of the American Water Resources Association*, 33(5), 1077–1090.
- Borch, T., Masue, Y., Kukkadapu, R. K., and Fendorf, S. (2007) Phosphate imposed limitations on biological reduction and alteration of ferrihydrite. *Environmental Science & Technology*, 41(1), 166–172.
- Borggaard, O. K., Raben-Lange, B., Gimsing, A. L., and Strobel, B. W. (2005) Influence of humic substances on phosphate adsorption by aluminium and iron oxides. *Geoderma*, 127(3-4), 270–279.
- Bradford, S., Yates, S., Bettahar, M., and Simunek, J. (2002) Physical factors affecting the transport and fate of colloids in saturated porous media. *Water Resources Research*, 38(12).
- Bradley, I., Straub, A., Maraccini, P., Markazi, S., and Nguyen, T. H. (2011) Iron oxide amended biosand filters for virus removal. *Water Research*, 45(15), 4501–4510.
- Bratieres, K., Fletcher, T. D., Deletic, A., and Zinger, Y. (2008) Nutrient and sediment removal by stormwater biofilters: A large-scale design optimisation study. *Water Research*, 42(14), 3930–3940.
- Bright, T. M., Hathaway, J. M., Hunt, W. F., de los Reyes, F. L., and Burchell, M. R. (2010) Impact of storm-water runoff on clogging and fecal bacteria reduction in sand columns. *Journal of Environmental Engineering-ASCE*, 136(12), 1435–1441.
- Brizzolara, R. A. and Stamper, D. M. (2007) The effect of covalent surface immobilization on the bactericidal efficacy of a quaternary ammonium compound. *Surface and Interface Analysis*, 39(7), 559–566.
- Brownell, M. J., Harwood, V. J., Kurz, R. C., McQuaig, S. M., Lukasik, J., and Scott, T. M. (2007) Confirmation of putative stormwater impact on water quality at a Florida beach by microbial source tracking methods and structure of indicator organism populations. *Water Research*, 41(16), 3747–3757.
- Brown, J. and Sobsey, M. D. (2009) Ceramic media amended with metal oxide for the capture of viruses in drinking water. *Environmental Technology*, 30(4), 379–391.
- Byappanahalli, M. N., Yan, T., Hamilton, M. J., Ishii, S., Fujioka, R. S., Whitman, R. L., et al. (2012) The population structure of *Escherichia coli* isolated from subtropical and

- temperate soils. *Science of the Total Environment*, 417-418, 273–279.
- Campos, L. C., Su, M. F. J., Graham, N. J. D., and Smith, S. R. (2002) Biomass development in slow sand filters. *Water Research*, 36(18), 4543–4551.
- CDC (2011) *Surveillance for Waterborne Disease Outbreaks and Other Health Events Associated with Recreational Water - United States, 2007-2008*, Atlanta, GA, Centers for Disease Control and Prevention.
- Chandrasena, G. I., Deletic, A., Ellerton, J., and McCarthy, D. T. (2012) Evaluating *Escherichia coli* removal performance in stormwater biofilters: A laboratory-scale study. *Water Science and Technology*, 66(5), 1132–1138.
- Chandrasena, G. I., Pham, T., Payne, E. G., Deletic, A., and McCarthy, D. T. (2014) *E. coli* removal in laboratory scale stormwater biofilters: Influence of vegetation and submerged zone. *Journal of Hydrology*, 519, 814–822.
- Characklis, G. W., Dilts, M. J., Simmons III, O. D., Likirdopulos, C. A., Krometis, L.-A. H., and Sobsey, M. D. (2005) Microbial partitioning to settleable particles in stormwater. *Water Research*, 39(9), 1773–1782.
- Chattopadhyay, S. and Puls, R. W. (1999) Adsorption of bacteriophages on clay minerals. *Environmental Science & Technology*, 33(20), 3609–3614.
- Chen, G. and Walker, S. L. (2012) Fecal indicator bacteria transport and deposition in saturated and unsaturated porous media. *Environmental Science & Technology*, 46(16), 8782–8790.
- Chiew, H., Sampson, M. L., Huch, S., Ken, S., and Bostick, B. C. (2009) Effect of groundwater iron and phosphate on the efficacy of arsenic removal by iron-amended BioSand filters. *Environmental Science & Technology*, 43(16), 6295–6300.
- Chi, F. H. and Amy, G. L. (2004) Kinetic study on the sorption of dissolved natural organic matter onto different aquifer materials: The effects of hydrophobicity and functional groups. *Journal of Colloid and Interface Science*, 274(2), 380–391.
- Chu, Y. J., Jin, Y., Baumann, T., and Yates, M. V. (2003) Effect of soil properties on saturated and unsaturated virus transport through columns. *Journal of Environmental Quality*, 32(6), 2017–2025.
- Cizek, A. R., Characklis, G. W., Krometis, L.-A., Hayes, J. A., Simmons III, O. D., Di Lonardo, S., et al. (2008) Comparing the partitioning behavior of *Giardia* and *Cryptosporidium* with that of indicator organisms in stormwater runoff. *Water Research*, 42(17), 4421–4438.
- Clark, S. E. and Pitt, R. (2012) Targeting treatment technologies to address specific stormwater pollutants and numeric discharge limits. *Water Research*, 46(20), 6715–6730.
- Clasen, T. (2009) *Scaling Up Household Water Treatment Among Low-Income Populations*,

Geneva, World Health Organization.

- Clasen, T., Schmidt, W.-P., Rabie, T., Roberts, I., and Cairncross, S. (2007) Interventions to improve water quality for preventing diarrhoea: Systematic review and meta-analysis. *BMJ*, 334(7597), 782.
- Cohen, Y. and Metzner, A. (1981) Wall effects in laminar-flow of fluids through packed-beds. *Aiche Journal*, 27(5), 705–715.
- Colford, J. M., Schiff, K. C., Griffith, J. F., Yau, V., Arnold, B. F., Wright, C. C., et al. (2012) Using rapid indicators for *Enterococcus* to assess the risk of illness after exposure to urban runoff contaminated marine water. *Water Research*, 46(7), 2176–2186.
- Cornell, R. M. and Schwertmann, U. (2003) *The Iron Oxides: Structure, Properties, Reactions, Occurrence and Uses*, John Wiley and Sons.
- Curriero, F. C., Patz, J. A., Rose, J. B., and Lele, S. (2001) The association between extreme precipitation and waterborne disease outbreaks in the United States, 1948–1994. *American Journal of Public Health*, 91(8), 1194–1199.
- Czaczyk, K., Trojanowska, K., Stachowiak, B., and Dubisz, H. (2001) Changes in cell number and the ATP content during the composting process. *Polish Journal of Environmental Studies*, 10(3), 149–153.
- Daoud, N. N., Dickinson, N. A., and Gilbert, P. (1983) Anti-microbial activity and physicochemical properties of some alkyldimethylbenzylammonium chlorides. *Microbios*, 37(148), 73–85.
- Daou, T. J., Begin-Colin, S., Grenèche, J. M., Thomas, F., Derory, A., Bernhardt, P., et al. (2007) Phosphate adsorption properties of magnetite-based nanoparticles. *Chemistry of Materials*, 19(18), 4494–4505.
- Davis, A. P., Hunt, W. F., Traver, R. G., and Clar, M. (2009) Bioretention technology: Overview of current practice and future needs. *Journal of Environmental Engineering*, 135(3), 109.
- Davis, A. P., Shokouhian, M., Sharma, H., and Minami, C. (2001) Laboratory study of biological retention for urban stormwater management. *Water Environment Research*, 73(1), 5–14.
- Dong, H., Onstott, T. C., Ko, C.-H., Hollingsworth, A. D., Brown, D. G., and Mailloux, B. J. (2002) Theoretical prediction of collision efficiency between adhesion-deficient bacteria and sediment grain surface. *Colloids and Surfaces B: Biointerfaces*, 24(3–4), 229–245.
- Dowd, S. E., Pillai, S. D., Wang, S., and Corapcioglu, M. Y. (1998) Delineating the specific influence of virus isoelectric point and size on virus adsorption and transport through sandy soils. *Appl. Environ. Microbiol.*, 64(2), 405–410.
- Drayna, P., McLellan, S. L., Simpson, P., Li, S.-H., and Gorelick, M. H. (2010) Association between rainfall and pediatric emergency department visits for acute gastrointestinal

- illness. *Environmental Health Perspectives*, 118(10), 1439–1443.
- Du Pont de Nemours and Co (1992) Letter From DuPont Chem Co to US EPA: Toxicity Studies with DuPont 5700.
- Ek, S., Iiskola, E. I., Niinistö, L., Vaittinen, J., Pakkanen, T. T., Keränen, J., et al. (2003) Atomic layer deposition of a high-density aminopropylsiloxane network on silica through sequential reactions of γ -aminopropyltrialkoxysilanes and water. *Langmuir*, 19(25), 10601–10609.
- Elimelech, M. (1994) Effect of particle size on the kinetics of particle deposition under attractive double layer interactions. *Journal of Colloid and Interface Science*, 164(1), 190–199.
- Elimelech, M. and Song, L. (1992) Theoretical investigation of colloid separation from dilute aqueous suspensions by oppositely charged granular media. *Separations Technology*, 2(1), 2–12.
- Elliott, M. A., DiGiano, F. A., and Sobsey, M. D. (2011) Virus attenuation by microbial mechanisms during the idle time of a household slow sand filter. *Water Research*, 45(14), 4092–4102.
- Elliott, M. A., Stauber, C. E., Koksal, F., DiGiano, F. A., and Sobsey, M. D. (2008) Reductions of *E. coli*, Echovirus type 12 and bacteriophages in an intermittently operated household-scale slow sand filter. *Water Research*, 42(10-11), 2662–2670.
- Erickson, A. J., Gulliver, J. S., and Weiss, P. T. (2012) Capturing phosphates with iron enhanced sand filtration. *Water Research*, 46(9), 3032–3042.
- Erickson, A. J., Gulliver, J. S., and Weiss, P. T. (2007) Enhanced sand filtration for storm water phosphorus removal. *Journal of Environmental Engineering-ASCE*, 133(5), 485–497.
- Fewtrell, L., Kaufmann, R., Kay, D., Enanoria, W., Haller, L., and Colford, J. M. (2005) Water, sanitation, and hygiene interventions to reduce diarrhoea in less developed countries: A systematic review and meta-analysis. *The Lancet Infectious Diseases*, 5(1), 42–52.
- Foppen, J. W. A., Oklety, S., and Schijven, J. F. (2006) Effect of goethite coating and humic acid on the transport of bacteriophage PRD1 in columns of saturated sand. *Journal of Contaminant Hydrology*, 85(3-4), 287–301.
- Foppen, J. W., Liem, Y., and Schijven, J. (2008) Effect of humic acid on the attachment of *Escherichia coli* in columns of goethite-coated sand. *Water Research*, 42(1–2), 211–219.
- Fox, K., Miltner, R., Logsdon, G., Dicks, D., and Drolet, L. (1984) Pilot-plant studies of slow-rate filtration. *Journal American Water Works Association*, 76(12), 62–68.
- Fraise, A., Lambert, P. A., and Maillard, J.-Y. (2008) *Russell, Hugo & Ayliffe's Principles and Practice of Disinfection, Preservation & Sterilization*, John Wiley and Sons.

- Furukawa, Y., Kim, J., Watkins, J., and Wilkin, R. T. (2002) Formation of ferrihydrite and associated iron corrosion products in permeable reactive barriers of zero-valent iron. *Environmental Science & Technology*, 36(24), 5469–5475.
- Gerba, C. P. (1984) “Applied and Theoretical Aspects of Virus Adsorption to Surfaces” in A. I. Laskin (ed.), *Advances in Applied Microbiology*. Academic Press, 133–168.
- Gerba, C. P. and Rose, J. B. (1990) “Viruses in Source and Drinking Water” in G. A. McFeters (ed.), *Drinking Water Microbiology*. Brock/Springer Series in Contemporary Bioscience. Springer New York, 380–396.
- Gerke, J. (1993) Phosphate adsorption by humic/Fe-oxide mixtures aged at pH 4 and 7 and by poorly ordered Fe-oxide. *Geoderma*, 59(1–4), 279–288.
- Gerke, J. and Hermann, R. (1992) Adsorption of orthophosphate to humic-Fe-complexes and to amorphous Fe-oxide. *Zeitschrift Fur Pflanzenernahrung Und Bodenkunde*, 155(3), 233–236.
- Gilbert, P. and Al-taae, A. (1985) Antimicrobial activity of some alkyltrimethylammonium bromides. *Letters in Applied Microbiology*, 1(6), 101–104.
- Gilbert, P. and Moore, L. E. (2005) Cationic antiseptics: Diversity of action under a common epithet. *Journal of Applied Microbiology*, 99(4), 703–715.
- Gimsing, A. L. and Borggaard, O. K. (2007) Phosphate and glyphosate adsorption by hematite and ferrihydrite and comparison with other variable-charge minerals. *Clays and Clay Minerals*, 55(1), 108–114.
- Grebel, J. E., Mohanty, S. K., Torkelson, A. A., Boehm, A. B., Higgins, C. P., Maxwell, R. M., et al. (2013) Engineered infiltration systems for urban stormwater reclamation. *Environmental Engineering Science*, 30(8), 437–454.
- Gu, B., Phelps, T. J., Liang, L., Dickey, M. J., Roh, Y., Kinsall, B. L., et al. (1999) Biogeochemical dynamics in zero-valent iron columns: Implications for permeable reactive barriers. *Environmental Science & Technology*, 33(13), 2170–2177.
- Hammes, F. A. and Egli, T. (2005) New method for assimilable organic carbon determination using flow-cytometric enumeration and a natural microbial consortium as inoculum. *Environmental Science & Technology*, 39(9), 3289–3294.
- Hammes, F., Berger, C., Köster, O., and Egli, T. (2010) Assessing biological stability of drinking water without disinfectant residuals in a full-scale water supply system. *Journal of Water Supply: Research and Technology—AQUA*, 59(1), 31.
- Hammes, F., Berney, M., Wang, Y., Vital, M., Köster, O., and Egli, T. (2008) Flow-cytometric total bacterial cell counts as a descriptive microbiological parameter for drinking water treatment processes. *Water Research*, 42(1–2), 269–277.

- Hammes, F. and Egli, T. (2010) Cytometric methods for measuring bacteria in water: advantages, pitfalls and applications. *Analytical and Bioanalytical Chemistry*, 397(3), 1083–1095.
- Hanna, K. (2007) Adsorption of aromatic carboxylate compounds on the surface of synthesized iron oxide-coated sands. *Applied Geochemistry*, 22(9), 2045–2053.
- Hans, K. and Maranzana, S. (2006) *University of California, Berkeley Strawberry Creek Water Quality - 2006 Status Report*, Office of Environment, Health & Safety University of California, Berkeley.
- Harvey, R. W. and Ryan, J. N. (2004) Use of PRD1 bacteriophage in groundwater viral transport, inactivation, and attachment studies. *FEMS Microbiology Ecology*, 49(1), 3–16.
- Hathaway, J. M., Hunt, W. F., Graves, A. K., and Wright, J. D. (2011) Field evaluation of bioretention indicator bacteria sequestration in Wilmington, North Carolina. *Journal of Environmental Engineering-ASCE*, 137(12), 1103–1113.
- Hatt, B. E., Fletcher, T. D., Walsh, C. J., and Taylor, S. L. (2004) The influence of urban density and drainage infrastructure on the concentrations and loads of pollutants in small streams. *Environmental Management*, 34(1), 112–124.
- Hermes, K. P. and Suttle, C. A. (1995) Direct counts of viruses in natural waters and laboratory cultures by epifluorescence microscopy. *Limnology and Oceanography*, 40(6), 1050–1055.
- He, Z. and Davis, A. P. (2011) Process modeling of storm-water flow in a bioretention cell. *Journal of Irrigation and Drainage Engineering*, 137(3), 121.
- Hipp, J. A., Ogunseitan, O., Lejano, R., and Smith, C. S. (2006) Optimization of stormwater filtration at the urban/watershed interface. *Environmental Science & Technology*, 40(15), 4794–4801.
- Huisman, L. and Wood, W. E. (1974) *Slow Sand Filtration*, Geneva, World Health Organization.
- Hunter, P. R., MacDonald, A. M., and Carter, R. C. (2010) Water supply and health. *PLoS Med*, 7(11), e1000361.
- Huysman, F. and Verstraete, W. (1993) Water-facilitated transport of bacteria in unsaturated soil columns: Influence of inoculation and irrigation methods. *Soil Biology & Biochemistry*, 25(1), 91–97.
- Ingram, D. T., Callahan, M. T., Ferguson, S., Hoover, D. G., Shelton, D. R., Millner, P. D., et al. (2012) Use of zero-valent iron biosand filters to reduce *Escherichia coli* O157:H12 in irrigation water applied to spinach plants in a field setting. *Journal of Applied Microbiology*, 112(3), 551–560.
- International Stormwater BMP Database (2014) *Developed by Wright Water Engineers, Inc. and Geosyntec Consultants for the Water Environment Research Foundation (WERF), the*

American Society of Civil Engineers (ASCE)/Environmental and Water Resources Institute (EWRI), the American Public Works Association (APWA), the Federal Highway Administration (FHWA), and U.S. Environmental Protection Agency (EPA).

- Inwood, W. B., Hall, J. A., Kim, K.-S., Fong, R., and Kustu, S. (2009) Genetic evidence for an essential oscillation of transmembrane-spanning segment 5 in the *Escherichia coli* ammonium channel AmtB. *Genetics*, 183(4), 1341–1355.
- Isquith, A. J., Abbott, E. A., and Walters, P. A. (1972) Surface-bonded antimicrobial activity of an organosilicon quaternary ammonium chloride. *Applied Microbiology*, 24(6), 859–863.
- Jenkins, M. W., Tiwari, S. K., and Darby, J. (2011) Bacterial, viral and turbidity removal by intermittent slow sand filtration for household use in developing countries: Experimental investigation and modeling. *Water Research*, 45(18), 6227–6239.
- Jensen, P. K., Ensink, J. H. J., Jayasinghe, G., Van Der Hoek, W., Cairncross, S., and Dalsgaard, A. (2002) Domestic transmission routes of pathogens: The problem of in-house contamination of drinking water during storage in developing countries. *Tropical Medicine & International Health*, 7(7), 604–609.
- Johnson, W. P. and Logan, B. E. (1996) Enhanced transport of bacteria in porous media by sediment-phase and aqueous-phase natural organic matter. *Water Research*, 30(4), 923–931.
- Jones, A. M., Pham, A. N., Collins, R. N., and Waite, T. D. (2009) Dissociation kinetics of Fe(III)- and Al(III)-natural organic matter complexes at pH 6.0 and 8.0 and 25 °C. *Geochimica et Cosmochimica Acta*, 73(10), 2875–2887.
- Karl, D. (1980) Cellular nucleotide measurements and applications in microbial ecology. *Microbiological Reviews*, 44(4), 739–796.
- Kasozi, G. N., Zimmerman, A. R., Nkedi-Kizza, P., and Gao, B. (2010) Catechol and humic acid sorption onto a range of laboratory-produced black carbons (biochars). *Environmental Science & Technology*, 44(16), 6189–6195.
- Kim, J.-W., Choi, H., and Pachepsky, Y. A. (2010) Biofilm morphology as related to the porous media clogging. *Water Research*, 44(4), 1193–1201.
- Kim, J. Y., Lee, C., Sedlak, D. L., Yoon, J., and Nelson, K. L. (2010) Inactivation of MS2 coliphage by Fenton's reagent. *Water Research*, 44(8), 2647–2653.
- Kim, M. H., Sung, C. Y., Li, M.-H., and Chu, K.-H. (2012) Bioretention for stormwater quality improvement in Texas: Removal effectiveness of *Escherichia coli*. *Separation and Purification Technology*, 84, 120–124.
- Kohn, T., Livi, K. J. T., Roberts, A. L., and Vikesland, P. J. (2005) Longevity of granular iron in groundwater treatment processes: Corrosion product development. *Environmental Science & Technology*, 39(8), 2867–2879.

- Kols, A. (2010) *Extended User Testing of Water Treatment Devices in Andhra Pradesh*, PATH. [online] <http://www.path.org/publications/detail.php?i=1841>.
- Kosmulski, M. (2011) The pH-dependent surface charging and points of zero charge V. Update. *Journal of Colloid and Interface Science*, 353(1), 1–15.
- Kostka, J. E., Stucki, J. W., Neelson, K. H., and Wu, J. (1996) Reduction of structural Fe(III) in smectite by a pure culture of *Shewanella putrefaciens* strain MR-1. *Clays and Clay Minerals*, 44(4), 522–529.
- Kügler, R., Bouloussa, O., and Rondelez, F. (2005) Evidence of a charge-density threshold for optimum efficiency of biocidal cationic surfaces. *Microbiology*, 151(5), 1341–1348.
- Lautenschlager, K., Hwang, C., Ling, F., Liu, W.-T., Boon, N., Köster, O., et al. (2014) Abundance and composition of indigenous bacterial communities in a multi-step biofiltration-based drinking water treatment plant. *Water Research*, 62, 40–52.
- Lawrence, J. R. and Hendry, M. J. (1996) Transport of bacteria through geologic media. *Canadian Journal of Microbiology*, 42(4), 410–422.
- Le Coustumer, S., Fletcher, T. D., Deletic, A., Barraud, S., and Lewis, J. F. (2009) Hydraulic performance of biofilter systems for stormwater management: Influences of design and operation. *Journal of Hydrology*, 376(1–2), 16–23.
- Le Coustumer, S., Fletcher, T. D., Deletic, A., Barraud, S., and Poelsma, P. (2012) The influence of design parameters on clogging of stormwater biofilters: A large-scale column study. *Water Research*, 46(20), 6743–6752.
- Lehtokari, M., Nikkola, P., and Paatero, J. (1983) Determination of ATP from compost using the firefly bioluminescence technique. *European Journal of Applied Microbiology and Biotechnology*, 17(3), 187–190.
- Leon Morales, C. F., Strathmann, M., and Flemming, H.-C. (2007) Influence of biofilms on the movement of colloids in porous media. Implications for colloid facilitated transport in subsurface environments. *Water Research*, 41(10), 2059–2068.
- Leupin, O. X., Hug, S. J., and Badruzzaman, A. B. M. (2005) Arsenic removal from Bangladesh tube well water with filter columns containing zerovalent iron filings and sand. *Environmental Science & Technology*, 39(20), 8032–8037.
- Li, H. and Davis, A. P. (2009) Water quality improvement through reductions of pollutant loads using bioretention. *Journal of Environmental Engineering*, 135(8), 567–576.
- Little, B. and Ray, R. (2002) A perspective on corrosion inhibition by biofilms. *Corrosion*, 58(5), 424–428.
- Litton, G. M. and Olson, T. M. (1993) Colloid deposition rates on silica bed media and artifacts related to collector surface preparation methods. *Environmental Science & Technology*,

27, 185–193.

- Liu, T., Tsang, D. C. W., and Lo, I. M. C. (2008) Chromium(VI) reduction kinetics by zero-valent iron in moderately hard water with humic acid: Iron dissolution and humic acid adsorption. *Environmental Science & Technology*, 42(6), 2092–2098.
- Li, Y. L., Deletic, A., Alcazar, L., Bratieres, K., Fletcher, T. D., and McCarthy, D. T. (2012) Removal of *Clostridium perfringens*, *Escherichia coli* and F-RNA coliphages by stormwater biofilters. *Ecological Engineering*, 49, 137–145.
- Logsdon, G. and Lippy, E. (1982) The role of filtration in preventing waterborne disease. *Journal American Water Works Association*, 74(12), 649–655.
- Loosdrecht, M. C. van, Lyklema, J., Norde, W., Schraa, G., and Zehnder, A. J. (1987) The role of bacterial cell wall hydrophobicity in adhesion. *Applied and Environmental Microbiology*, 53(8), 1893–1897.
- Lovley, D. R. (1997) Microbial Fe(III) reduction in subsurface environments. *FEMS Microbiology Reviews*, 20(3-4), 305–313.
- Lovley, D. R. and Phillips, E. J. P. (1986) Organic matter mineralization with reduction of ferric iron in anaerobic sediments. *Applied and Environmental Microbiology*, 51(4), 683–689.
- Lukasik, J., Cheng, Y.-F., Lu, F., Tamplin, M., and Farrah, S. R. (1999) Removal of microorganisms from water by columns containing sand coated with ferric and aluminum hydroxides. *Water Research*, 33(3), 769–777.
- Luo, Y., Durenkamp, M., De Nobili, M., Lin, Q., Devonshire, B. J., and Brookes, P. C. (2013) Microbial biomass growth, following incorporation of biochars produced at 350 °C or 700 °C, in a silty-clay loam soil of high and low pH. *Soil Biology and Biochemistry*, 57, 513–523.
- Magic-Knezev, A. and van der Kooij, D. (2004) Optimisation and significance of ATP analysis for measuring active biomass in granular activated carbon filters used in water treatment. *Water Research*, 38(18), 3971–3979.
- Maillard, J. -Y (2002) Bacterial target sites for biocide action. *Journal of Applied Microbiology*, 92, 16S–27S.
- Marsalek, J. and Rochfort, Q. (2004) Urban wet weather flows: Sources of fecal contamination impacting on recreational waters and threatening drinking-water sources. *Journal of Toxicology and Environmental Health, Part A*, 67(20-22), 1765–1777.
- Mattioli, M. C., Boehm, A. B., Davis, J., Harris, A. R., Mrisho, M., and Pickering, A. J. (2014) Enteric pathogens in stored drinking water and on caregiver's hands in Tanzanian households with and without reported cases of child diarrhea. *PLoS ONE*, 9(1), e84939.
- Mattison, R. G., Taki, H., and Harayama, S. (2002) The bacterivorous soil flagellate *Heteromita*

- globosa* reduces bacterial clogging under denitrifying conditions in sand-filled aquifer columns. *Applied and Environmental Microbiology*, 68(9), 4539–4545.
- Mayer, B. K., Ryu, H., and Abbaszadegan, M. (2008) Treatability of U.S. Environmental Protection Agency contaminant candidate list viruses: Removal of Coxsackievirus and Echovirus using enhanced coagulation. *Environmental Science & Technology*, 42(18), 6890–6896.
- Mays, D. C. and Hunt, J. R. (2005) Hydrodynamic aspects of particle clogging in porous media. *Environmental Science & Technology*, 39(2), 577–584.
- Michen, B. and Graule, T. (2010) Isoelectric points of viruses. *Journal of Applied Microbiology*, 109(2), 388–397.
- Michen, B., Meder, F., Rust, A., Fritsch, J., Aneziris, C., and Graule, T. (2011) Virus removal in ceramic depth filters based on diatomaceous earth. *Environmental Science & Technology*, 46(2), 1170–1177.
- Mills, A. L., Herman, J. S., Hornberger, G. M., and DeJesús, T. H. (1994) Effect of solution ionic strength and iron coatings on mineral grains on the sorption of bacterial cells to quartz sand. *Applied and Environmental Microbiology*, 60(9), 3300–3306.
- Mohanty, S. K. and Boehm, A. B. (2014) *Escherichia coli* removal in biochar-augmented biofilter: Effect of infiltration rate, initial bacterial concentration, biochar particle size, and presence of compost. *Environmental Science & Technology*, 48(19), 11535–11542.
- Mohanty, S. K., Cantrell, K. B., Nelson, K. L., and Boehm, A. B. (2014) Efficacy of biochar to remove *Escherichia coli* from stormwater under steady and intermittent flow. *Water Research*, 61, 288–296.
- Mohanty, S. K., Torkelson, A. A., Dodd, H., Nelson, K. L., and Boehm, A. B. (2013) Engineering solutions to improve the removal of fecal indicator bacteria by bioinfiltration systems during intermittent flow of stormwater. *Environmental Science & Technology*, 47(19), 10791–10798.
- Murata, H., Koepsel, R. R., Matyjaszewski, K., and Russell, A. J. (2007) Permanent, non-leaching antibacterial surfaces-2: How high density cationic surfaces kill bacterial cells. *Biomaterials*, 28(32), 4870–4879.
- Nakagawa, Y., Hayashi, H., Tawaratani, T., Kourai, H., Horie, T., and Shibasaki, I. (1984) Disinfection of water with quaternary ammonium salts insolubilized on a porous glass surface. *Applied and Environmental Microbiology*, 47(3), 513–518.
- Neumann, A., Kaegi, R., Voegelin, A., Hussam, A., Munir, A. K. M., and Hug, S. J. (2013) Arsenic removal with composite iron matrix filters in Bangladesh: A field and laboratory study. *Environmental Science & Technology*, 47(9), 4544–4554.
- Noubactep, C. (2010) Metallic iron for safe drinking water worldwide. *Chemical Engineering*

- Journal, 165(2), 740–749.
- Noubactep, C., Schoener, A., and Wofo, P. (2009) Metallic iron filters for universal access to safe drinking water. *Clean-Soil Air Water*, 37(12), 930–937.
- NRC (2008) *Urban Stormwater Management in the United States*, Washington, D.C., National Research Council.
- Olivieri, A. W., Boehm, A., Sommers, C. A., Soller, J. A., Eisenberg, J. N., and Danielson, R. (2007) *Development of a Protocol for Risk Assessment of Microorganisms in Separate Stormwater Systems*, Water Environment Research Foundation.
- Or, D., Phutane, S., and Dechesne, A. (2007) Extracellular polymeric substances affecting pore-scale hydrologic conditions for bacterial activity in unsaturated soils. *Vadose Zone Journal*, 6(2), 298–305.
- Ott, E.-M., Müller, T., Müller, M., Franz, C., Ulrich, A., Gabel, M., et al. (2001) Population dynamics and antagonistic potential of *Enterococci* colonizing the phyllosphere of grasses. *Journal of Applied Microbiology*, 91(1), 54–66.
- Parfitt, R. L., Fraser, A. R., and Farmer, V. C. (1977) Adsorption on hydrous oxides. III. Fulvic acid and humic acid on goethite, gibbsite and imogolite. *Journal of Soil Science*, 28(2), 289–296.
- Parker, J. K., McIntyre, D., and Noble, R. T. (2010) Characterizing fecal contamination in stormwater runoff in coastal North Carolina, USA. *Water Research*, 44(14), 4186–4194.
- Park, S.-J. and Kim, S.-B. (2009) Adhesion of *Escherichia coli* to iron-coated sand in the presence of humic acid: A column experiment. *Water Environment Research*, 81(2), 125–130.
- Park, S.-J., Lee, C.-G., and Kim, S.-B. (2009) The role of phosphate in bacterial interaction with iron-coated surfaces. *Colloids and Surfaces B-Biointerfaces*, 68(1), 79–82.
- Park, S. K., Choi, S. C., and Kim, Y. K. (2007) The rate of iron corrosion for different organic carbon sources during biofilm formation. *Water Science and Technology*, 55(8-9), 489–497.
- Passeport, E., Hunt, W. F., Line, D. E., Smith, R. A., and Brown, R. A. (2009) Field study of the ability of two grassed bioretention cells to reduce storm-water runoff pollution. *Journal of Irrigation and Drainage Engineering-ASCE*, 135(4), 505–510.
- Pham, M., Mintz, E. A., and Nguyen, T. H. (2009) Deposition kinetics of bacteriophage MS2 to natural organic matter: Role of divalent cations. *Journal of Colloid and Interface Science*, 338(1), 1–9.
- Phillips, D. H., Gu, B., Watson, D. B., Roh, Y., Liang, L., and Lee, S. Y. (2000) Performance evaluation of a zerovalent iron reactive barrier: Mineralogical characteristics.

- Environmental Science & Technology, 34(19), 4169–4176.
- Pickering, A. J., Julian, T. R., Marks, S. J., Mattioli, M. C., Boehm, A. B., Schwab, K. J., et al. (2012) Fecal contamination and diarrheal pathogens on surfaces and in soils among Tanzanian households with and without improved sanitation. *Environmental Science & Technology*, 46(11), 5736–5743.
- Pitt, R. and Clark, S. (2012) *Stormwater Non-Potable Beneficial Uses and Effects on Urban Infrastructure*, WERF.
- Pitt, R. and Clark, S. E. (2008) Integrated storm-water management for watershed sustainability. *Journal of Irrigation and Drainage Engineering-ASCE*, 134(5), 548–555.
- Pitt, R., Clark, S., and Field, R. (1999) Groundwater contamination potential from stormwater infiltration practices. *Urban Water*, 1(3), 217–236.
- Prest, E. I., Hammes, F., Köttsch, S., van Loosdrecht, M. C. M., and Vrouwenvelder, J. S. (2013) Monitoring microbiological changes in drinking water systems using a fast and reproducible flow cytometric method. *Water Research*, 47(19), 7131–7142.
- Prüss-Ustün, A., Bartram, J., Clasen, T., Colford, J. M., Cumming, O., Curtis, V., et al. (2014) Burden of disease from inadequate water, sanitation and hygiene in low- and middle-income settings: A retrospective analysis of data from 145 countries. *Tropical Medicine & International Health*, 19(8), 894–905.
- Quigley, M., Rangarajan, S., Pankani, D., and Henning, D. (2008) “New Directions in Real-Time and Dynamic Control for Stormwater Management and Low Impact Development” in *American Society of Civil Engineers*, 1–7.
- Ram, J. L., Thompson, B., Turner, C., Nechvatal, J. M., Sheehan, H., and Bobrin, J. (2007) Identification of pets and raccoons as sources of bacterial contamination of urban storm sewers using a sequence-based bacterial source tracking method. *Water Research*, 41(16), 3605–3614.
- Rangsvivek, R. and Jekel, M. R. (2005) Removal of dissolved metals by zero-valent iron (ZVI): Kinetics, equilibria, processes and implications for stormwater runoff treatment. *Water Research*, 39(17), 4153–4163.
- Reddy, K. R., Xie, T., and Dastgheibi, S. (2014) Evaluation of biochar as a potential filter media for the removal of mixed contaminants from urban storm water runoff. *Journal of Environmental Engineering*, 140(12), 04014043.
- Redman, J. A., Grant, S. B., Olson, T. M., Hardy, M. E., and Estes, M. K. (1997) Filtration of recombinant Norwalk virus particles and bacteriophage MS2 in quartz sand: Importance of electrostatic interactions. *Environmental Science & Technology*, 31(12), 3378–3383.
- Roberson, E. and Firestone, M. (1992) Relationship between desiccation and exopolysaccharide production in a soil *Pseudomonas Sp.* *Applied and Environmental Microbiology*, 58(4),

1284–1291.

- Ronen, D., Berkowitz, B., and Magaritz, M. (1989) The development and influence of gas bubbles in phreatic aquifers under natural flow conditions. *Transport in Porous Media*, 4(3), 295–306.
- Rosenberg, M. and Kjelleberg, S. (1986) “Hydrophobic Interactions: Role in Bacterial Adhesion” in K. C. Marshall (ed.), *Advances in Microbial Ecology*. Advances in Microbial Ecology. Springer US, 353–393.
- Rusch, B., Hanna, K., and Humbert, B. (2010) Coating of quartz silica with iron oxides: Characterization and surface reactivity of iron coating phases. *Colloids and Surfaces A: Physicochemical and Engineering Aspects*, 353(2–3), 172–180.
- Rusciano, G. M. and Obropta, C. C. (2007) Bioretention column study: Fecal coliform and total suspended solids reductions. *Transactions of the ASABE*, 50(4), 1261–1269.
- Ryan, J. N., Harvey, R. W., Metge, D., Elimelech, M., Navigato, T., and Pieper, A. P. (2002) Field and laboratory investigations of inactivation of viruses (PRD1 and MS2) attached to iron oxide-coated quartz sand. *Environmental Science & Technology*, 36(11), 2403–2413.
- Rydman, P. S., Caldentey, J., Butcher, S. J., Fuller, S. D., Rutten, T., and Bamford, D. H. (1999) Bacteriophage PRD1 contains a labile receptor-binding structure at each vertex. *Journal of Molecular Biology*, 291(3), 575–587.
- Sauer, E. P., VandeWalle, J. L., Bootsma, M. J., and McLellan, S. L. (2011) Detection of the human specific *Bacteroides* genetic marker provides evidence of widespread sewage contamination of stormwater in the urban environment. *Water Research*, 45(14), 4081–4091.
- Schiff, K. C., Morton, J., and Weisberg, S. B. (2003) Retrospective evaluation of shoreline water quality along Santa Monica Bay beaches. *Marine Environmental Research*, 56(1-2), 245–253.
- Schriewer, A., Odagiri, M., Wuertz, S., Misra, P. R., Panigrahi, P., Clasen, T., et al. (2015) Human and animal fecal contamination of community water sources, stored drinking water and hands in rural India measured with validated microbial source tracking assays. *The American Journal of Tropical Medicine and Hygiene*, 93(3), 509–516.
- Seki, Miyazaki, and Nakano (1998) Effects of microorganisms on hydraulic conductivity decrease in infiltration. *European Journal of Soil Science*, 49(2), 231–236.
- Selvakumar, A. and Borst, M. (2006) Variation of microorganism concentrations in urban stormwater runoff with land use and seasons. *Journal of Water and Health*, 4(1), 109–124.
- Senesi, N., Griffith, S. M., Schnitzer, M., and Townsend, M. G. (1977) Binding of Fe³⁺ by humic materials. *Geochimica et Cosmochimica Acta*, 41(7), 969–976.

- Sercu, B., Van De Werfhorst, L. C., Murray, J. L. S., and Holden, P. A. (2011) Sewage exfiltration as a source of storm drain contamination during dry weather in urban watersheds. *Environmental Science & Technology*, 45(17), 7151–7157.
- Shi, C., Wei, J., Jin, Y., Kniel, K. E., and Chiu, P. C. (2012) Removal of viruses and bacteriophages from drinking water using zero-valent iron. *Separation and Purification Technology*, 84, 72–78.
- Sidhu, J. P. S., Ahmed, W., Gernjak, W., Aryal, R., McCarthy, D., Palmer, A., et al. (2013) Sewage pollution in urban stormwater runoff as evident from the widespread presence of multiple microbial and chemical source tracking markers. *Science of The Total Environment*, 463–464, 488–496.
- Sidhu, J. P. S., Hodggers, L., Ahmed, W., Chong, M. N., and Toze, S. (2012) Prevalence of human pathogens and indicators in stormwater runoff in Brisbane, Australia. *Water Research*, 46(20), 6652–6660.
- Siegrist, R. and Boyle, W. (1987) Waste-water-induced soil clogging development. *Journal of Environmental Engineering-ASCE*, 113(3), 550–566.
- Sobsey, M. D., Stauber, C. E., Casanova, L. M., Brown, J. M., and Elliott, M. A. (2008) Point of use household drinking water filtration: A practical, effective solution for providing sustained access to safe drinking water in the developing world. *Environmental Science & Technology*, 42(12), 4261–4267.
- Staley, C., Reckhow, K. H., Lukasik, J., and Harwood, V. J. (2012) Assessment of sources of human pathogens and fecal contamination in a Florida freshwater lake. *Water Research*, 46(17), 5799–5812.
- Stauber, C. E., Elliott, M. A., Koksal, F., Ortiz, G. M., DiGiano, F. A., and Sobsey, M. D. (2006) Characterisation of the biosand filter for *E. coli* reductions from household drinking water under controlled laboratory and field use conditions. *Water Science and Technology*, 54(3), 1–7.
- Syngouna, V. I. and Chrysikopoulos, C. V. (2015) Experimental investigation of virus and clay particles cotransport in partially saturated columns packed with glass beads. *Journal of Colloid and Interface Science*, 440, 140–150.
- Theis, T. L. and Singer, P. C. (1974) Complexation of iron(II) by organic matter and its effect on iron(II) oxygenation. *Environmental Science & Technology*, 8(6), 569–573.
- Tiquia, S. M., Wan, J. H. C., and Tam, N. F. Y. (2002) Dynamics of yard trimmings composting as determined by dehydrogenase activity, ATP content, arginine ammonification, and nitrification potential. *Process Biochemistry*, 37(10), 1057–1065.
- Torkelson, A. A., da Silva, A. K., Love, D. C., Kim, J. Y., Alper, J. P., Coox, B., et al. (2012) Investigation of quaternary ammonium silane-coated sand filter for the removal of bacteria and viruses from drinking water. *Journal of Applied Microbiology*, 113(5),

1196–1207.

- Triszcz, J. M., Porta, A., and Einschlag, F. S. G. (2009) Effect of operating conditions on iron corrosion rates in zero-valent iron systems for arsenic removal. *Chemical Engineering Journal*, 150(2–3), 431–439.
- Tseng, D. Y., Chalmers, J. J., and Tuovinen, O. H. (1996) ATP measurement in compost. *Compost Science & Utilization*, 4(3), 6–17.
- Tufenkji, N. and Elimelech, M. (2004) Correlation equation for predicting single-collector efficiency in physicochemical filtration in saturated porous media. *Environmental Science & Technology*, 38(2), 529–536.
- Ulrich, B. A., Im, E. A., Werner, D., and Higgins, C. P. (2015) Biochar and activated carbon for enhanced trace organic contaminant retention in stormwater Infiltration systems. *Environmental Science & Technology*, 49(10), 6222–6230.
- UNICEF/WHO (2009) *Diarrhoea: Why Children Are Still Dying and What Can Be Done*, New York, Geneva, United Nations Children’s Fund, World Health Organization.
- U.S. EPA (2000) *Low Impact Development (LID): A Literature Review*, Washington, D.C., United States Environmental Protection Agency.
- U.S. EPA (2001) *Method 1601: Male-Specific (F+) and Somatic Coliphage in Water by Two-Step Enrichment Procedure*, Washington, D.C., United States Environmental Protection Agency.
- U.S. EPA (2001) *Method 1602: Male-specific (F+) and Somatic Coliphage in Water by a Single Agar Layer(SAL) Procedure*, Washington, D.C., United States Environmental Protection Agency.
- U.S. EPA (1983) *Methods for chemical analysis of water and wastes*, Washington, D.C., United States Environmental Protection Agency.
- U.S. EPA *National Recommended Water Quality Criteria*, Washington, D.C., United States Environmental Protection Agency.
- U.S. EPA (2009) *National Water Quality Inventory: Report to Congress*, Washington, D.C., United States Environmental Protection Agency.
- U.S. EPA (2009) *Technical Guidance on Implementing the Stormwater Runoff Requirements for Federal Projects under Section 438 of the Energy Independence and Security Act*, Washington, D.C., United States Environmental Protection Agency.
- Vandevivere, P. and Baveye, P. (1992) Saturated hydraulic conductivity reduction caused by aerobic-bacteria in sand columns. *Soil Science Society of America Journal*, 56(1), 1–13.
- Velten, S., Boller, M., Köster, O., Helbing, J., Weilenmann, H.-U., and Hammes, F. (2011)

- Development of biomass in a drinking water granular active carbon (GAC) filter. *Water Research*, 45(19), 6347–6354.
- Velten, S., Hammes, F., Boller, M., and Egli, T. (2007) Rapid and direct estimation of active biomass on granular activated carbon through adenosine tri-phosphate (ATP) determination. *Water Research*, 41(9), 1973–1983.
- Viollier, E., Inglett, P. W., Hunter, K., Roychoudhury, A. N., and Van Cappellen, P. (2000) The ferrozine method revisited: Fe(II)/Fe(III) determination in natural waters. *Applied Geochemistry*, 15(6), 785–790.
- Vital, M., Dignum, M., Magic-Knezev, A., Ross, P., Rietveld, L., and Hammes, F. (2012) Flow cytometry and adenosine tri-phosphate analysis: Alternative possibilities to evaluate major bacteriological changes in drinking water treatment and distribution systems. *Water Research*, 46(15), 4665–4676.
- Waddington, H., Fewtrell, L., Snilstveit, B., and White, H. (2009) *Water and Sanitation Interventions to Combat Childhood Diarrhoea in developing Countries.*, International Initiative for Impact Evaluation.
- Walters, S. P., Thebo, A. L., and Boehm, A. B. (2011) Impact of urbanization and agriculture on the occurrence of bacterial pathogens and *stx* genes in coastal waterbodies of central California. *Water Research*, 45(4), 1752–1762.
- Wang, H., Narihiro, T., Straub, A. P., Pugh, C. R., Tamaki, H., Moor, J. F., et al. (2014) MS2 bacteriophage reduction and microbial communities in biosand filters. *Environmental Science & Technology*, 48(12), 6702–6709.
- Wang, Y., Hammes, F., Boon, N., Chami, M., and Egli, T. (2009) Isolation and characterization of low nucleic acid (LNA)-content bacteria. *ISME Journal*, 3(8), 889–902.
- Wan, J., Wilson, J., and Kieft, T. (1994) Influence of the gas-water interface on transport of microorganisms through unsaturated porous-media. *Applied and Environmental Microbiology*, 60(2), 509–516.
- Weber, K. A., Achenbach, L. A., and Coates, J. D. (2006) Microorganisms pumping iron: Anaerobic microbial iron oxidation and reduction. *Nature Reviews Microbiology*, 4(10), 752–764.
- Weber-Shirk, M. L. and Dick, R. I. (1997) Biological mechanisms in slow sand filters. *American Water Works Association Journal*, 89(2), 72–83.
- Westerhoff, P. and James, J. (2003) Nitrate removal in zero-valent iron packed columns. *Water Research*, 37(8), 1818–1830.
- Wheeler, D., Bartram, J., and Lloyd, B. J. (1988) “The Removal of Viruses by Filtration Through Sand” in *Slow Sand Filtration: Recent Developments in Water Treatment Technology*. Chichester, England, Ellis Horwood Ltd., 207–229.

- WHO (2007) *Combating Waterborne Disease at the Household Level*, Geneva, World Health Organization.
- WHO (2011) *Evaluating Household Water Treatment Options: Health-based Targets and Microbiological Performance Specifications*, Geneva, World Health Organization.
- WHO (2009) *Global Health Risks: Mortality and Burden of Disease Attributable to Selected Major Risks*, Geneva, World Health Organization.
- WHO (2015) *Progress on Sanitation and Drinking Water: 2015 Update and MDG Assessment*, Geneva, World Health Organization.
- Wingender, J., Neu, T. R., and Flemming, H.-C. (1999) “What are Bacterial Extracellular Polymeric Substances?” in D. J. Wingender, D. T. R. Neu, and P. D. H.-C. Flemming (eds.), *Microbial Extracellular Polymeric Substances*. Springer Berlin Heidelberg, 1–19.
- Witucki, G. L. (1993) A silane primer: Chemistry and applications of alkoxy silanes. *Journal of Coating Technology*, 65(822), 57–60.
- Xie, T., Reddy, K. R., Wang, C., Yargicoglu, E., and Spokas, K. (2015) Characteristics and applications of biochar for environmental remediation: A review. *Critical Reviews in Environmental Science and Technology*, 45(9), 939–969.
- Yang, H., Kim, H., and Tong, M. (2012) Influence of humic acid on the transport behavior of bacteria in quartz sand. *Colloids and Surfaces B: Biointerfaces*, 91(0), 122–129.
- Yao, Y., Gao, B., Inyang, M., Zimmerman, A. R., Cao, X., Pullammanappallil, P., et al. (2011) Removal of phosphate from aqueous solution by biochar derived from anaerobically digested sugar beet tailings. *Journal of Hazardous Materials*, 190(1–3), 501–507.
- Yates, M. and Yates, S. (1987) Modeling microbial fate in the subsurface environment. *Critical Reviews in Environmental Control*, 17(4), 307–344.
- Young, K. D. and Thackston, E. L. (1999) Housing density and bacterial loading in urban streams. *Journal of Environmental Engineering*, 125(12), 1177–1180.
- Young-Rojanschi, C. and Madramootoo, C. (2014) Intermittent versus continuous operation of biosand filters. *Water Research*, 49, 1–10.
- You, Y. W., Han, J., Chiu, P. C., and Jin, Y. (2005) Removal and inactivation of waterborne viruses using zerovalent iron. *Environmental Science & Technology*, 39(23), 9263–9269.
- Yuan, B., Pham, M., and Nguyen, T. H. (2008) Deposition kinetics of bacteriophage MS2 on a silica surface coated with natural organic matter in a radial stagnation point flow cell. *Environmental Science & Technology*, 42(20), 7628–7633.
- Zhang, L., Seagren, E. A., Davis, A. P., and Karns, J. S. (2011) Long-term sustainability of *Escherichia Coli* removal in conventional bioretention media. *Journal of Environmental*

Engineering, 137(8), 669.

Zhang, L., Seagren, E. A., Davis, A. P., and Karns, J. S. (2010) The capture and destruction of *Escherichia coli* from simulated urban runoff using conventional bioretention media and iron oxide-coated sand. *Water Environment Research*, 82(8), 701–714.

Zhuang, J. and Jin, Y. (2008) Interactions between viruses and goethite during saturated flow: Effects of solution pH, carbonate, and phosphate. *Journal of Contaminant Hydrology*, 98(1-2), 15–21.